Geophysics Open-File Report 53
Geoscience Department and
Geophysical Research Center
New Mexico Tech
Socorro, NM 87801
June, 1985

Apparent Qp for Upper Crustal Rock in the Rio Grande Rift near Socorro, New Mexico, from the Pulse Width of the Initial P-phase of Microearthquakes

by

Grant D. Goodyear

Submitted in partial fulfillment
of the requirement for
Geophysics 590
and the
Master's Degree Program

at

New Mexico Institute of
Mining and Technology

June, 1985

ABSTRACT

Measurements of the first half-cycle of waveforms for microearthquakes occurring near Socorro, New Mexico and recorded between January, 1977 and November, 1983, were used in calculating apparent Qp values for the Socorro area from the pulse rise-time equation of Gladwin and Stacey (1974). Apparent Qp for this study is a measure of the attenuation of seismic energy caused by intrinsic absorption and scattering.

A series of criteria were instituted to select the events for the study. First, a cross-correlation coefficient of the P phase of events of 0.700 or above was required so events could be separated into duplicate groups. Criteria were established to exclude events whose initial motion possessed appreciable noise, abnormal shape or broadening due to the source. Pulse broadening resulting from instrument impulse response of the recording systems was removed from the first half cycle of events. From the duplicate groups, average pulse width values satisfying all criteria were obtained. After correction for instrument broadening, apparent Qp values for the raypaths from the general hypocentral locations to the stations were calculated.

Three different procedures for obtaining apparent Qp values were used in this study. First, using a half-space model, whole-path average apparent Qp values were obtained for the Socorro area using three different values for the parameter C in the pulse rise-time equation. Average apparent Qp values using C = 0.773 corresponded best with apparent Qp values obtained by Carpenter (1984) for the Socorro area.

Next, the area was modeled as a low Q, low-velocity layer of varying thickness overlying a relatively high Q, high-velocity half-space. Apparent Qp values for the low-velocity layer (LVL) were obtained from Carpenter (1984) and apparent Qp values for the half-space were calculated using the same three values for C used in the first procedure. As the value of C increased the apparent Qp values of the half-space became increasingly negative implying the values for apparent Qp in the LVL were too small and/or the LVL thicknesses too great such that all the pulse broadening was be attributable to travel through the LVL. The negative values could also suggest the model used was an oversimplification of the actual physical setting.

The third procedure used was a linear inversion of the corrected pulse widths to obtain apparent Qp values for the LVL under each station and for the half-space based upon the same layer over a half-space model. No obvious "best" group of apparent Qp values was evident from the runs of the

inversion program for the different values of C. The scalar R parameter, which gives a measure of the appropriateness of the model, implied the model used was too simplistic a representation of the actual physical setting for the area.

ACKNOWLEDGMENTS

I wish to thank Dr. Allan Sanford for the many valuable discussions during the research of this study and for his critical reviews of this text. I would also like to thank some of my fellow students for their help and support, in particular, Jon Ake, Paul Singer and Kevin King. A very special thanks is extended to Leanna Grossman for her many hours of assistance in the preparation of this manuscript.

TABLE OF CONTENTS

Introduction

Objective and Scope

The attenuative properties of rocks can be extremely important diagnostic tools in unmasking and delineating the composition and physical state of the earth. The attenuation of seismic energy can be caused by a variety of processes such as geometrical spreading, absorption, and the partitioning of energy at acoustic discontinuities. Geometrical spreading is fairly well understood, but the comprehension of the mechanisms of absorption and the affects of scattering are much more difficult to ascertain.

The seismic quality factor, Q, is one of the most common measures of energy lost from an acoustic wave by irreversible conversion to heat. An assortment of loss mechanisms can cause absorption such as friction along cracks, interstitial fluid flow and viscous dissipation, thermoelastic relaxation, as well as energy absorbed in systems undergoing phase changes. By obtaining a measure of Q a quantitative picture of the make up and physical state of the rocks beneath the surface of the earth can be obtained since different geologic materials absorb energy in different amounts and different ways. If the earth is seen as a filter of seismic waves, then the magnitude of Q is a direct measure of some characteristics of just such a filter and can serve as an important parameter in the construction

of synthetic seismograms and ultimately in a more accurate description of the composition and state of the earth.

This study was based upon a pulse propagation technique which employs the width of the first half cycle of a natural acoustic wave to obtain a quantitative measure of Qp. The relationship of the pulse width, or pulse rise time, to Q was introduced by Gladwin and Stacey (1974) and takes the form

$$T = Ts + Ct/Q \qquad (1)$$

where tau is the pulse rise time of the first half cycle of the waveform, tau s the initial rise time at the source due to a finite duration of the source, C a constant generally taken as equal to 0.5, and t the travel time of the wave through a medium of quality factor Q. Generalizing equation (1) over any wavepath of variable Q gives

$$T = Ts + C \int_0^t dt/Q \qquad (2)$$

(Gladwin and Stacey, 1974).

It has been shown that in a given material any consistent operational definition of rise time will yield the rock Q (Kjartannson, 1979; Blair and Spathis, 1982). For this study the rise time is equivalent to the pulse width of the first half cycle of the waveform because a ground velocity rather than ground displacement seismometer was used.

The major objectives of this study were based upon equations (1) and (2). First, average whole path apparent Qp values were to be obtained for the Socorro area. Second, the area was modeled as a low Q, low-velocity layer overlying a relatively high Q, high-velocity half-space. Apparent Qp values for the half-space were obtained from equation (2) using a priori knowledge of apparent Qp values for the low velocity-layer derived from results of Carpenter (1984) for the Socorro area. Finally, using the same layer over a half-space model, average pulse widths obtained for the area were linearly inverted to find apparent Qp values for the layer and for the half-space.

Brief Description of Method

A series of criteria were established to select the events for this study. First, events were separated into duplicate groups based on the cross-correlation of the P phase of events. A cross-correlation coefficient of 0.700 or above was required to confirm duplication of waveforms. This criterion permitted an average pulse width and thus a Qp value along the raypath to be obtained from the general hypocentral location of a swarm to a specific station.

Next, a noise criterion was established to limit the noise superimposed on the first half cycle of any event. An event in which twice the standard deviation from the average amplitude of the 35 data points preceding the onset of the

event exceeded 10% of the maximum amplitude of the first half cycle of that event was considered to possess appreciable noise and thus rejected from this study.

Pulse widths for each event were then graphed using a standardized technique. Any abnormality in the shape of the first half cycle resulted in either a separation of such abnormal waveforms from the "normal" group or rejection altogether of such a waveform. Measurement of the pulse width and associated error of each event was then obtained.

The pulse widths for a duplicate group were plotted against their respective duration magnitudes. Pulse widths below a certain magnitude level were generally found to be independent of magnitude implying that these pulse widths were only dependent on path and instrument response. This allowed tau s in equation (1) and (2), which takes into account the effects of the source, to be set equal to zero. An average pulse width and associated standard deviation was then calculated for the source-free events of the swarm group.

Calibration tests were run on the digital recording systems employed in the study and determinations of the pulse broadening due to instrument impulse response of each system for various filter settings were obtained. This pulse broadening was subtracted from the average measured durations of the first half cycle for each group of events which left a pulse width dependent on path only.

The corrected average pulse widths were employed in equation (1) along with their respective hypocentral distances and average velocities along the raypaths and apparent Qp values were obtained for the Socorro area. Next, the area was modeled as a low Q, low-velocity layer of varying thickness overlying a relatively high Q, high-velocity half-space. Apparent Qp values of the layer were estimated from results taken from Carpenter (1984) and half-space apparent Qp values were obtained for the Socorro area. Finally, the corrected average pulse widths were linearly inverted, based on the same layer over a half-space model, and apparent Qp values were obtained for the layer and for the half-space.

Geology and Geophysics of the Study Area

The setting of this study is the central Rio Grande rift near Socorro, New Mexico. The Rio Grande rift is a series of en-echelon grabens and basins trending roughly north-south and extending from near Leadville, Colorado on the north into northern Mexico in the south (Chapin, 1971). East-west crustal extension has been occurring in the rift for approximately the past 30 million years (Chapin and Seager, 1975). Major physiographic and geologic features of the rift are discussed in Chapin (1971), Chapin and Seager (1975), Sanford et al. (1977), Cordell (1978), and the volume Rio Grande Rift: Tectonics and Magmatism edited by Riecker (1979). Figure 1a shows the major physiographic and

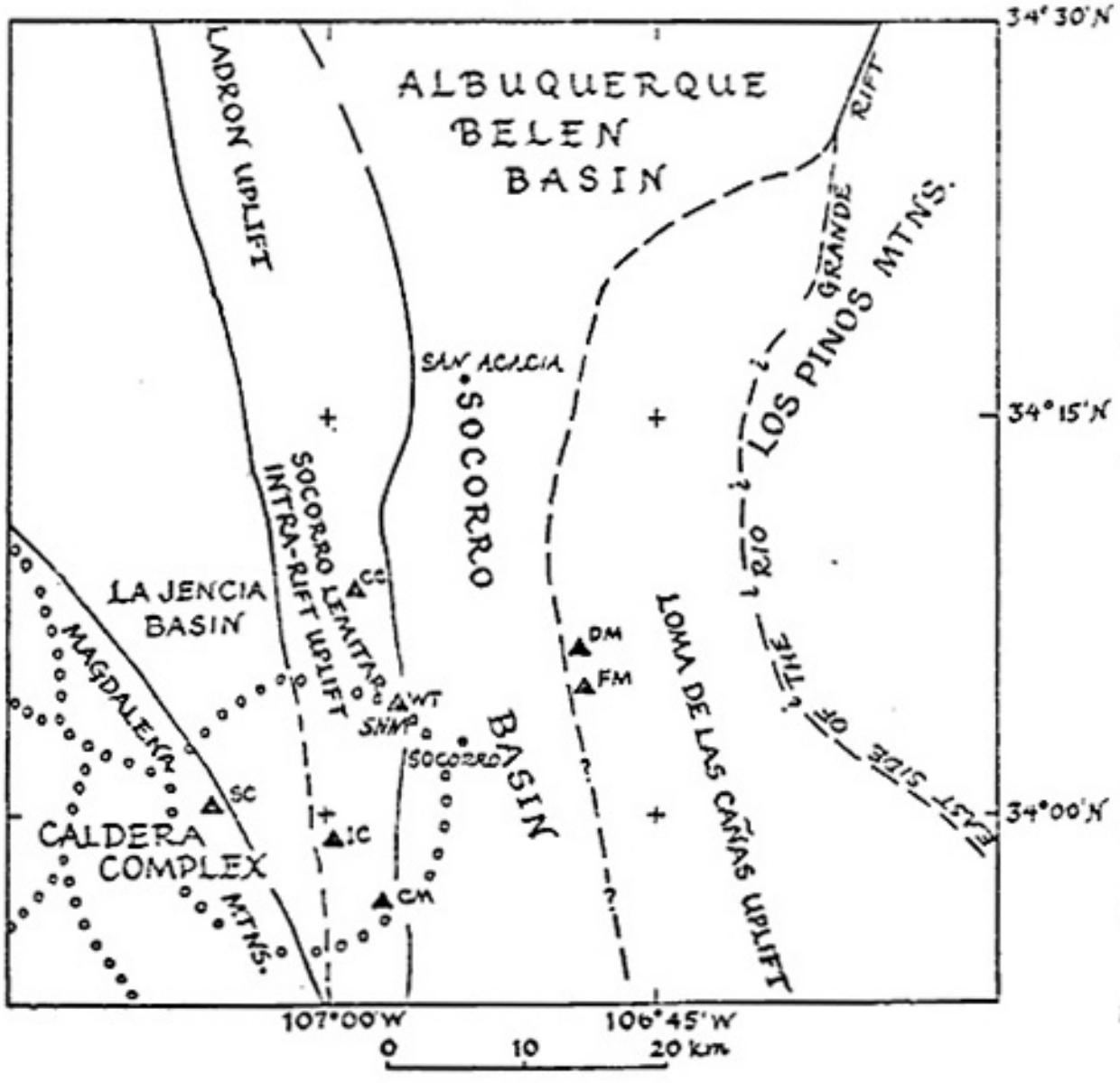

Figure 1a. Major physiographic and geological features near Socorro and the locations of the seismic recording stations (after Rinehart, 1979).

geologic features of the study area along with the locations of the seismic stations which sit on either intrarift horst blocks or on the elevated structural borders of the rift. Figure 1b is a simplified geologic map of the area which also exhibits the seismic stations in the network.

Significant distinguishing features of the rift in the Socorro area include deep alluvial basins (Sanford, 1968; Chapin and Seager, 1975), Quaternary bounding faults trending roughly north-south (Rejas, 1965; Chamberlin, 1980), the intersection of two volcanic lineaments (Chapin et al., 1978), a broad sill-like magma body approximately 19 km deep (Rinehart et al., 1979), an area of positive surface uplift centered north of Socorro (Reilinger et al., 1978), high heat flow (Reiter and Smith, 1977) and high seismicity (Sanford et al., 1979).

Seismicity in the Socorro area historically includes major earthquakes, major to minor swarms and more or less continuous microearthquake activity (Sanford et al., 1979). Most recent shocks are thought to be caused by the injection of magma into the upper crust (Sanford et al., 1977). Microearthquake swarms occurring above the intersection of a transverse shear zone and the mid-crustal magma body (Chapin et al., 1978) as well as in regions of high Poisson's ratio and low velocities (Caravella, 1976; Ward et al., 1981) support this conclusion. Abnormally high heat flows also suggest upper crustal magma injection. Figure 2 shows the

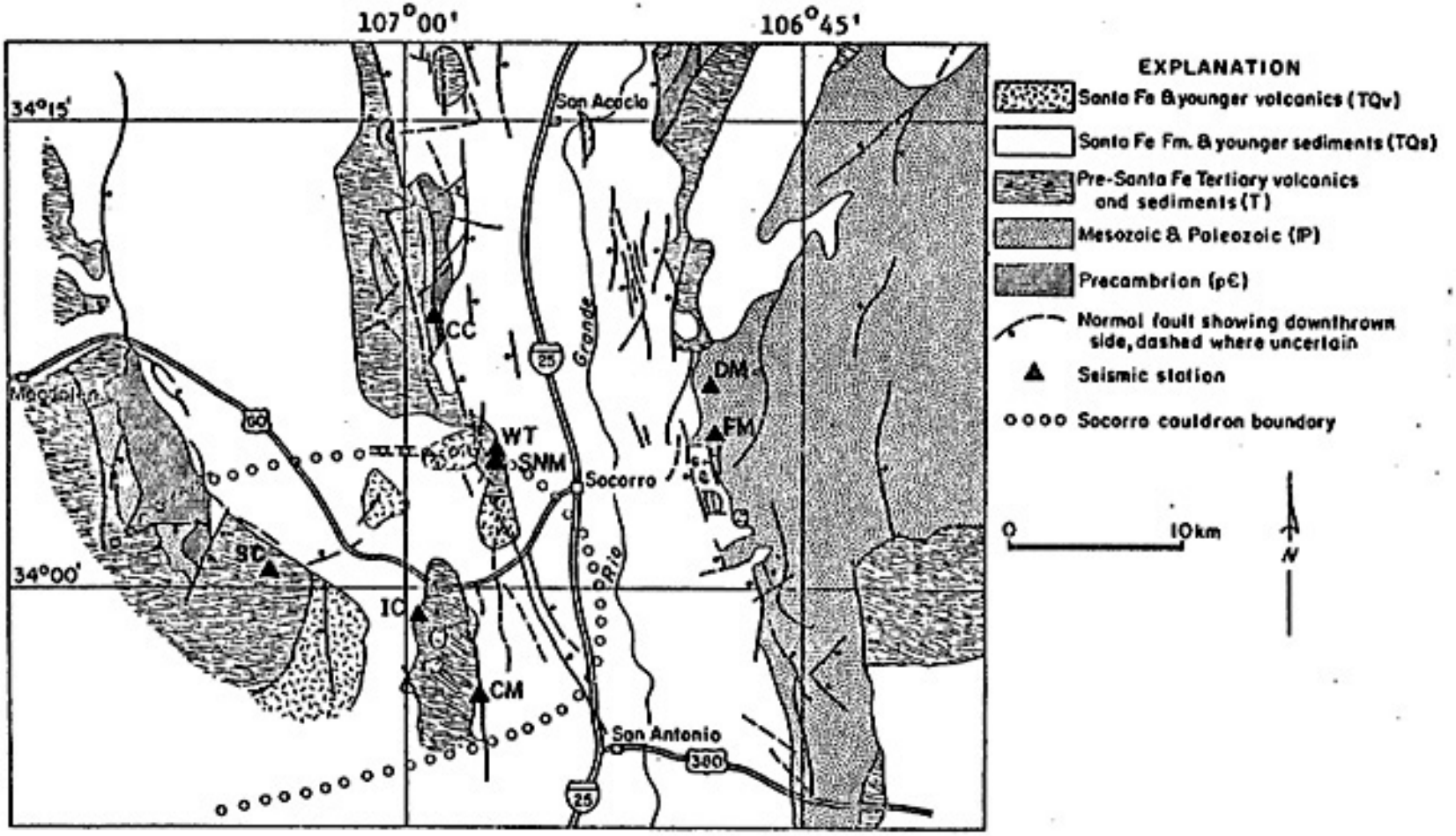

Figure 1b. Simplified geological map of the study area. Stations used for digital recording are marked with triangles (after Sanford et al., 1972).

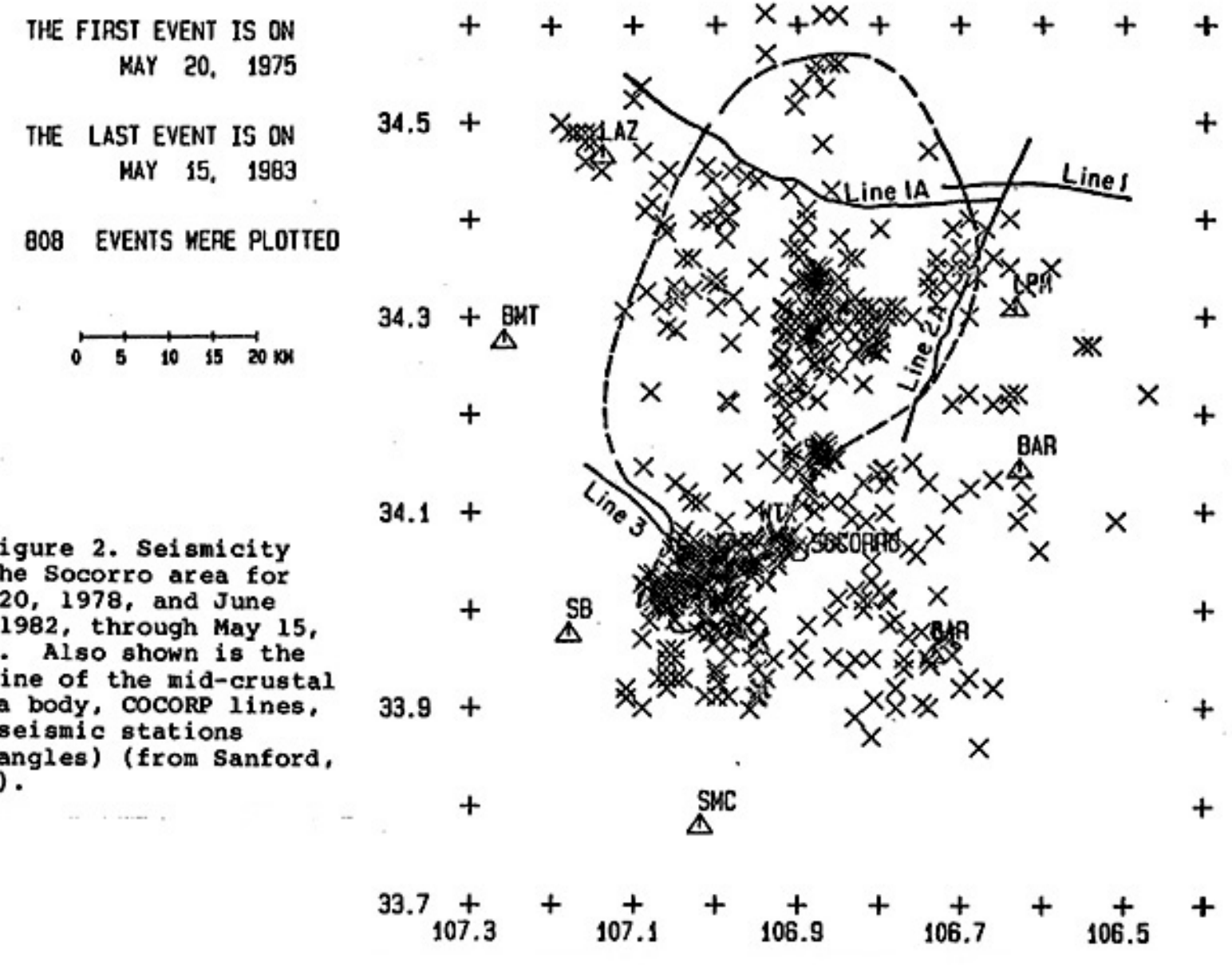

Figure 2. Seismicity of the Socorro area for May 20, 1978, and June 13, 1982, through May 15, 1983. Also shown is the outline of the mid-crustal magma body, COCORP lines, and seismic stations (triangles) (from Sanford, 1983).

seismicity of the Socorro area between 1975 and 1983 as well as an outline of the mid-crustal magma body which was identified in part on the seismic reflection lines obtained by the Consortium for Continental Reflection Profiling (COCORP) north of Socorro.

General History of Q Studies

Measurements of attenuation in the laboratory center around four techniques, each based largely on the range of frequencies used, the actual attenuation parameter desired and the physical conditions applied to the sample. The four methods are (Zener, 1948; Kolsky, 1953; Schreiber et al., 1973):

a.) free vibration,

b.) forced vibration,

c.) wave propagation and

d.) stress-strain curve observations.

In the free vibration method, the amplitude decay of successive cycles of free vibrations in the sample are measured and related to the logarithmic decrement which is in turn related to Q.. (Toksoz and Johnston, 1981). The forced vibration method involves forced longitudinal, flexural, or torsional vibrations of long bars and is based on the principle of standing waves (Toksoz and Johnston, 1981). Stress-strain curve observations deal with measuring the energy lost by loading and unloading a sample at

specific cycles, confined to be substantially different from the resonance frequency of the sample, and computing the area under the stress-strain curves (Gordon and Davis, 1968; McKavanagh and Stacey, 1974; Brennan and Stacey, 1977; Peselnick et al., 1979). Wave propagation methods generally assume an exponential decay of amplitude of the seismic wave with distance or time. It also assumes corrections for intrinsic attenuation can be made. This method is important because the loss parameters are very similar to field attenuation measurements and thereby are directly applicable to field studies (Toksoz and Johnston, 1981). Each of the above methods can be separated into subgroups and a good general description of each can be found in Toksoz and Johnston (1981).

There are several parameters that have been, and some of which are still being, investigated which have an effect on attenuation. A brief discussion on some of the historical work done on the dependence of attenuation on frequency, pressure, wave strain amplitude, temperature and saturation will follow.

Frequency

There have been a number of investigations which have verified the independence of Q on frequency, at least for dry rocks (Birch and Bancroft, 1938; Born, 1941; Peselnick and OuterBridge, 1961; Knopoff, 1964; Pandit and Savage,

1973; Nur and Winkler, 1980; Tittman et al., 1981) over a broad frequency range (10^{-2} to 10^{7} Hz). Under certain conditions, however, some studies have found a frequency dependence of Q. In fluid-saturated rock a flow type mechanism has been found to generate attenuation and create a frequency dependent Q. Born (1941) studied sandstones in the lab containing varying amounts of interstitial water injected into the sample. A Q independent of frequency was found for dry rocks while Q^{-1} showed a linearly increasing dependence on frequency as increasing amounts of water were injected into the sample. (Knopoff, 1964). More recently, Nur and Winkler (1980) found Q^{-1} apparently peaked for saturated limestone at approximately 4 kHz, but was frequency independent for the dry case. As the pressure was increased the attenuation peak increased to higher frequencies. Spencer (1981) also found attenuation peaks at low frequencies. Nur and Winkler (1980) and Spencer (1981) stated that an apparent constant Q might possibly exist over limited frequency bands. They went on to state that a narrow range of flow relaxation times might be adding to the overall attenuation in rock.

Extrapolation from laboratory to field data requires a detailed description of the operative attenuation mechanism and geometry of the pore space involved. Even if such a description was obtainable, the effect is probably not worth considering in this study since the frequency dependent component of attenuation in highly porous and permeable rock

may be negligible at seismic frequencies, even in unconsolidated marine sediments (Hamilton,1972).

Pressure

It is generally agreed that attenuation decreases (Q increases) as pressure increases leveling off to a constant value at high pressures. This result seems to be valid for all frequencies and saturation conditions studied in the lab (Gardner et al., 1964; Klima et al., 1964; Levykin, 1965; Gordon and Davis, 1968; Al-Sinawi, 1968; Walsh et al., 1970; Toksoz et al., 1979; Winkler and Nur, 1979; Johnston and Toksoz, 1980a, among others). The rate of change of attenuation, however, does depend on the physical state of microcracks in the rocks (Toksoz and Johnston, 1981). Dilatancy can originate from high differential stresses resulting in the opening of cracks and thus increased attenuation (Lockner et al., 1977).

Strain Amplitude

For strains $< 10^{-6}$, such as those generally associated with seismic waves, attenuation is independent of strain while strains greater than this show an amplitude dependent behavior possibly associated with some non-linear mechanism such as frictional sliding (Peselnick and Outerbridge, 1961; Gordon and Davis, 1968; Gordon and Rader, 1971; McKavanagh and Stacey, 1974; Brennan and Stacey, 1977; Winkler et

al., 1979; Johnston and Toksoz, 1980b). Cyclic loading tests at low strain amplitudes exhibit elliptical stress-strain loops suggesting a linear mechanism while stains > 10^{-6} show cusped ends to the stress-strain hysteresis loops implying non-linearity (Toksoz and Johnston, 1981).

Temperature

Although little data has been collected on this subject, Volarovich and Gurevich (1957) and Gordon and Davis (1968) have found that Q seems to be generally independent of temperature at low temperatures (relative to the melting temperature of the material). Attenuation was found to increase with temperature above 150 degrees C in quartzite (Gordon and Davis, 1968) possibly due to thermal cracking in the rock (Toksoz and Johnston, 1981). When temperatures approach the boiling temperature of pore fluids, for instance in geothermal areas, thermally activated attenuation mechanisms may play a substantial role (Toksoz and Johnston, 1981). It has been documented that in systems undergoing partial melting attenuation values will also depend significantly on temperature (Spetzler and Anderson, 1968; Stocker and Gordon, 1975).

Saturation

It appears that the degree of saturation and the type of saturate involved (primarily its viscosity) may have a significant effect on attenuation. As mentioned previously, Born (1941) found partial saturation may exhibit a frequency dependence. Other experimental work on partial saturation has indicated little difference between partially and fully saturated states on attenuation (Wyllie et al., 1962; Gardner et al., 1964). However, more recent experiments have shown Q_p for partial saturation can be less than for complete saturation (DeVilbiss-Munoz, 1980). As the degree of partial saturation increases, Q declines significantly, presumably due to a wetting effect of water entering fine cracks, reacting with intergranular material and softening the rock (Johnston et al., 1978). Pressure will reduce the effect of saturation by closing the cracks (Johnston et al., 1978).

Laboratory results on the effect of fluid type (viscosity) on Q indicate that highly viscous fluids (e.g. glycerol) have little effect on attenuation (Johnston et al., 1978). Nur and Simmons (1969a) found that the effect of viscosity is frequency dependent.

Q and Wave Propagation

Fundamental to the propagation of stress waves in real material is the absorption of energy and the resulting change in waveform. The shape of the wave, propagating in a medium of finite Q, will change with distance and time. Observing this effect in the frequency domain, higher frequencies decay more rapidly than low frequencies. When laboratory studies of attenuation were being initiated, an energy loss per cycle that was independent of frequency was observed. At that time there wasn't a linear attenuation theory that could explain this effect. It was advanced that the loss was due to some rate independent frictional mechanism quite like when two surfaces slide past each other (Born, 1941). Collins and Lee (1956) and Knopoff and MacDonald (1958) showed that a simple linear mechanism could not explain this completely flat Q spectrum. Evidence was later observed which implied that the Q spectrum was not in fact exactly flat (Zemanek and Rudnick, 1961; Donato et al., 1962; Usher, 1962) and thus linear mechanisms had already been advanced which possessed Q spectrums at least as flat as those observed (Kolsky, 1956; Lominitz, 1957).

Even though the original motivation for a non-linear mechanism no longer existed and the fact that a realistic prediction of pulse propagation in an attenuative media by a non-linear mechanism was never produced, non-linear friction has been widely assumed to be the dominant mechanism,

especially in crustal rocks (McDonal et al., 1958; Knopoff, 1964; White, 1965; Gordon and Davis, 1968; Lockner et al., 1977; Johnston and Toksoz, 1977).

Ricker (1953,1977) advanced a different approach to attenuation theory. He accounted for absorption by adding a single term to the wave equation. Because of this simplistic approach wavelets based on Ricker's theory have been used regularly in producing synthetic seismograms (Boore et al., 1971; Munasinghe and Farrell, 1973) even though Ricker's theory implies a Q which is strongly frequency dependent and this is a contradiction to almost all experimental observations.

Currently there are basically two approaches to seismic pulse propagation and dispersion in an attenuative solid:

1.) A viscoelastic rheology is assumed and its effect on wave propagation is ascertained (Kolsky, 1953, 1956; Ricker, 1953, 1977). This Kelvin-Voigt model, as it is sometimes referred to, shows a frequency dependence that corresponds exactly to viscous dissipation in fluids and thus viscous damping is probably the mechanism for attenuation in fluids (Knopoff, 1964).

2.) A constant or nearly constant Q (CQ or NCQ) model for the media is assumed and used to find pulse broadening and dispersion effect (Futterman, 1962; Strick, 1967, 1970, 1971; Carpenter, 1966; Fuchs and Muller, 1971; Gladwin and Stacey, 1974; Liu et al., 1976; Kjartannson,

1979).

The constant Q model is probably a better representation for most crustal rocks than the Voigt model and has thereby gained greater acceptance in the past ten years (Johnston and Toksoz, 1981).

This study will deal with a nearly constant Q (NCQ) model based initially on work by Gladwin and Stacey (1974) and extended to a constant Q regime by Kjartannson (1979). In the frequency range of interest (0 - 100 Hz) Q independent of frequency will be assumed. Also, dispersion effects will be considered negligible in this frequency band.

Attenuation in the Socorro Area

The Socorro area is a region of intense fracturing and elevated temperatures. These physical characteristics can have a substantial effect on Q as discussed above. Through geologic mapping, seismicity maps, geochemical analysis and tectonic modeling zones of intense fracturing have been ascertained within the area. Three areas of profound, deep-seated fracturing have been identified and demarcated in the Socorro area by Chapin et al. (1978):

1.) Major N-S trending rift faults.

2.) Cauldron ring fractures.

3.) A transverse shear zone extending from South Canyon in the Magdalena Mountains beneath Socorro Peak and

to the east.

All three areas of fracturing could furnish routes for the ascent of magma (Chapin et al., 1978) which if still molten could diminish apparent Q values for raypaths passing through it. In addition, because of scattering and water saturation effects, fracturing could possibly lead to decreases in Q (Walsh, 1966; Gordon and Davis, 1968; O'Connell and Budiansky, 1977). Meteoric waters have been shown to have circulated as deep as 4 km in an ancient hydrothermal system in the southern Socorro cauldron (Eggleston et al., 1983). Many other parts of the cauldron exhibit permeable volcanic tuffs which formed another ancient geothermal reservoir (Chapin et al.,1978).

Carpenter (1984), using a spectral slope technique, obtained apparent Qs and Qp values for the Socorro area from spectra of microearthquakes. He found apparent Q, which incorporated intrinsic absorption and scattering, increased with event distance for all stations in the digital array and successfully modeled this increase with a laterally varying low Q, low-velocity layer overlying a high Q, high-velocity half-space. The average upper crustal Qs was found to have a value of 535 (2 s.d. range = 374-938) in the central Rio Grande rift. Carpenter (1984) went on to find Q(p)/Q(s) ratios that had an average value of 0.66 +/- 0.08 (1 s.d.) but which varied substantially over the array. Four anomalously low Q(s) regions located southwest of

Socorro were identified, possibly indicating small magmatic intrusions or regions of high fracture density (Carpenter, 1984).

Data

Digital Recording

The data in this study consist of microearthquakes digitally recorded at 100 samples/second at eight field stations in the Socorro network between January, 1977 and November, 1983. A thorough explanation of the digital recording systems used, station locations, digital playback and initial processing of the data can be found in Carpenter (1984). A listing of the duration of the pulse broadening due to the impulse responses for the two recording systems with respect to various filter settings is given in Appendix 1.

Cross-Correlation

Events which appeared to have similar waveforms were cross-correlated to verify that they were indeed originating from the same source area and thus traveled similar, if not identical, paths (See Appendix 2 for results). Duplication of wave forms for events from the same microearthquake swarms over a broad range in amplitudes indicates that the frequency content of the waveforms is not modified by the strength of an event and thus essentially independent of

source.

Since this study deals only with the first half cycle of the seismogram, P wave cross-correlations are more important than full waveform cross-correlations. P phase cross-correlations included only the first 0.6 seconds (60 digital samples) of the waveform to ensure exclusive P phase information. Only those events which showed a P phase maximum correlation coefficient of 0.700 or greater were included in groups for further analysis. Cross-correlation coefficients thus ranged from 0.700 to 0.993 and extended from duration based magnitudes of -2.95 to 1.65. The duplication of waveforms (excluding amplitudes) covering a wide range of magnitudes indicates the waveforms of these events are approximately the impulse response of the path and instrument (Frankel and Kanamori, 1983).

Documentation for direct P phase duplication is presented for events with magnitudes less than 1.2 by Sanford et al. (1983b) and for S waves with magnitudes less than 1.0 by Sanford et al. (1983c). Ake (1984) also found waveform duplication existed over a wide range of magnitudes ($-0.8<M.<1.2$) for a May-July, 1983 swarm group in the Socorro area. A precise determination of where duplication ended was not obtained due to the lack of relatively large magnitude events in the swarm. An amplitude based magnitude scale was used in that study.

The P phase cross-correlations generally, but not exclusively, showed higher average cross-correlations than the full waveform correlation-coefficients. This suggests the latter portion of the wavetrain (i.e. the portion following the P phase) is effected more by multipathing and reverberations than the P phase. For this reason, the first cycle of motion in the P phase for local events, which will travel the minimum time path, will be least effected by multipathing and reverberations. Thus, this generally higher cross correlation coefficient for the P phase with respect to the entire waveform correlation coefficient supports the inferrence that studying the pulse rise time of a wave to obtain information on path, instrument response and source properties of an event will inherently be a "cleaner" technique than studying the entire waveform as required by the commonly used spectral ratios method.

Pulse Width

The pulse rise time defined by Gladwin and Stacey (1974) as "the interval between the intersections of the steepest rise of a pulse onset with the zero level and the peak pulse amplitude" is equivalent to the pulse width measurement used in this study. Gladwin and Stacey (1974) based their definition on measurements recorded by displacement transducers while this study employed velocity transducers as recording instruments. Thus the pulse width, defined here as the time between the onset of the wave and

its first zero crossing, is synonymous with Gladwin and Stacey's pulse rise time.

Measurements of pulse widths for the events of this study consisted of a systematic process of normalizing the digital amplitudes of the first half cycle of an event's waveform to the maximum digital amplitude of that half cycle. Normalized amplitudes were graphed with respect to time, the onset and first zero crossing were picked and associated errors of each determined. Although a degree of subjectivity was inherent to each measurement,especially in the drawing of the shape of the first half cycle and thus the onset and zero crossing, any such subjectivity was minimized (or at least decreased) by this systematic approach.

After the digital amplitudes were normalized and each normalized value was plotted, a smooth curve was drawn through the points (figure 3 shows an example of a pulse width measurement for this study). The zero level was established as the average normalized amplitude of the 35 points preceding the onset of the event. Almost all events exhibited a gentle roll off at the beginning of the wave which comprised the majority of the uncertainty in the onset. In general, the uncertainty of onset was taken as the interval between (1) the intersection of the zero amplitude level with a line drawn tangent to the point of roll off exhibiting the highest curvature and (2) the

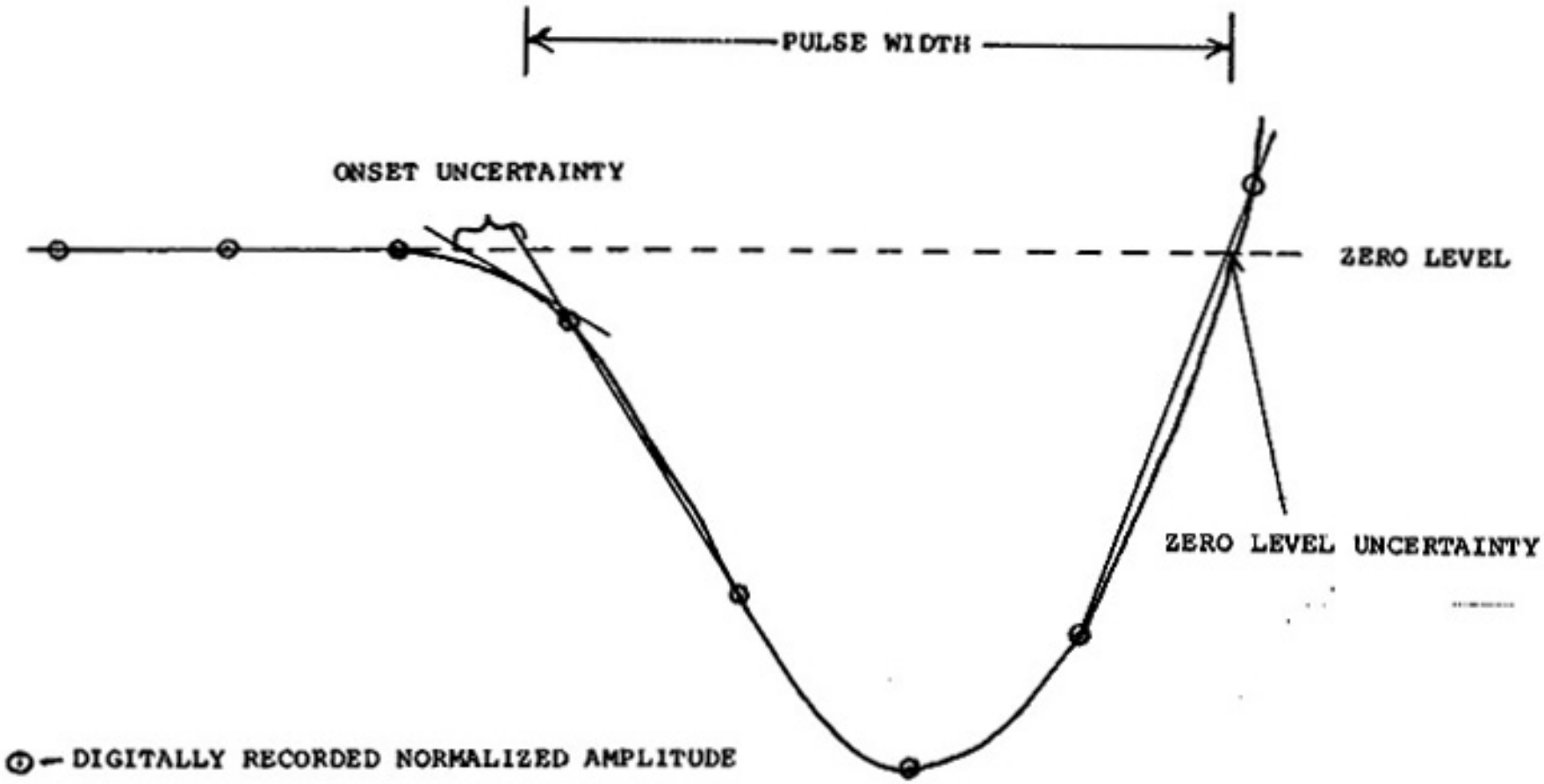

Figure 3. An example of a pulse width measurement displaying the uncertainty of the onset and first zero crossing of the first half cycle of an event.

intersection of the zero amplitude level with a line through the steepest rise of the onset of the pulse. The critical area with respect to the onset was the segment of the roll off of the onset displaying the highest curvature. In an attempt to minimize the error of onset, the point of inflection of this segment was taken, when possible, as an actual recorded sample point, thus giving more weight to the data than to the interpolated segments between data points.

The uncertainty associated with the first zero crossing generally contributed less to the overall uncertainty than did the uncertainty of the onset. The first zero crossing uncertainty was taken to be the interval between (1) the intersection of the zero amplitude level with a line connecting the last point of the first half cycle with the first point after the zero crossing and (2) the intersection of the zero amplitude level with a smooth curve connecting these same two data points. The ambiguity is introduced in drawing the smooth curve in that several different curves may be drawn through the same set of points. The difference in shape of the various possible curves, however, was slight and thus was assumed to have a negligible effect on the measurements.

A noise criterion was set for each pulse width measurement. If the ratio of twice the standard deviation of the average amplitude of 35 points preceding the onset of the pulse to the maximum amplitude of the first half cycle

exceeded 0.10 (i.e. 10% of maximum amplitude), the event was rejected. This was to ensure that significant noise was not superimposed onto the pulse width. Only those events which met the cross-correlation and noise criteria were used in the study.

Source Effects

In most pulse propagation studies it is necessary to remove the source spectrum from the observed spectrum if dependable Q values are to be obtained. In the pulse rise time technique of Gladwin and Stacey (1974), the source effects are taken into account with just one parameter, tau s, which is the initial rise time at the source due to finite duration of the source. There has been some controversy over the simplicity of Gladwin and Stacey's model. In particular, Blair and Spathis (1982), working in a massive silicia dolomite region in Queensland, Australia and using two different non-impulsive sources concluded that the values of tau s were highly dependent upon the high frequency components of the source. Therefore it is possible to have two different sources result in the same value for tau s yet differ in spectral content, especially in the low frequency range. When propagated through an attenuative material, the two sources could give different values of pulse width (rise time). They infer that the use of tau s to correct for the source is an oversimplification of the real processes at the source. Blair and Spathis

(1982) do state, however, that the rise time equation is strictly valid if we have an impulsive source (i.e. tau s = 0). Assuming the source model of Brune (1970) is applicable, this suggests that microearthquakes having impulsive sources are composed of source spectra whose corner frequencies fall above the associated path attenuation curves and thus the source functions are "delta-like". These waveforms will therefore contain information pertaining only to the path and instrument responses of the system. Ake (1984) gives a brief but concise discussion of this effect. Sanford et al. (1983b), studying P phase duplication from swarms between 1977 to 1983 spanning a magnitude scale of 0.6 to 1.2, also concluded this source independent implication. The events used in this study will be assumed to have a flat source spectrum (i.e. tau s = 0).

Magnitudes

In order to establish that the events used in this study are source independent, it was necessary to look at the dependence of the pulse width on magnitude. All magnitudes calculated in this study were found using a duration based magnitude scale derived by Los Alamos National Laboratory (LANL) for northern New Mexico (Newton et al., 1976). Ake et al. (1983) found that the LANL formula

$$M(d) = 2.79 \log(tau) - 3.63, \qquad (3)$$

where tau is the measured signal duration in seconds, is also appropriate for earthquakes occurring in central New Mexico. The accuracy of this equation is questionable for events with magnitudes less than 0.0 because this magnitude relationship was derived using data between magnitudes one and four. However, for this study it will be assumed that any uncertainty associated with the possible inaccuracy of this duration based magnitude relation will not effect the source information cutoff level since only relative magnitude effects will be considered.

Durations were measured from analog records recorded at stations within the Socorro array. For events in which no analog record existed, duration based magnitudes were obtained by using an empirical relation between duration and maximum amplitudes of digitally recorded events.

Duration based magnitudes for all events were plotted against values of pulse width for individual groups recorded at particular stations. It was anticipated that at higher magnitudes the pulse widths would increase with increasing magnitude. Below a certain magnitude, however, no such dependency was expected because pulse broadening due to the source would be negligible compared to the effects of attenuation and instrumentation. Therefore, the assumption of a delta-like impulsive source (Blair and Spathis, 1982) is applicable. This result would be consistent with the

conclusion drawn previously that the frequency content of the P waveform was not influenced by event strength. For the remainder of this study, any reference to magnitudes will be assumed to be referring to duration magnitudes unless explicitly stated otherwise.

The events selected and separated into groups for this study met the following criteria:

1) A cross correlation coefficient for the P-phase of 0.700 or above to confirm the duplication of waveforms.

2) Twice the standard deviation of the average amplitude of the 35 data points preceding the onset of an event must be less than 10% of the maximum amplitude of the first half cycle of the events so that appreciable noise is not superimposed onto the pulse.

3) Abnormality in the shape of the first half-cycle of an event resulted in either its rejection or separation into a group of events of similar anomalous pulse shape.

4) Any events which exhibited clipped waveforms were rejected because some uncertainty existed as to their duration magnitudes and waveforms.

5) Magnitude cutoff levels for each station were imposed and are listed below. Events with magnitudes greater than these levels were considered to contain source propagation effects and thus were rejected:

a) WT - 0.00

b) SC - 0.00

c) IC - 0.60

d) CC - 0.65

e) DM - 0.00

f) CM - 0.30

g) FM - 0.00

h) SNM - 0.00

6) Any unusual wave character preceding the onset of an event resulted in rejection of the event.

The groups which exhibited an independence of pulse width with magnitude are displayed in figures 4 through 23 and listed in Appendix 3. Groups of events which met all the criteria set forth above but exhibited anomalous characteristics either for individual events or as a group are discussed below.

Group 77-13

This two event group, shown in figure 24, is questionable, at best, in assuming the pulse width shows no dependence on magnitude. The limits of the uncertainties of the pulse widths just overlap. It was decided to keep this group because of the extremely high correlation coefficient between P phases (0.965) and the lack of any other data for station CM. Hence, the reliability of information derived from this group is open to doubt and any conclusions drawn

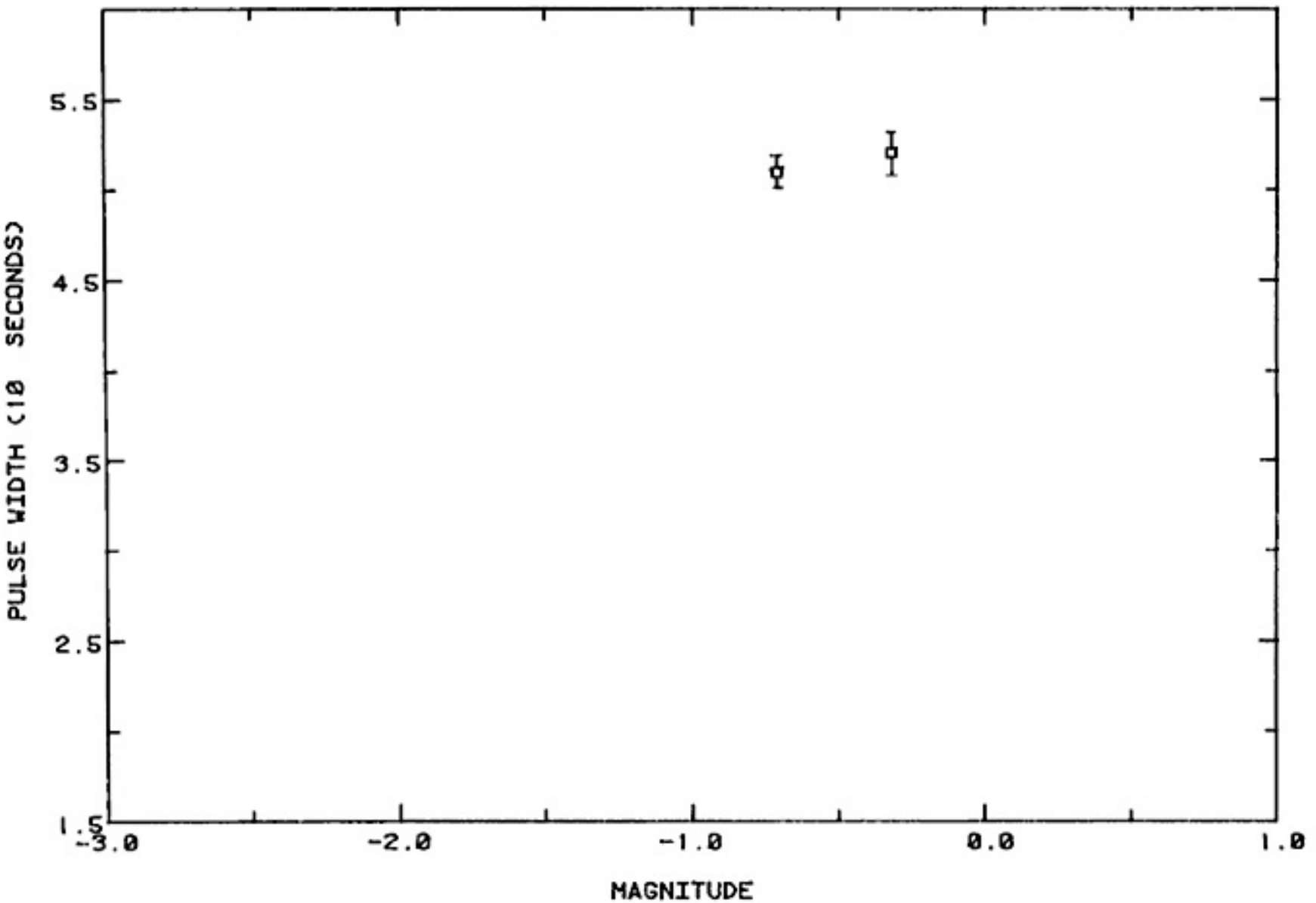

Figure 10. Pulse width verses magnitude for group 77-17. The calculated average pulse width for the group is 0.0515 +/- 0.0006 seconds (1 s.d.).

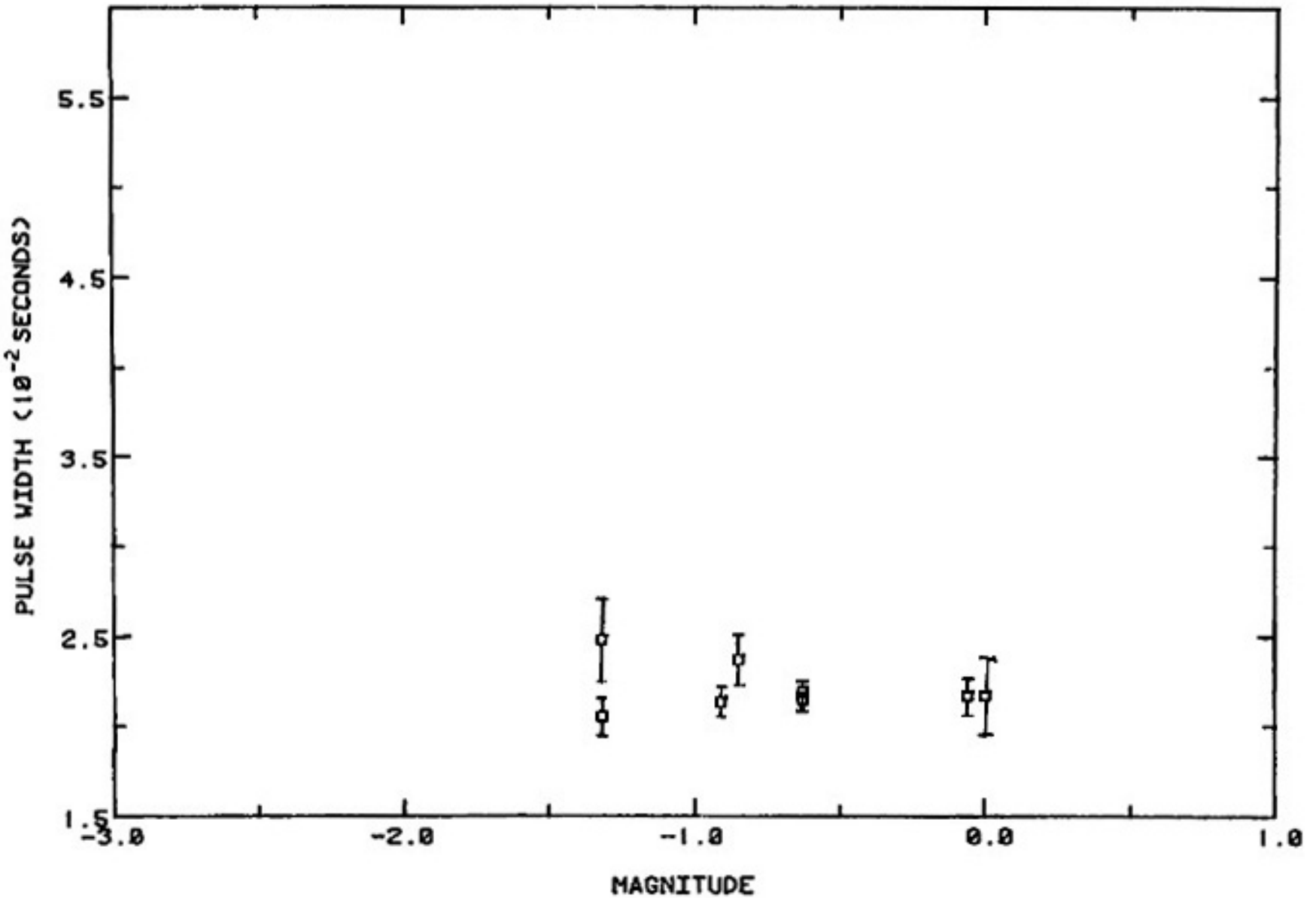

Figure 4. Pulse width verses magnitude for group 77-2. The calculated average pulse width for the group is 0.0221 +/- 0.0013 seconds (1 s.d.).

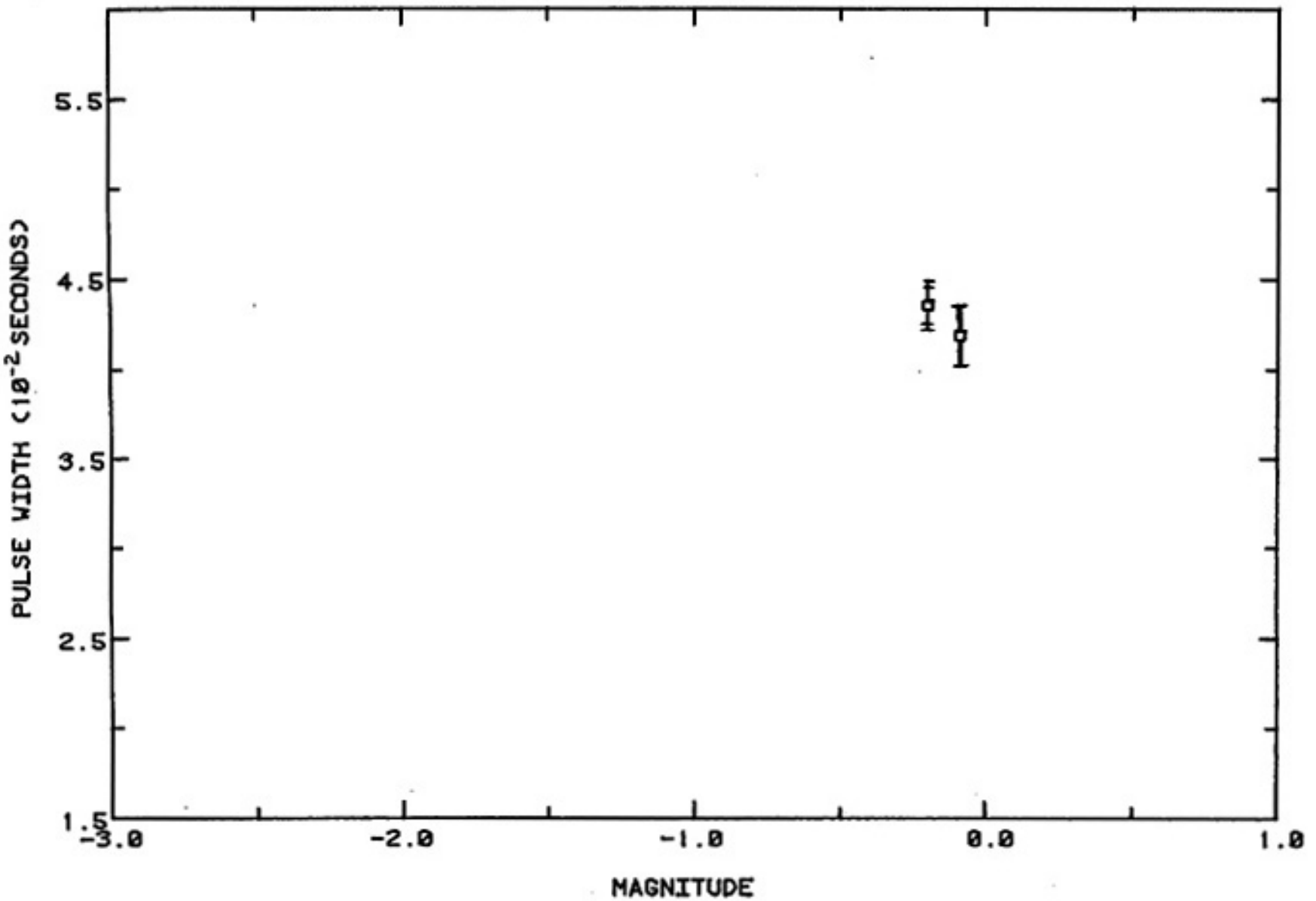

Figure 5. Pulse width verses magnitude for group 77-3. The calculated average pulse width for the group is 0.0429 +/- 0.0008 seconds (1 s.d.).

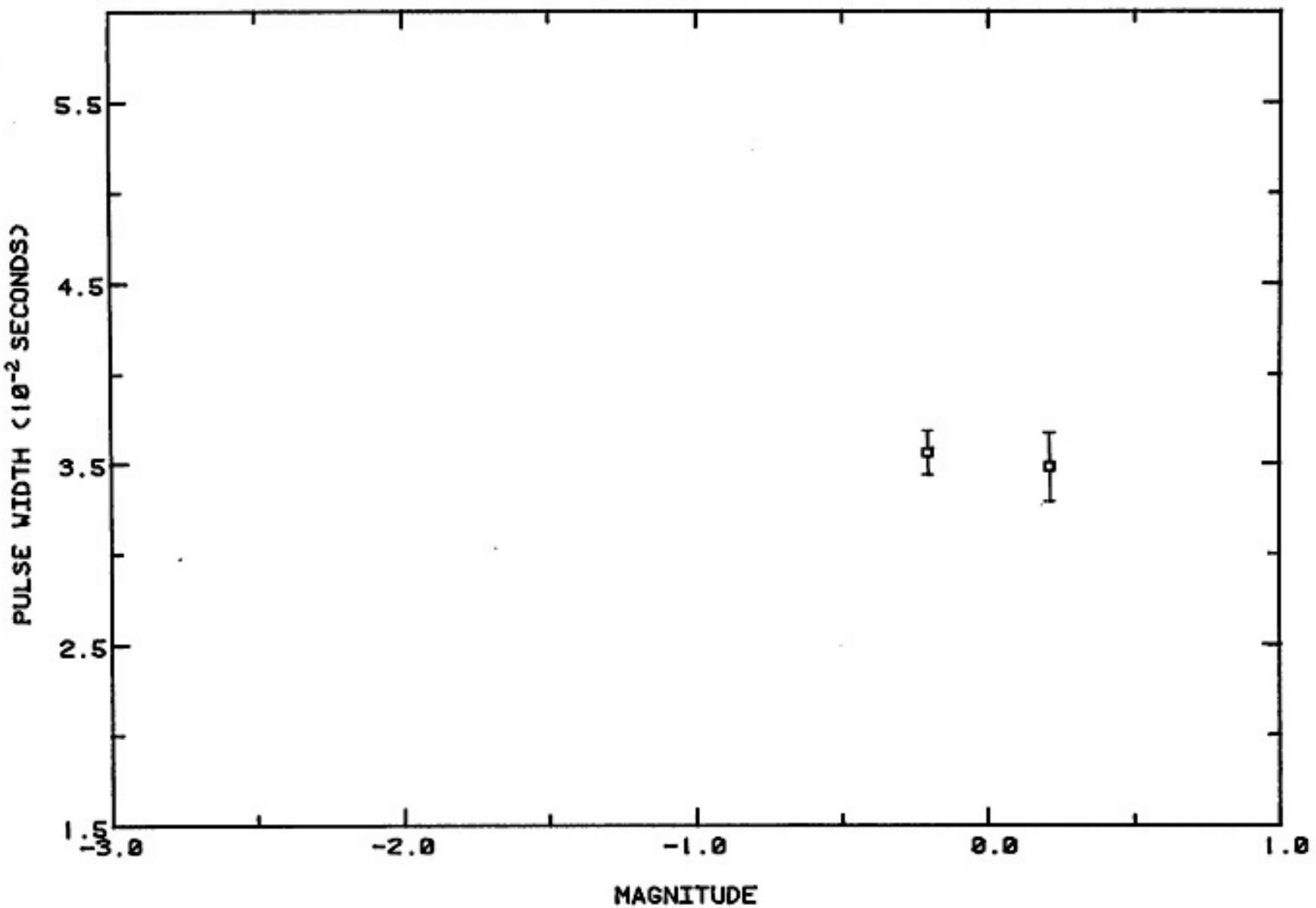

Figure 6. Pulse width verses magnitude for group 77-4. The calculated average pulse width for the group is 0.0352 +/- 0.0004 seconds (1 s.d.).

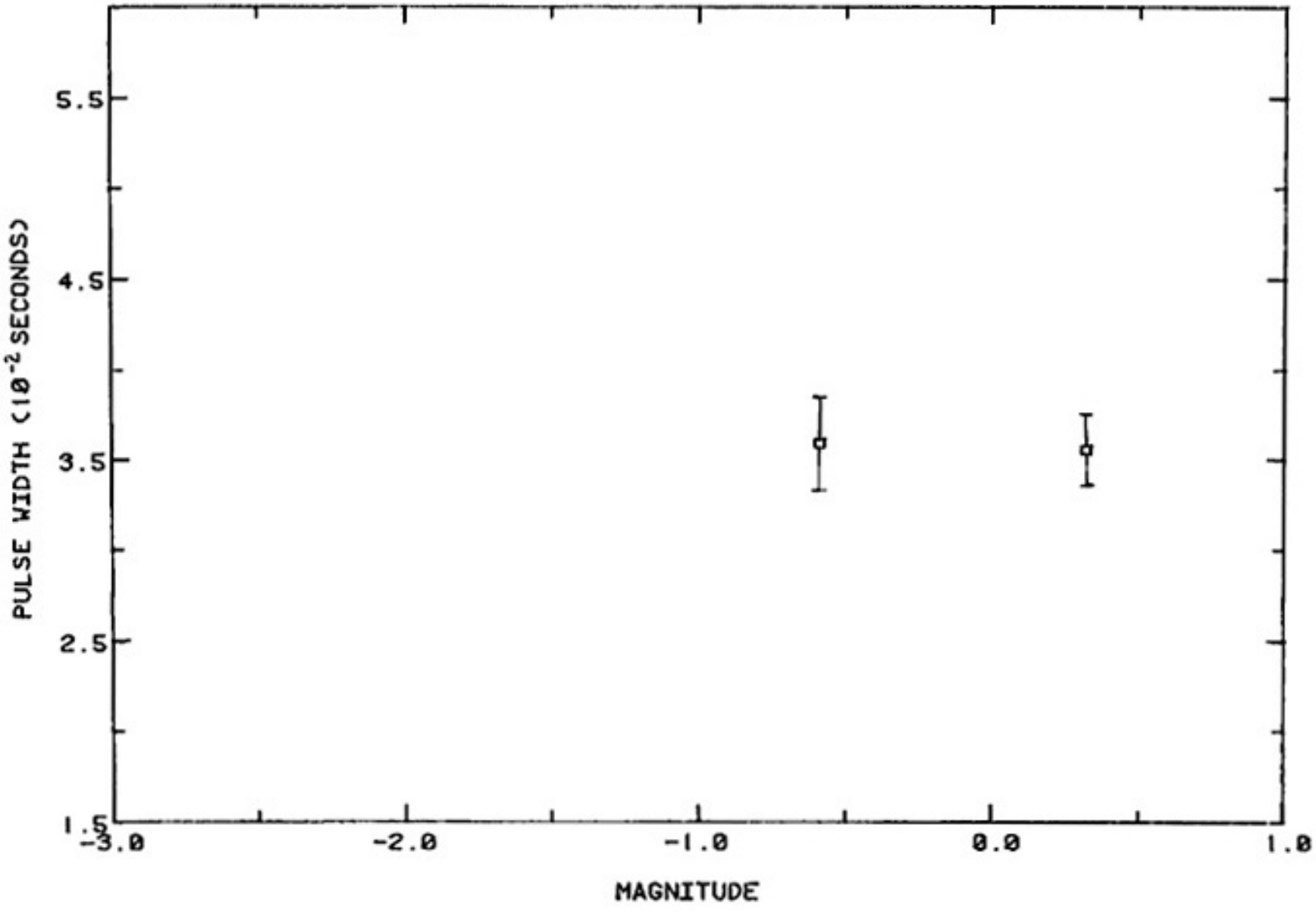

Figure 7. Pulse width verses magnitude for group 77-5. The calculated average pulse width for the group is 0.0357 +/- 0.0002 seconds (1 s.d.).

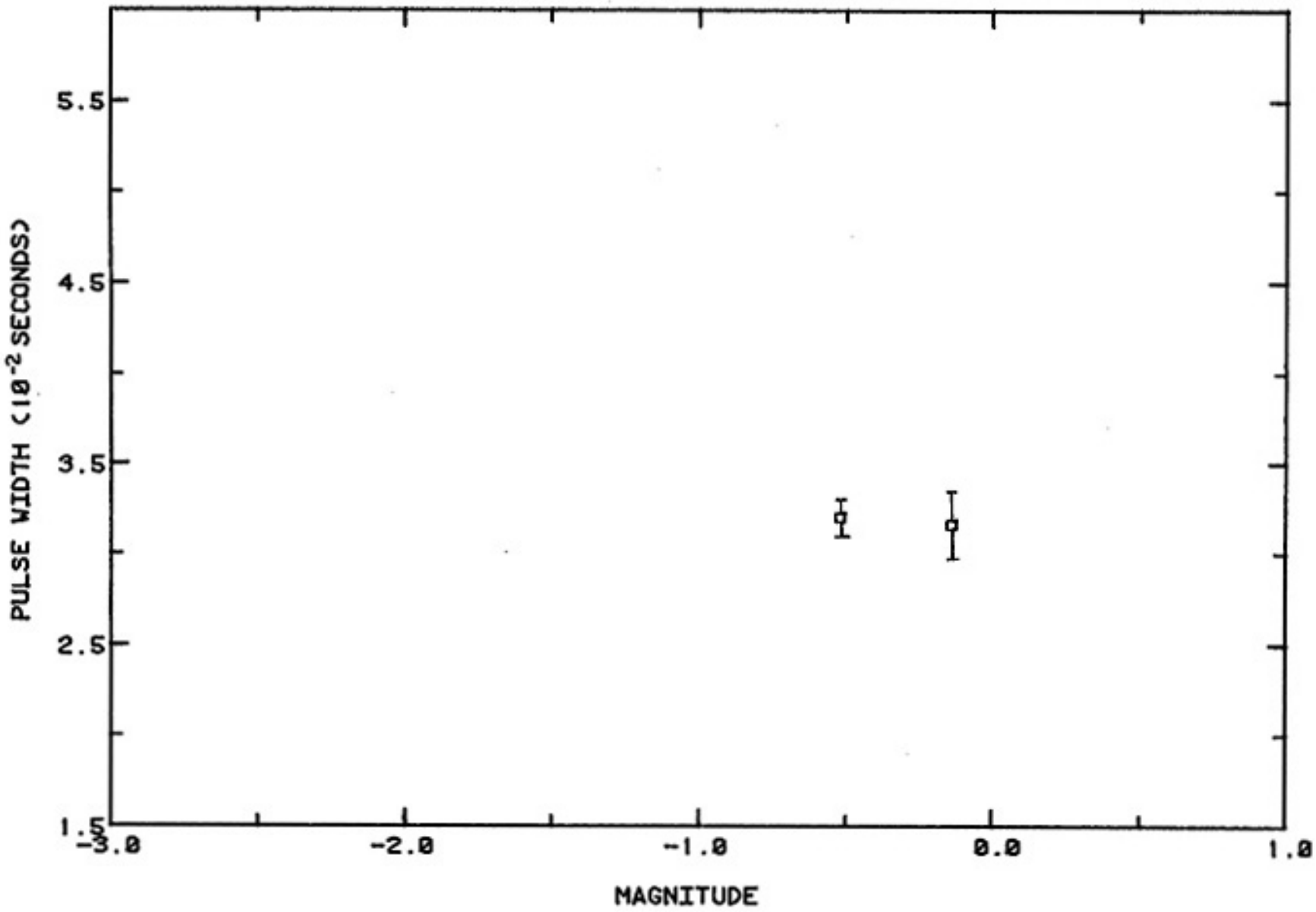

Figure 9. Pulse width verses magnitude for group 77-16. The calculated average pulse width for the group is 0.0318 +/- 0.0002 seconds (1 s.d.).

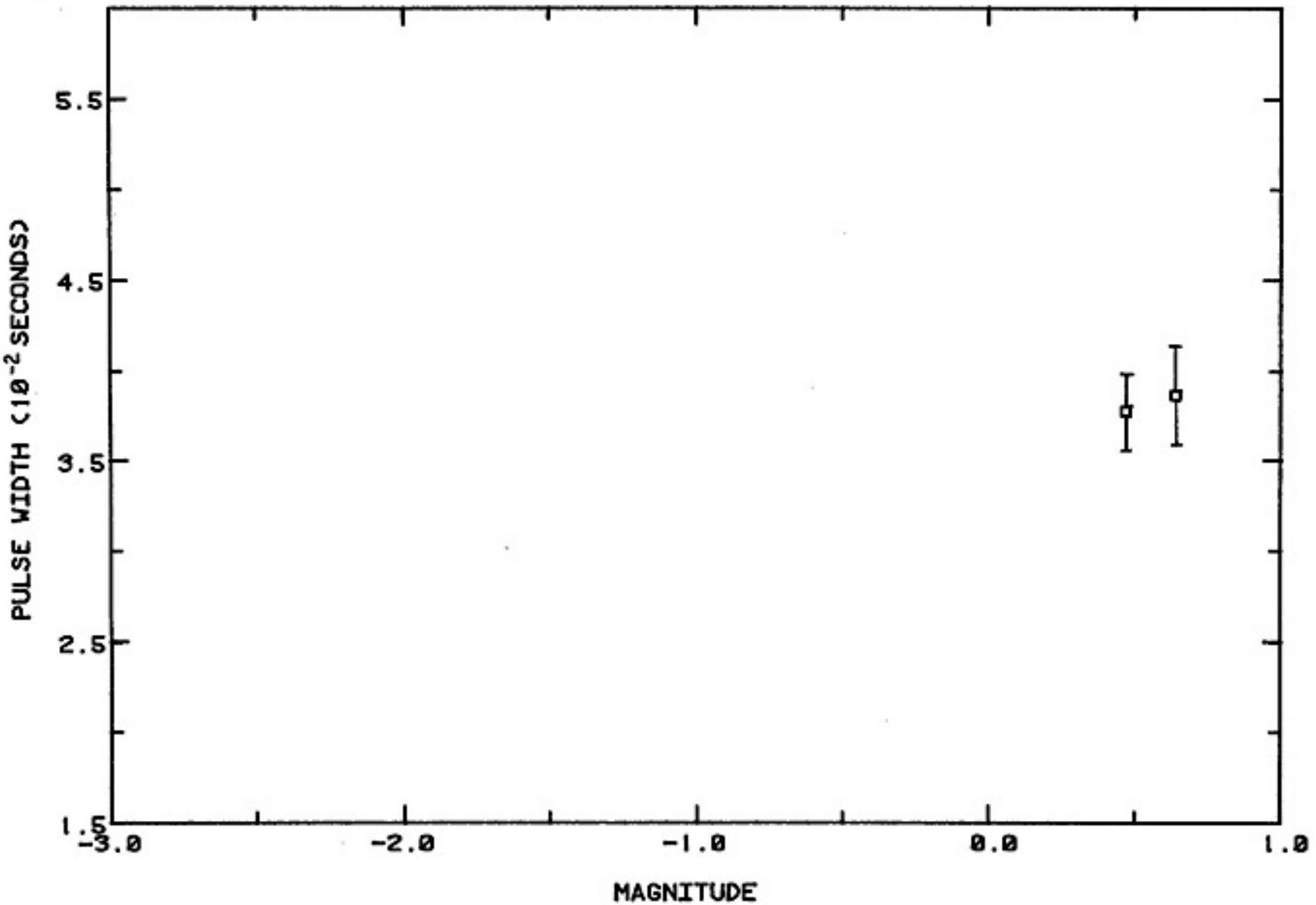

Figure 8. Pulse width verses magnitude for group 77-15. The calculated average pulse width for the group is 0.0382 +/- 0.0005 seconds (1 s.d.).

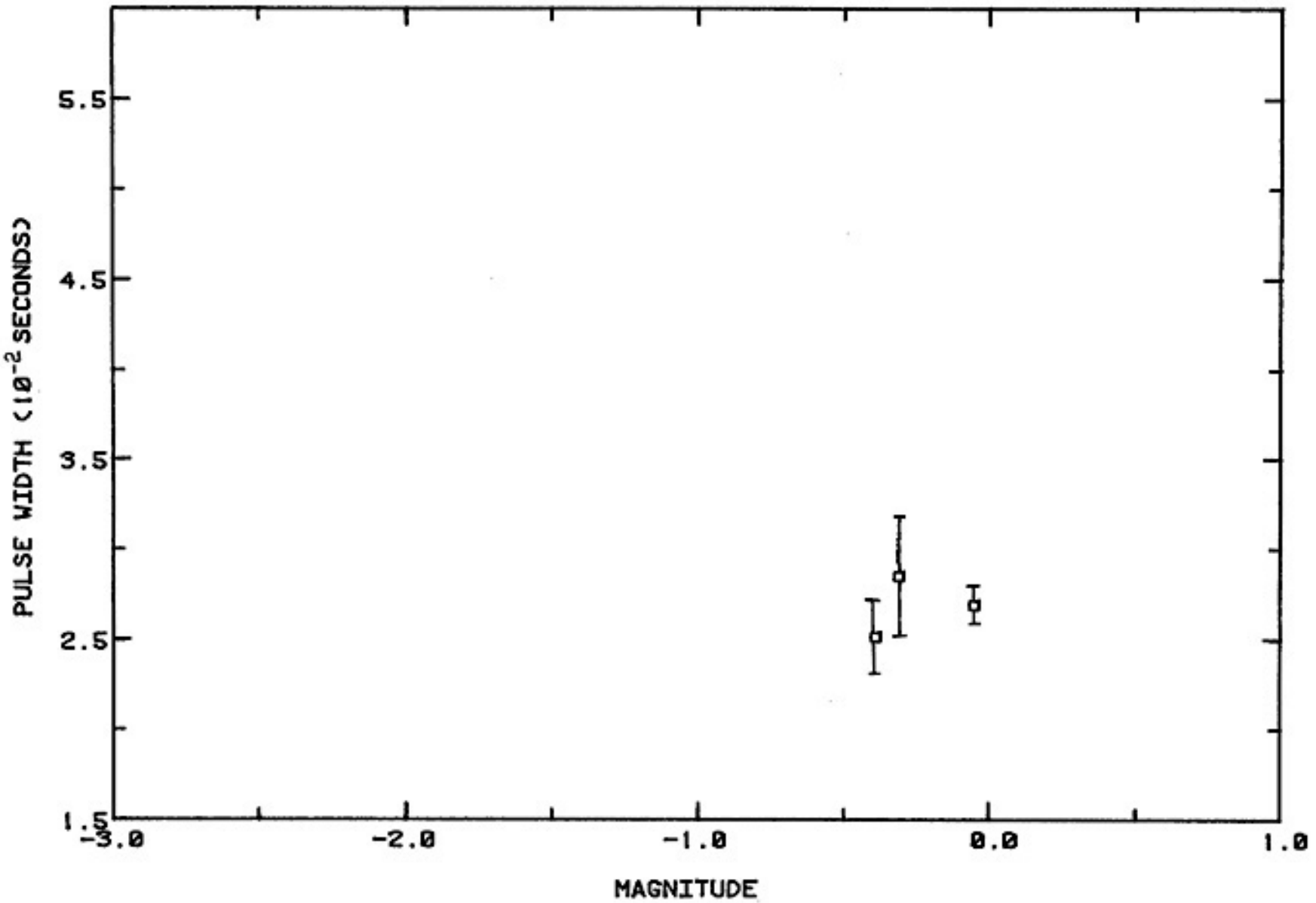

Figure 11. Pulse width verses magnitude for group 77-18. The calculated average pulse width for the group is 0.0268 +/- 0.0014 seconds (1 s.d.).

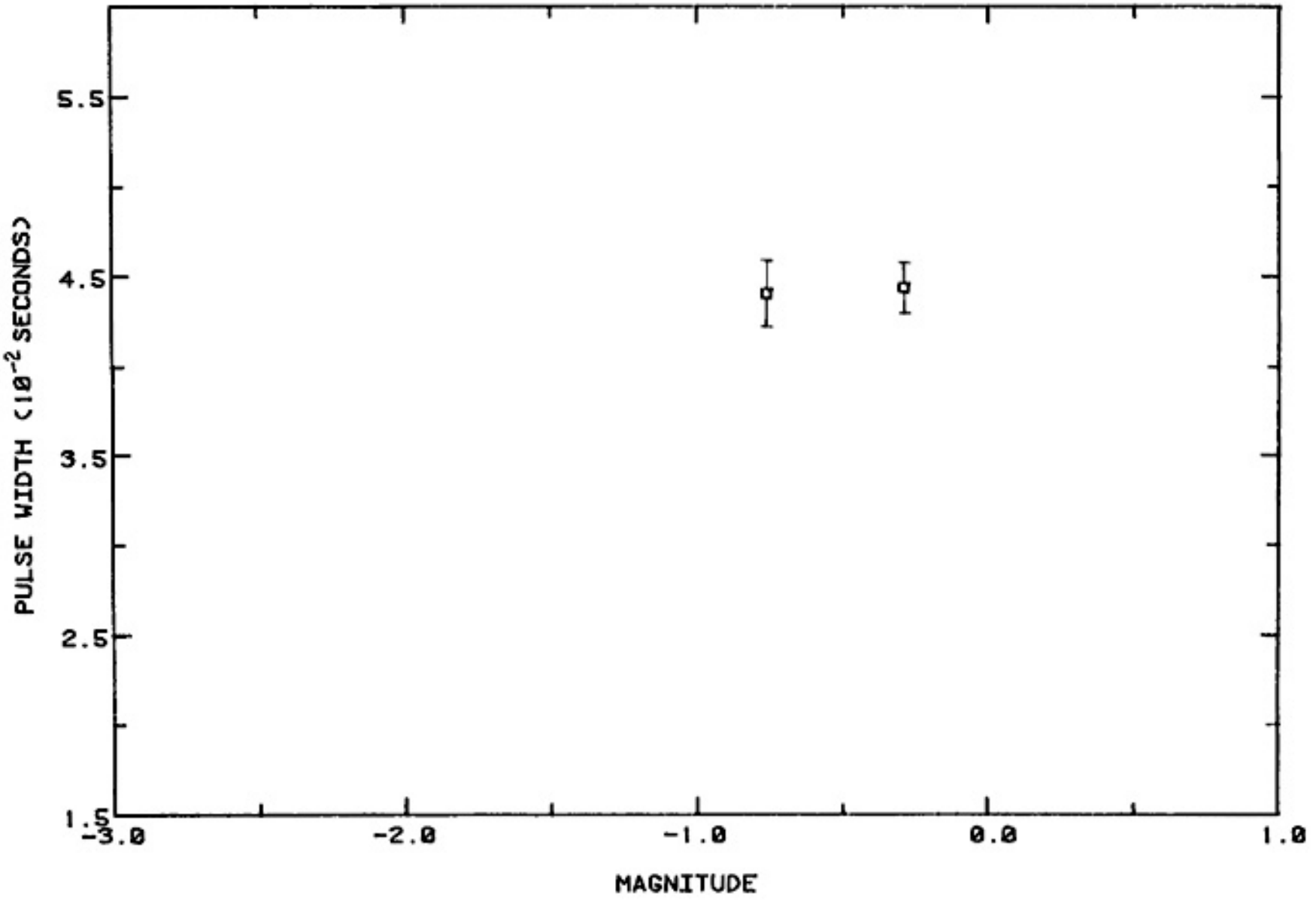

Figure 12. Pulse width verses magnitude for group 81-4. The calculated average pulse width for the group is 0.0442 +/- 0.0002 seconds (1 s.d.).

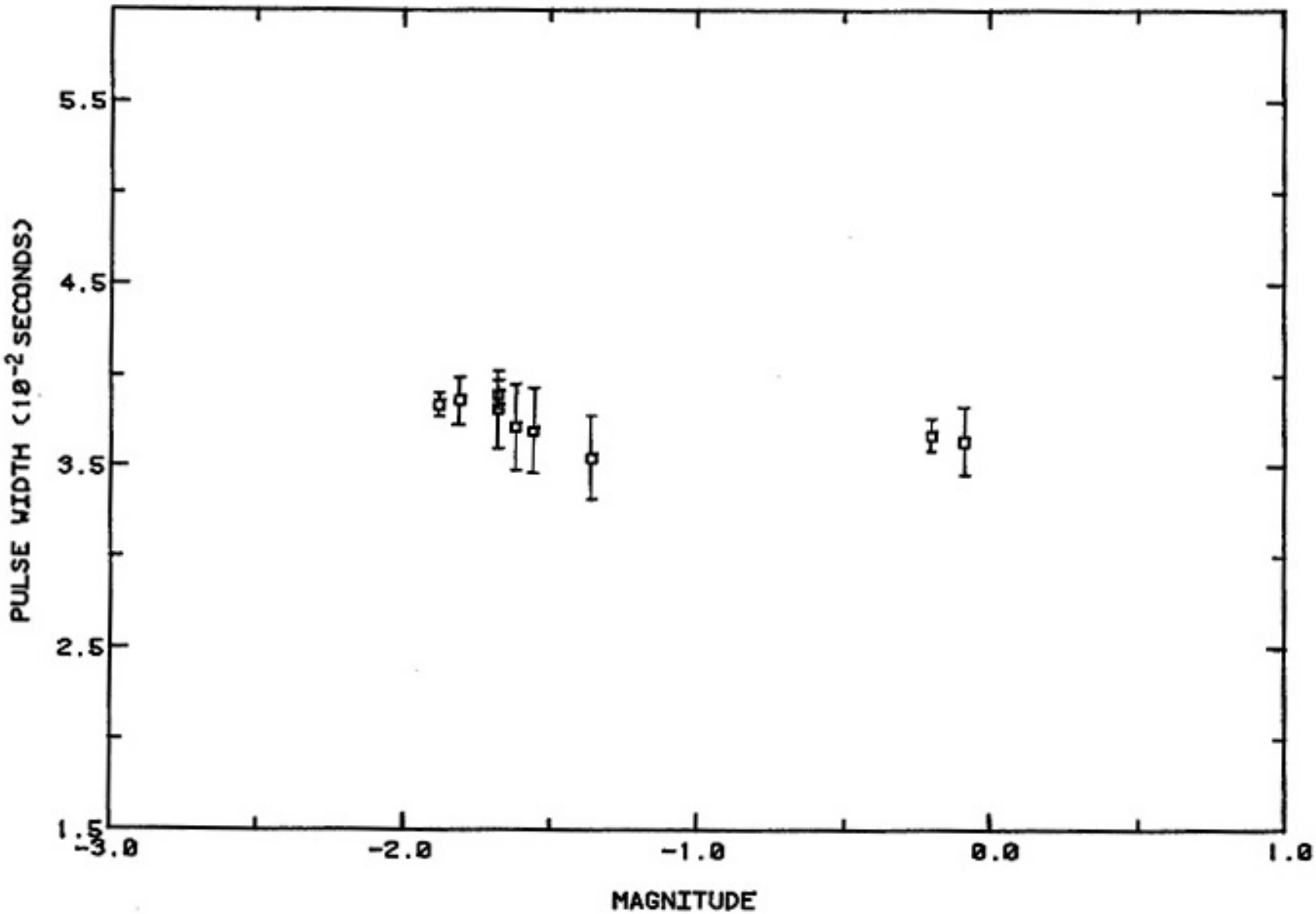

Figure 13. Pulse width verses magnitude for group 83-1. The calculated average pulse width for the group is 0.0374 +/- 0.0011 seconds (1 s.d.).

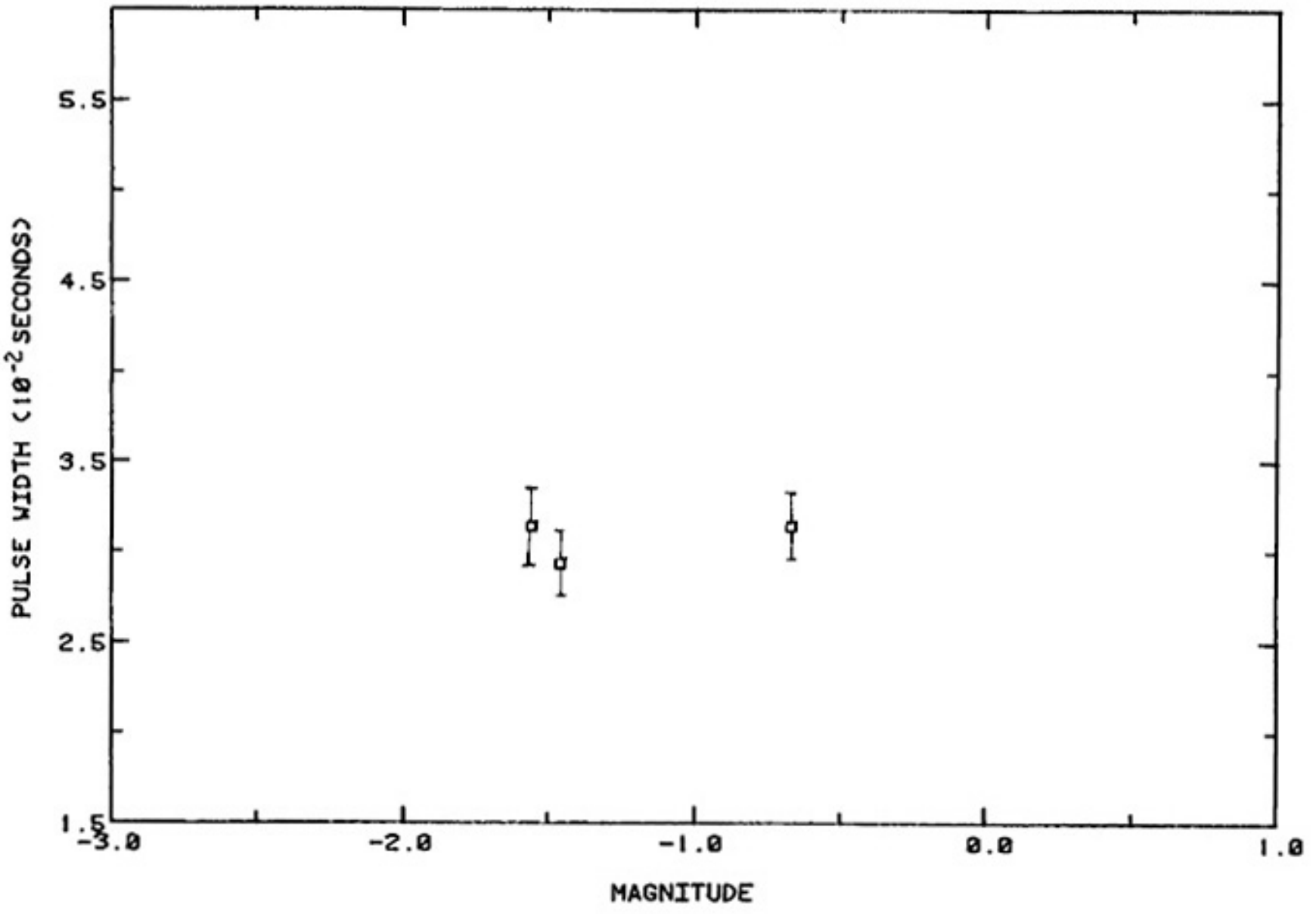

Figure 14. Pulse width verses magnitude for group 83-3. The calculated average pulse width for the group is 0.0314 +/- 0.0000 seconds (1 s.d.).

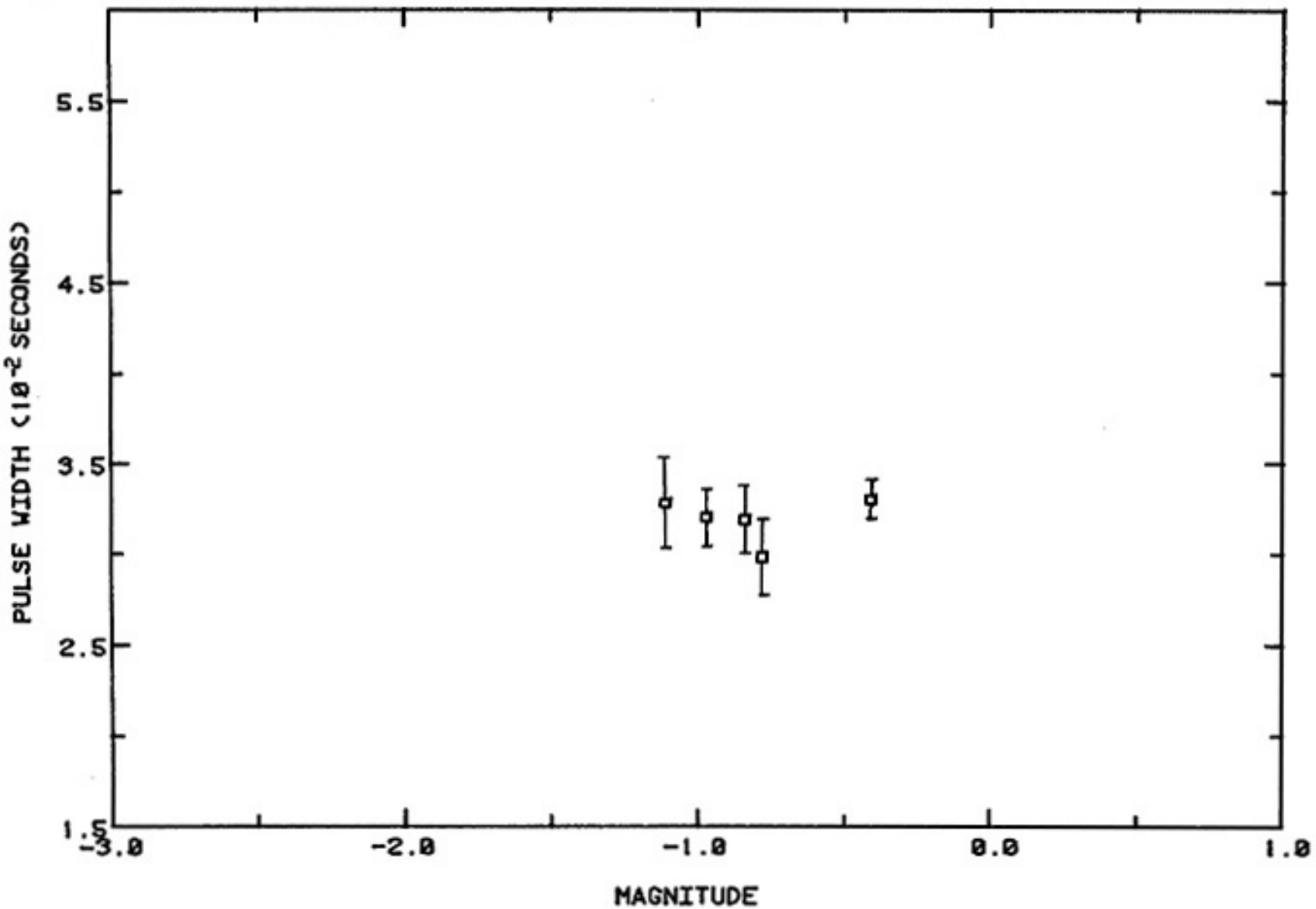

Figure 15. Pulse width verses magnitude for group 83-5. The calculated average pulse width for the group is 0.0319 +/- 0.0011 seconds (1 s.d.).

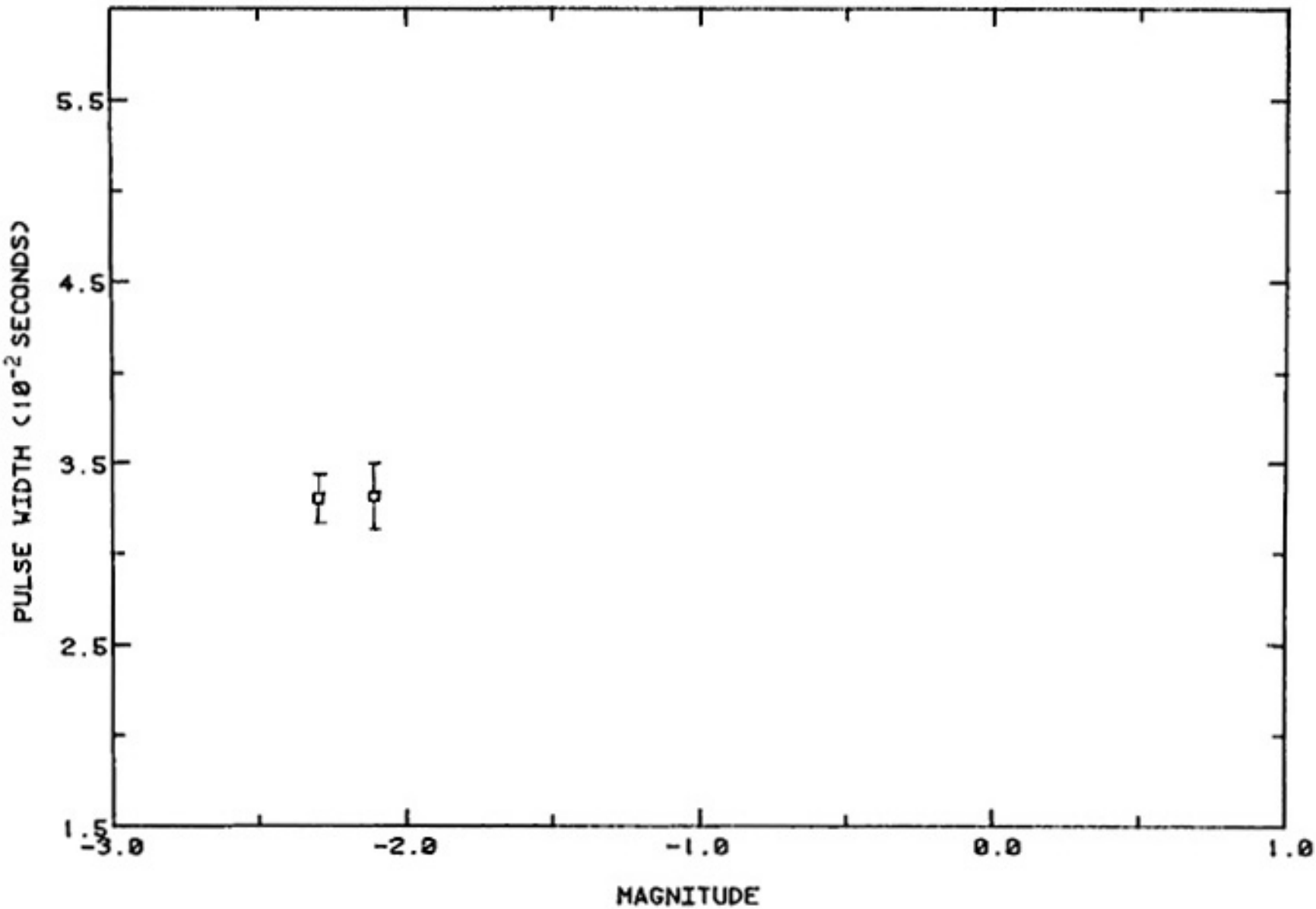

Figure 16. Pulse width verses magnitude for group 83-6. The calculated average pulse width for the group is 0.0331 +/- 0.0001 seconds (1 s.d.).

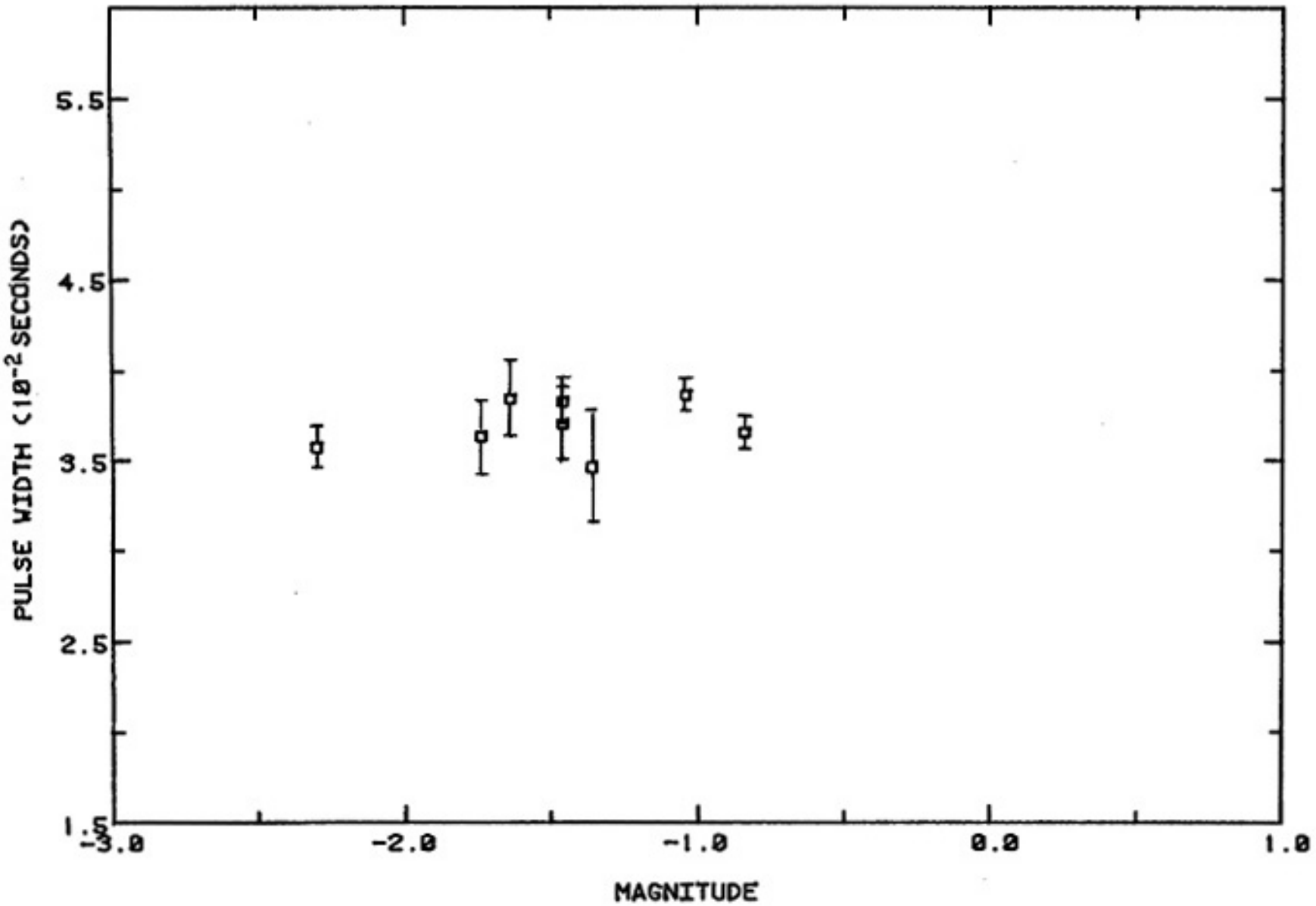

Figure 17. Pulse width verses magnitude for group 83-8a. The calculated average pulse width for the group is 0.0369 +/- 0.0013 seconds (1 s.d.).

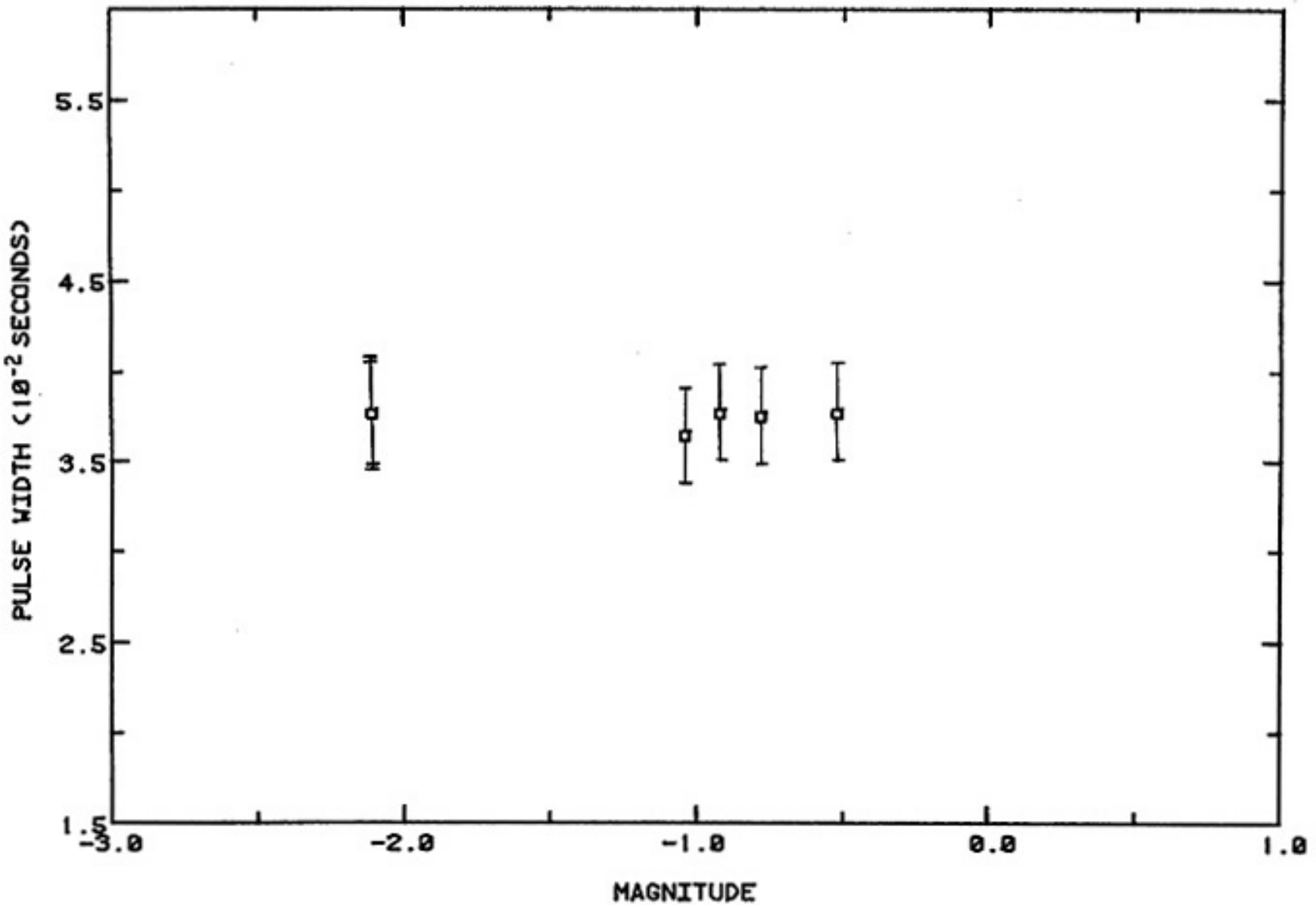

Figure 18. Pulse width verses magnitude for group 83-8b. The calculated average pulse width for the group is 0.0374 +/- 0.0004 seconds (1 s.d.).

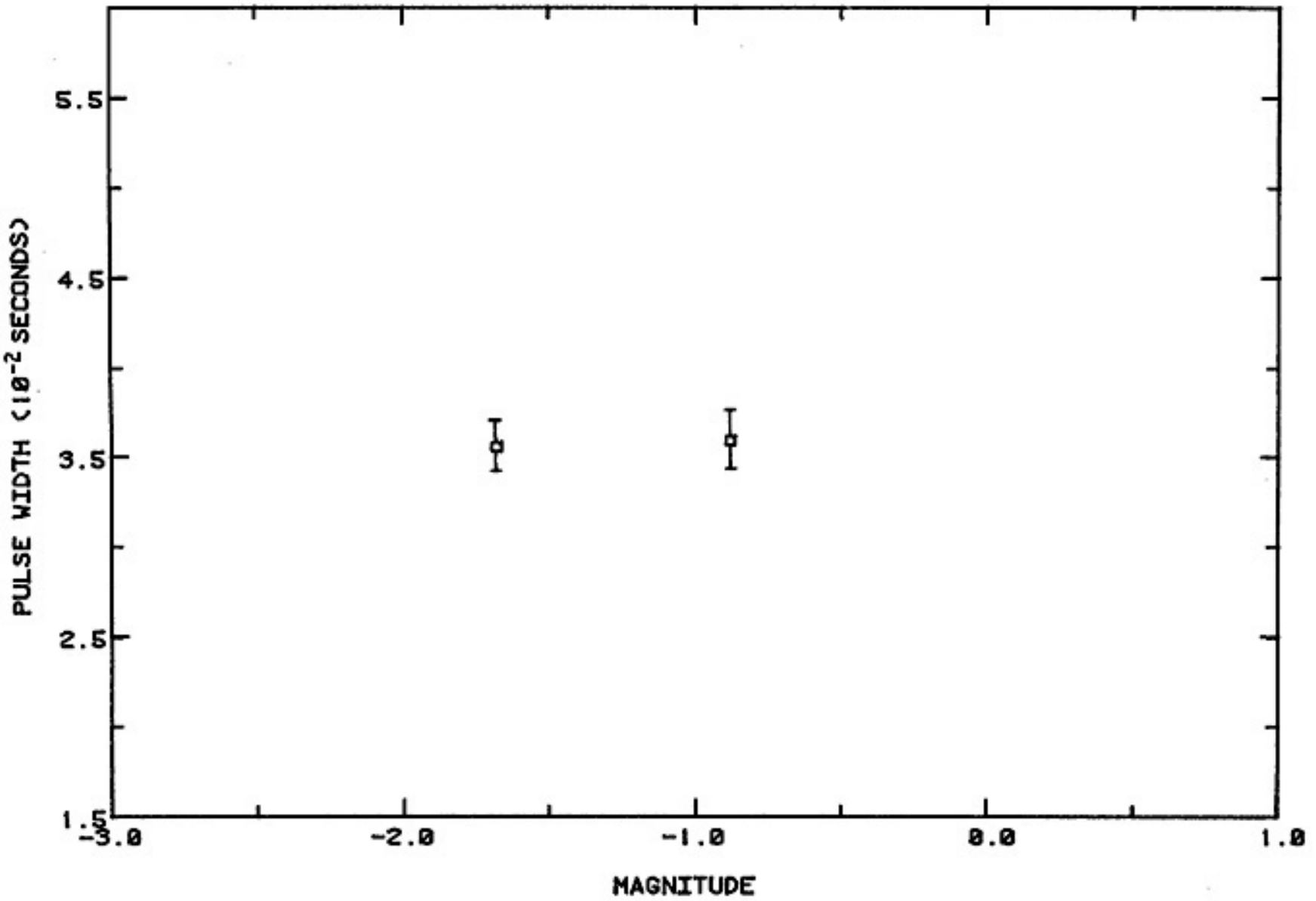

Figure 19. Pulse width verses magnitude for group 83-8c. The calculated average pulse width for the group is 0.0357 +/- 0.0002 seconds (1 s.d.).

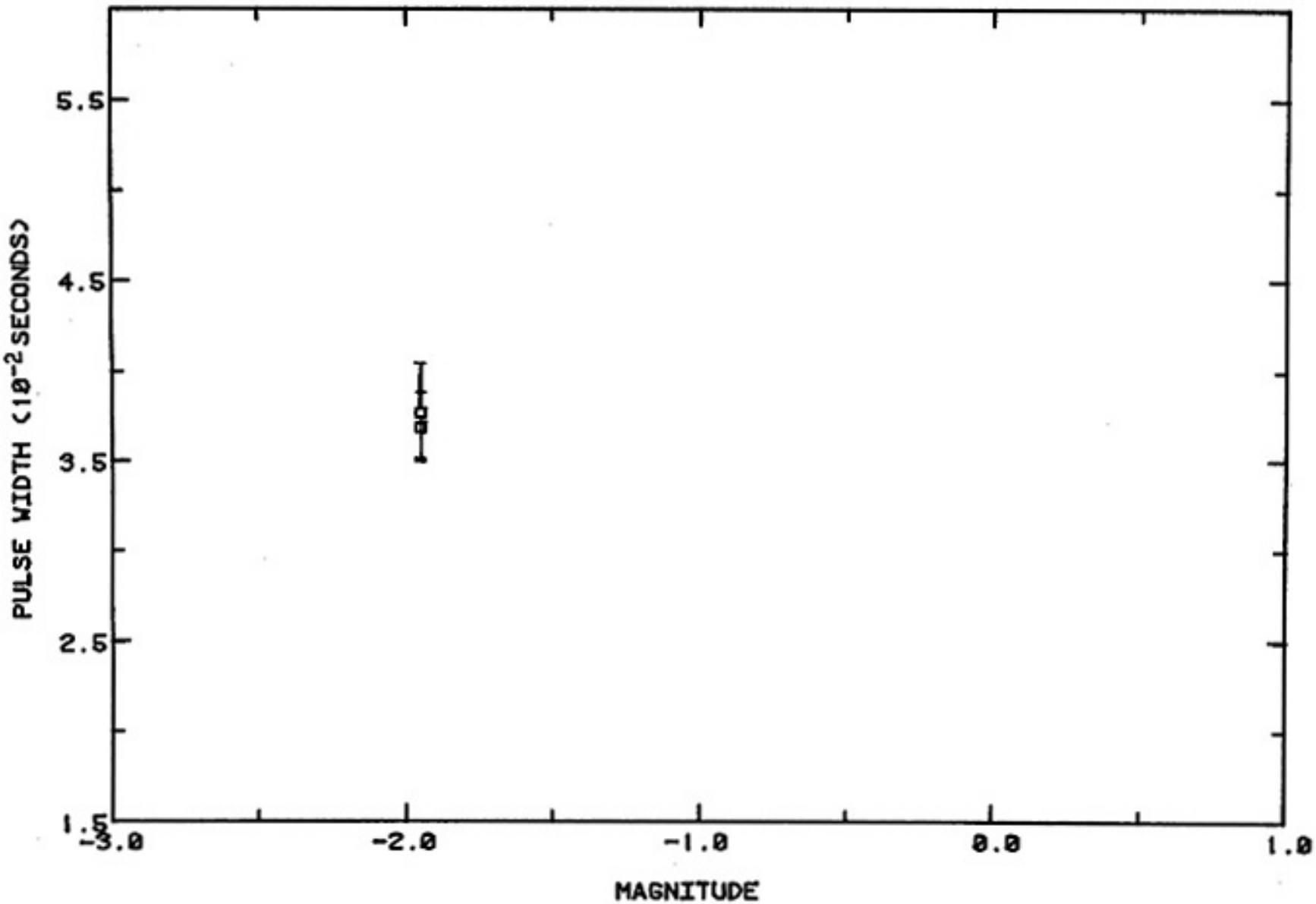

Figure 20. Pulse width verses magnitude for group 83-9. The calculated average pulse width for the group is 0.0372 +/- 0.0004 seconds (1 s.d.).

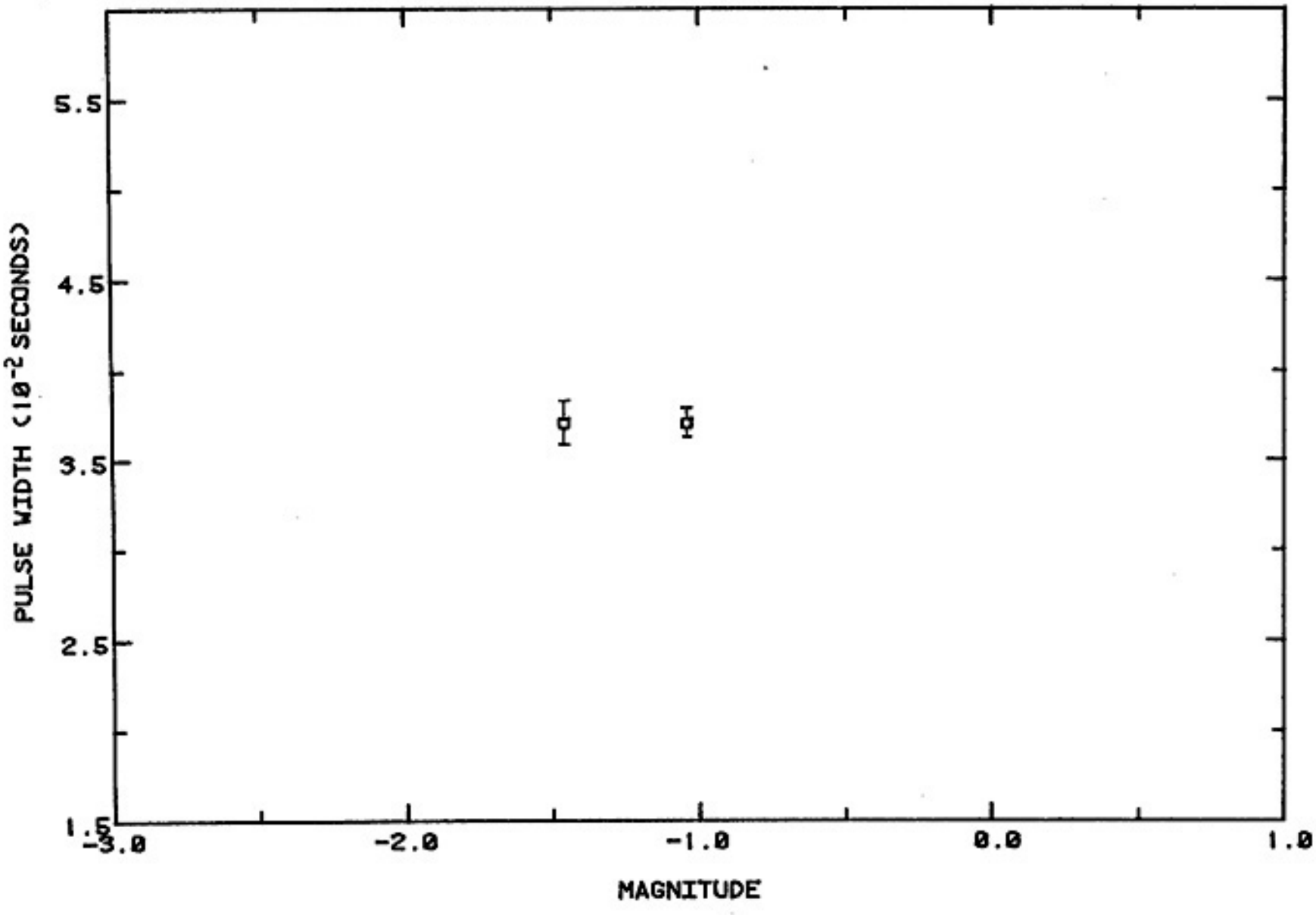

(48)

Figure 21. Pulse width verses magnitude for group 83-11. The calculated average pulse width for the group is 0.0370 +/- 0.0000 seconds (1 s.d.).

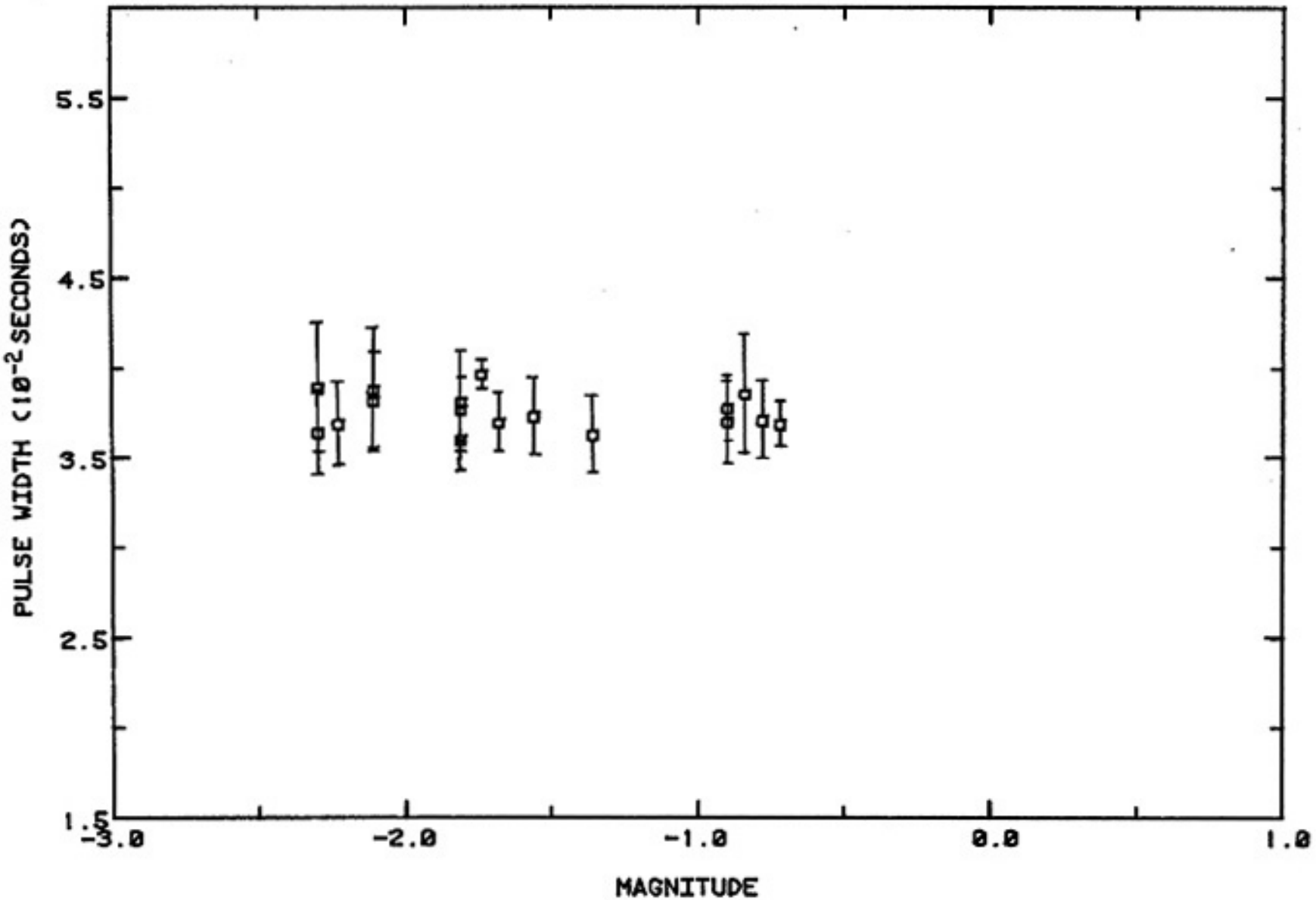

Figure 22. Pulse width verses magnitude for group 83-13b. The calculated average pulse width for the group is 0.0375 +/- 0.0010 seconds (1 s.d.).

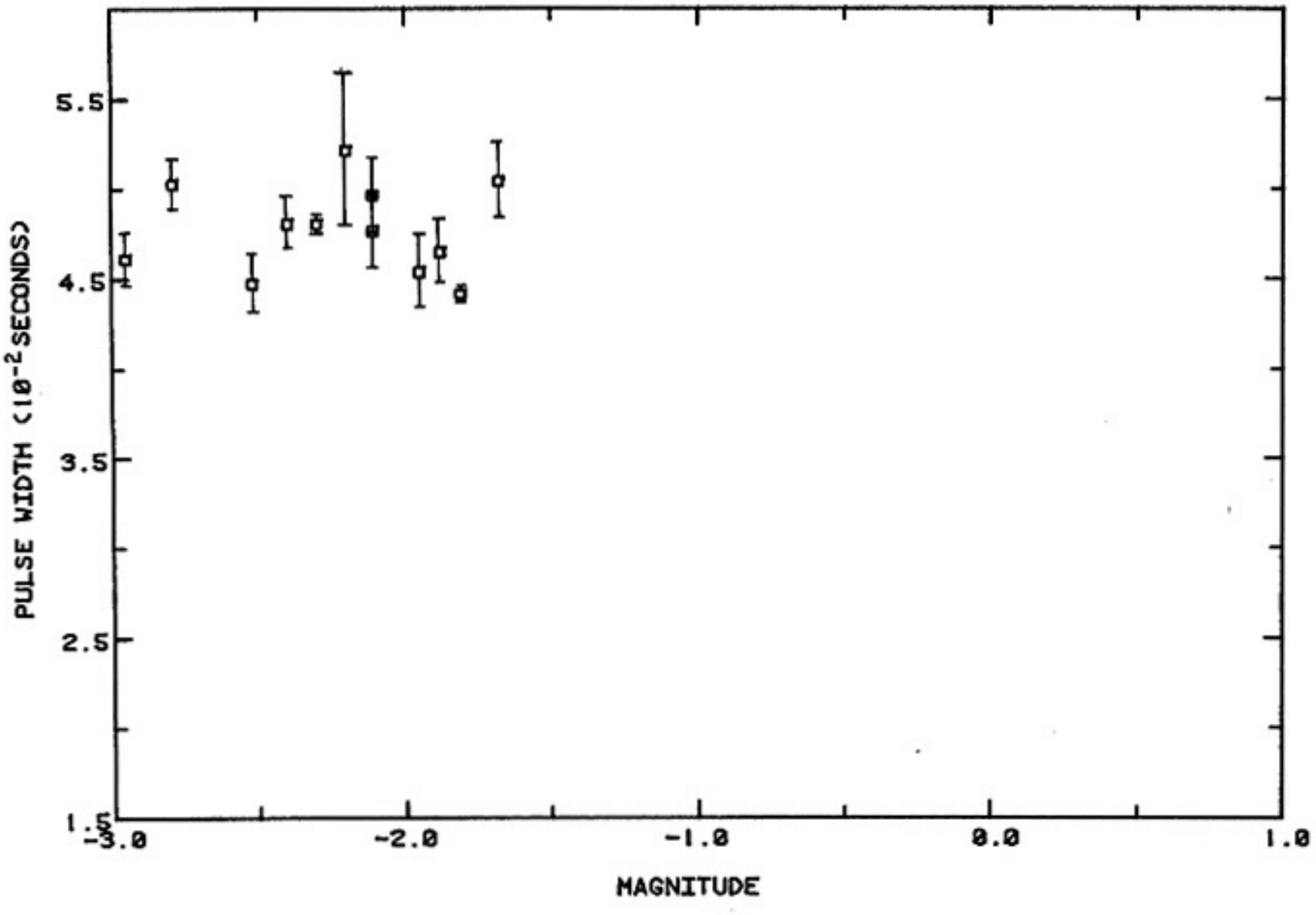

Figure 23. Pulse width verses magnitude for group 83-15. The calculated average pulse width for the group is 0.0477 +/- 0.0024 seconds (1 s.d.).

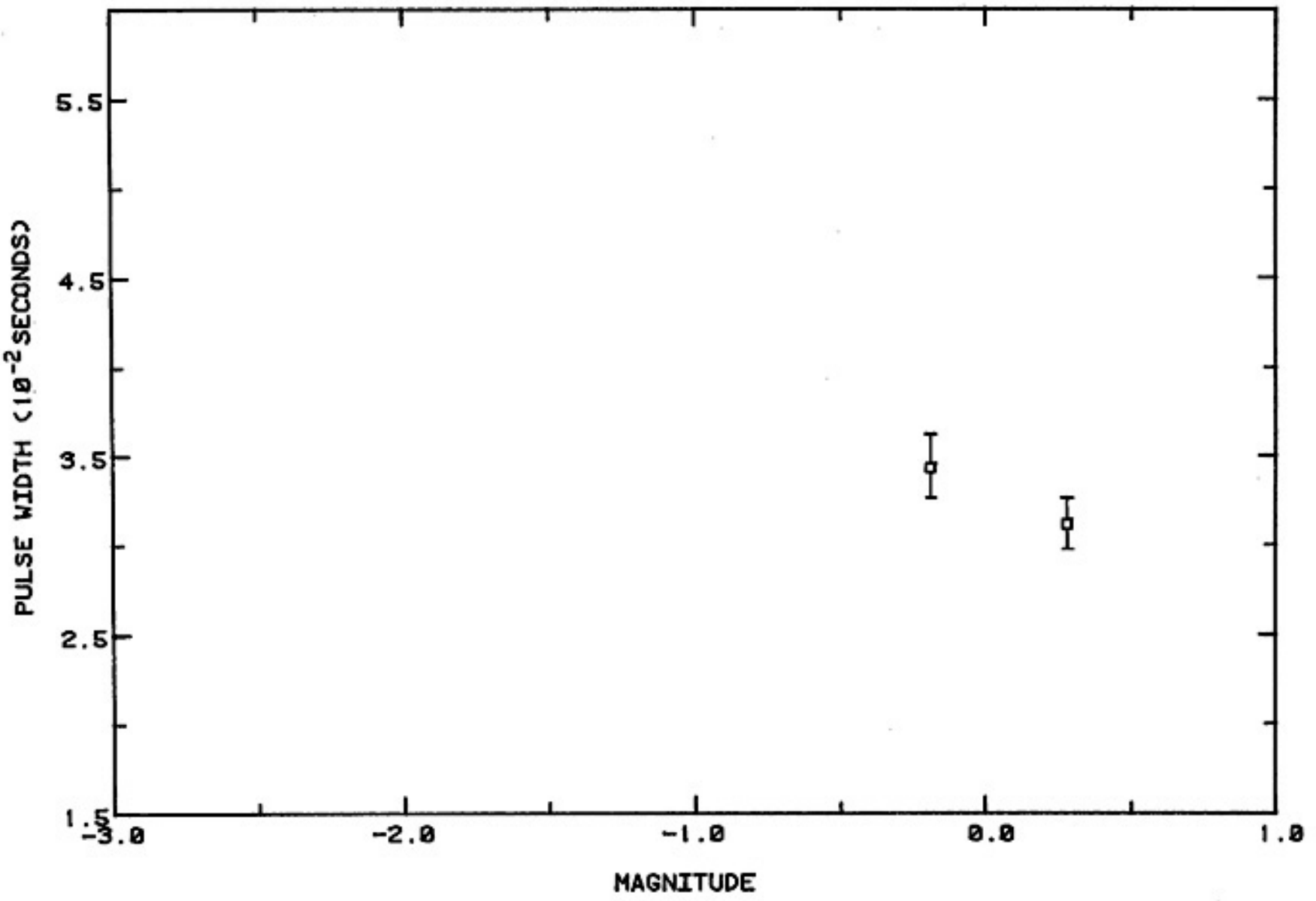

Figure 24. Pulse width verses magnitude for group 77-13. The calculated average pulse width for the group is 0.0327 +/- 0.0016 seconds (1 s.d.).

thereof should be interpreted carefully.

Group 77-22

This group consists of two events (figure 25) which exhibit a decreasing trend of pulse width with increasing magnitude. This group will therefore be excluded from further consideration since one if not both events possibly contain some source information in their waveforms.

Group 81-3

This group contains four events whose characteristics are shown in figure 26. These data do not display a constant pulse width over an extended magnitude range.

Group 81-5

Six events are included in this group with each event's characteristic values shown in figure 27. The figure suggests two separate trends for this group. The first sub-group, designated with an asterisk in Appendix 3, has a relatively constant pulse width value over a range of magnitudes from -0.78 to 0.60 implying a waveform lacking any source information.

The two events of relatively low pulse width values comprise the second sub-group. The consistency in pulse widths for these two events isn't as clear cut as the

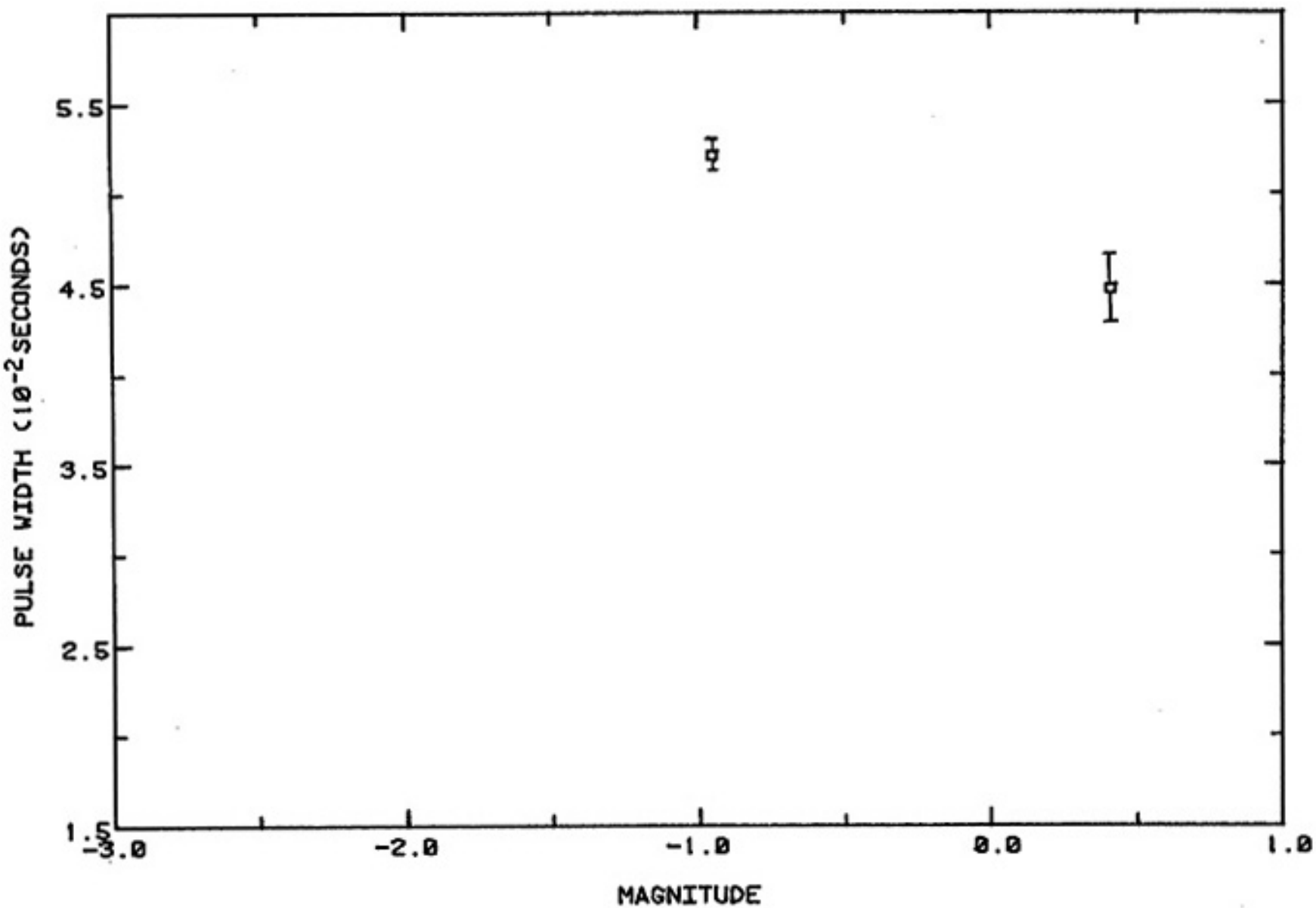

Figure 25. Pulse width verses magnitude for group 77-22. This group displays a pulse width dependence on magnitude and was therefore rejected.

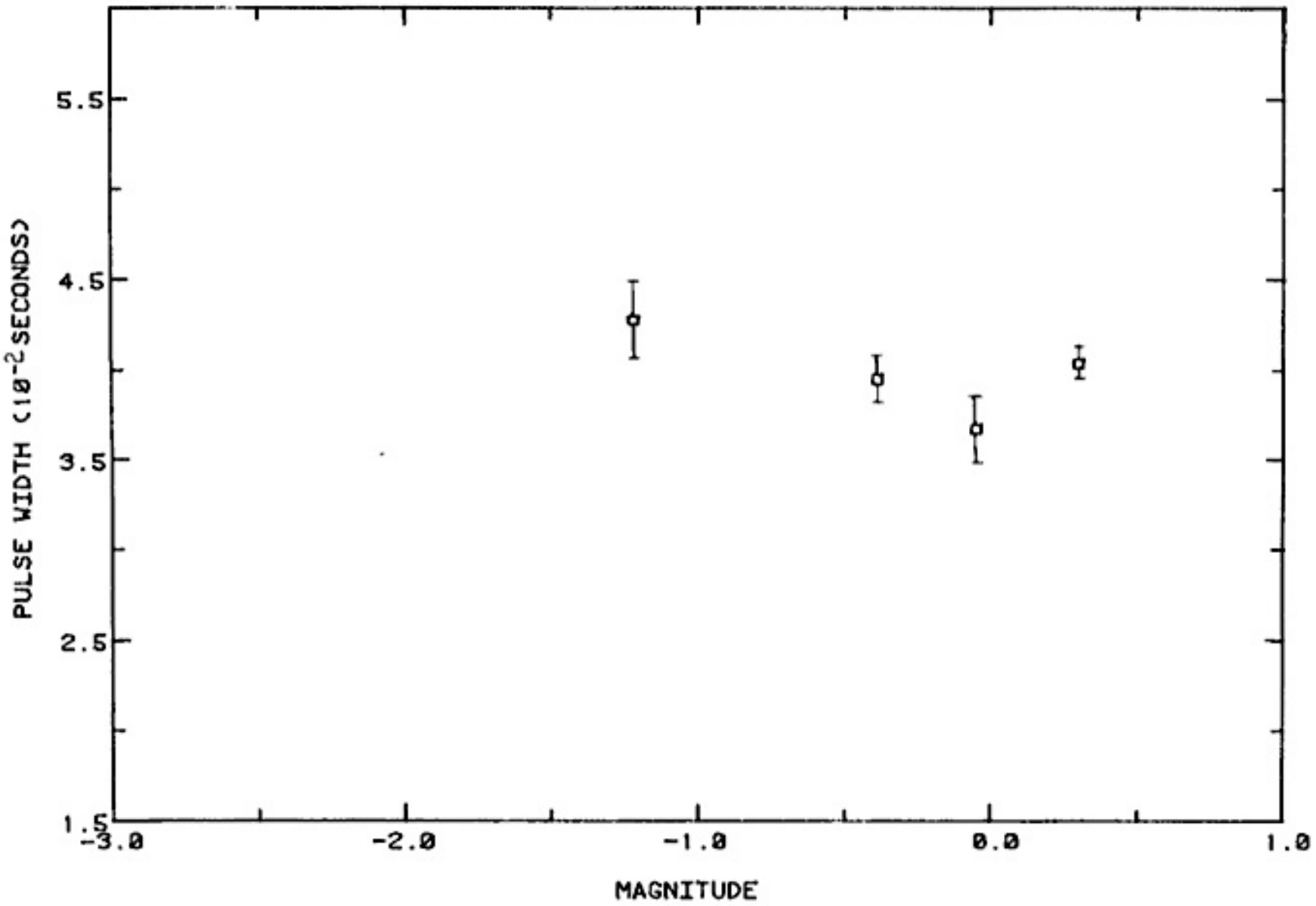

Figure 26. Pulse width verses magnitude for group 81-3. A constant pulse width over an extended magnitude range is not displayed and so this group was rejected.

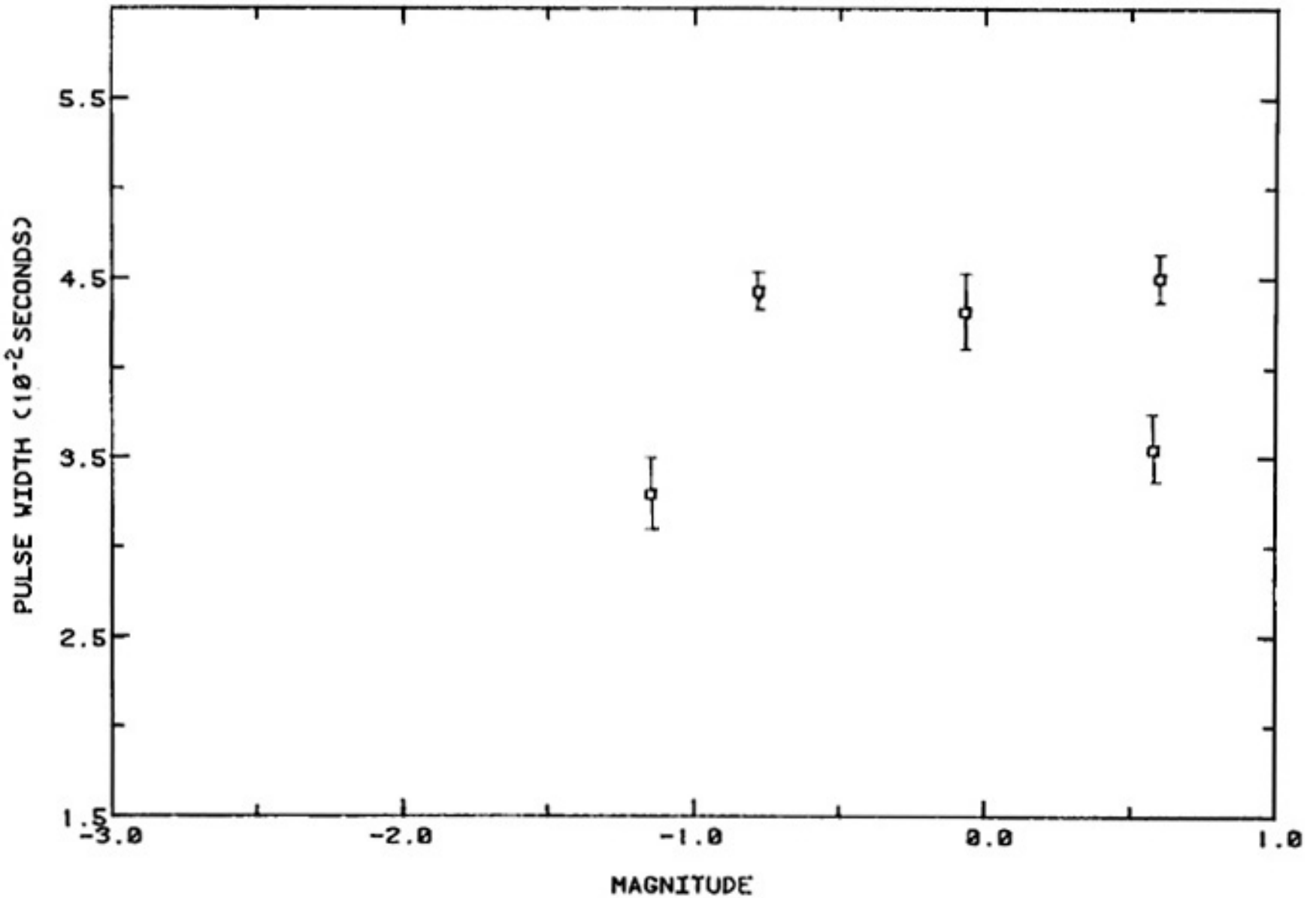

Figure 27. Pulse width verses magnitude for group 81-5. This group displays two trends. The calculated average pulse width for the first sub-group (81-5a) is 0.0441 +/- 0.0008 seconds (1 s.d.). The calculated average pulse width for the second sub-group (81-5b) is 0.0342 +/- 0.0013 seconds (1 s.d.).

previous sub-group, but their values overlap sufficiently and span a large magnitude range, and so are acceptable.

Group 83-10

This group is composed of eight events as shown in figure 28. Seven of the eight events show some semblance of magnitude independence but this tendency is questionable. It will be assumed that magnitude independence is valid for these seven events and that the standard deviation of the computed average pulse width for this group will lend some measure of uncertainty to any physical interpretation drawn from this group later on. The deviant event shows no obvious anomalous characteristics other than its pulse width and is unexplainable at this time. It will be excluded from the "normal" group.

Group 83-13a

This group consists of twenty events and is plotted in figure 29. Two events exhibit anomalously low pulse widths. No evidence was observed to explain this behavior. Because of their low pulse widths, albeit unaccounted for, these two events were omitted from further consideration. The pulse widths for the remaining 18 events displayed a general independence of magnitude for magnitudes less than 0.00.

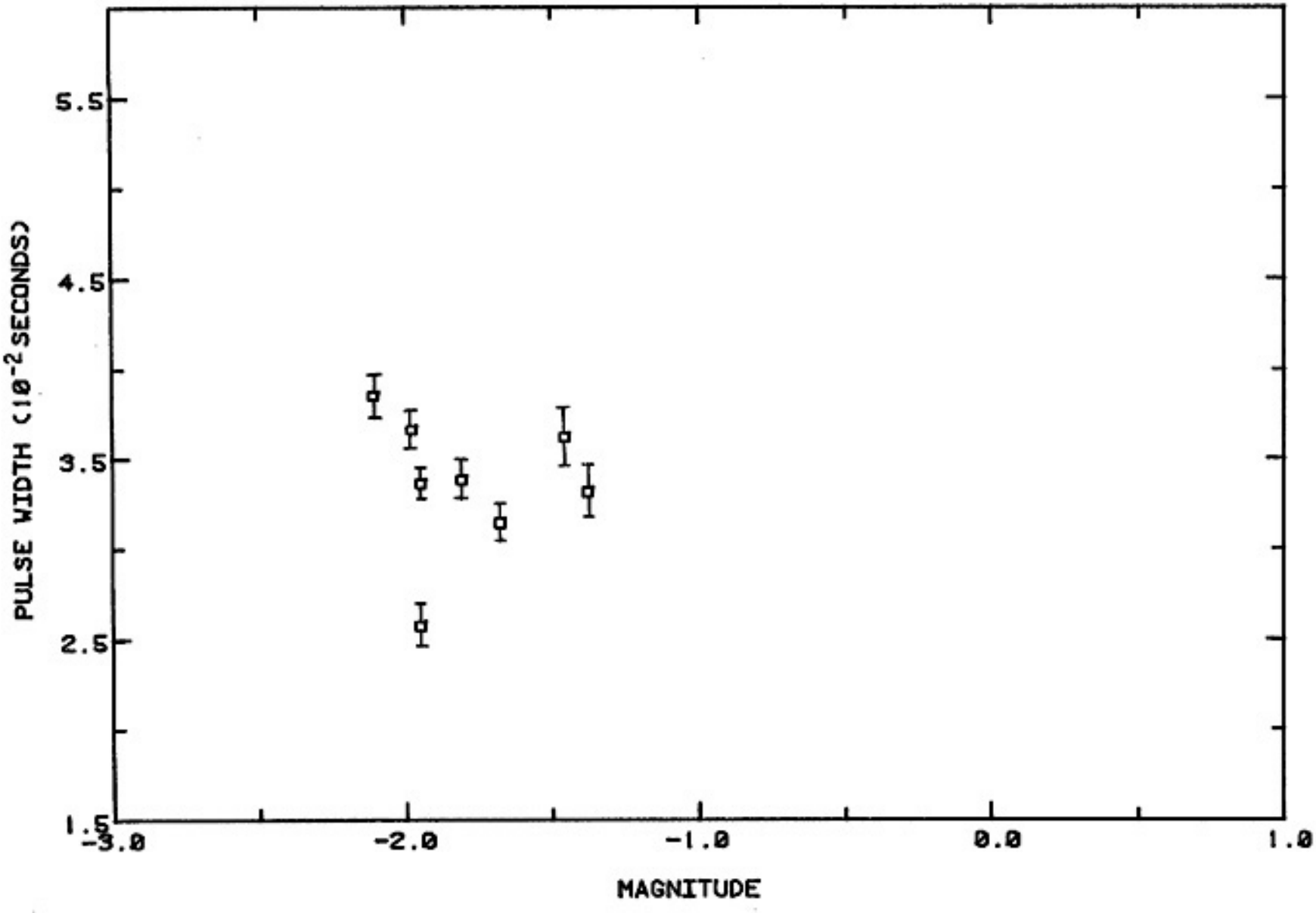

Figure 28. Pulse width verses magnitude for group 83-10. Excluding the anomalously low pulse width, the calculated average pulse width for the group is 0.0374 +/- 0.0023 seconds (1 s.d.).

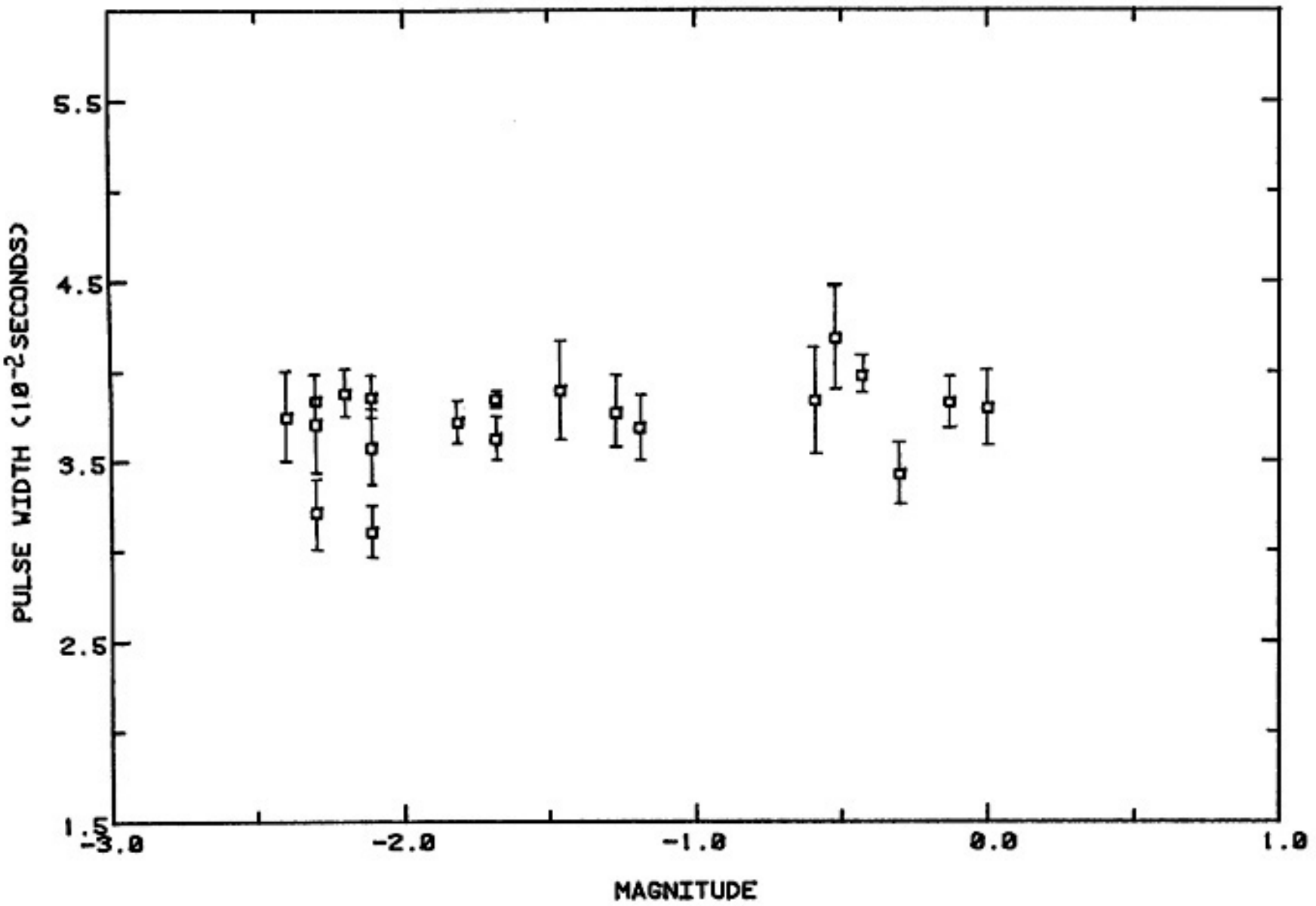

Figure 29. Pulse width verses magnitude for group 83-13a. Excluding the two anomalously low pulse widths, the calculated average pulse width for the group is 0.0378 +/- 0.0014 seconds (1 s.d.).

Group 83-17

Two events comprising this group are displayed in figure 30. The range of magnitudes for this group is relatively small, -0.23 to -0.13, and the uncertainties in the pulse widths for individual events barely coincide. These facts, combined with the occurrence of only two events in this group, make it difficult to believe an independence of pulse width from magnitude. This group will therefore be rejected from further consideration in this study.

Instrument Effects

All events were recorded by either a Sprengnether DR100 or a DR100-1A digital recorder. A Marks Products L4C (vertical component 1 Hz natural frequency) seismometer was used for the majority of the study although the vertical-component of a 3-component Sprengnether S-6000 seismometer was deployed at station WT for a short time (Carpenter, 1984). The manufacturer's manual indicates that the frequency response of the recording part of the digital recording systems possess flat spectrums from 0 to 300 Hz and thus should not appreciably effect the width of the initial P-pulse. Theoretically, the mechanical response of the seismometers is flat to very high frequencies and therefore they will be assumed to have no effect on the recorded pulse widths.

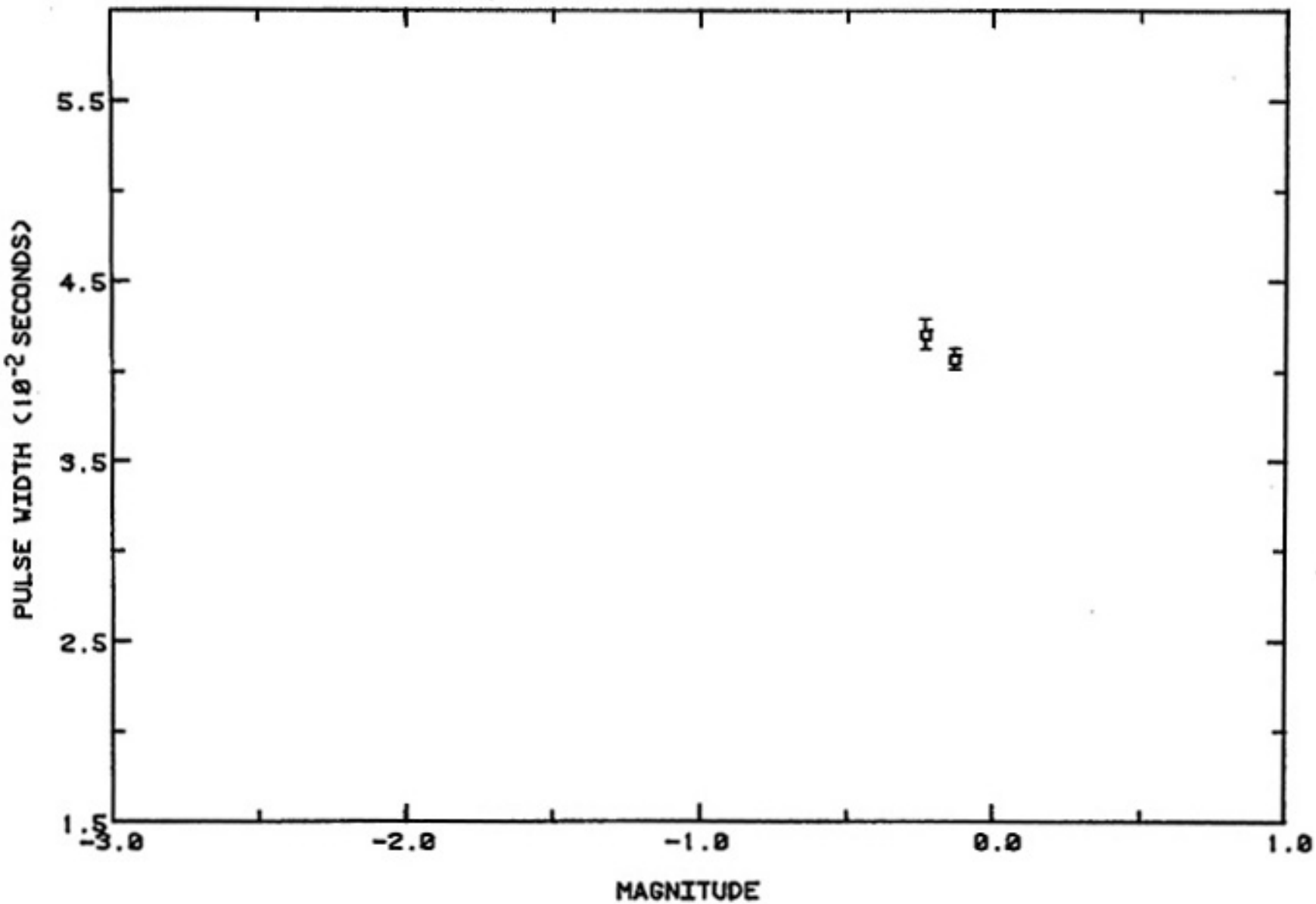

Figure 30. Pulse width verses magnitude for group 83-17. Pulse widths display little coincidence and extend over a small magnitude range, therefore this group was rejected.

The responses of the signal conditioning components of the two recording systems were tested in the laboratory. The pulse broadening effects for each filter setting for one millisecond input pulses are listed in Appendix 1. These values include the effect of the one millisecond input pulses. The instrumental pulse broadening for the appropriate filter setting was subtracted from the average pulse width for each group and the result is listed in Appendix 1.

Geometrical Spreading and Scattering

Geometrical spreading only affects the level of the spectrum of a waveform because it is independent of frequency. The effects of scattering were combined with absorptive effects altering the measured quality factor from a true to an apparent Q measurement.

Station Effects

Several studies advocate that near-surface conditions can have appreciable affects on the character of seismic waves recorded at the surface. Frankel (1982) has stated that over 90% of the observed attenuation for earthquakes that are less than 10 km from the station may be caused from absorption by surficial material. Experimental and field data (Gorden and Davis, 1968, Tittman, 1977) suggested that near-surface Q was low relative to rock 1-2 km beneath the

station implying an incompetent nature to the near-surface material. O'Neill (1984) observed that the minimum pulse widths did not systematically increase with distance and thus appeared to be site dependent, possibly implying that most of the attenuation and/or scattering occurs at shallow depths directly beneath stations, as Frankel and Hanks have alluded to in other areas (Frankel, 1982; Hanks, 1982; Frankel and Kanamori, 1983).

Scattering from inhomogenieties, short-path multiples and incompetent near-surface material acting as high-cut filters are the principle attenuation processes that can effect a waveform as it travels through the near-surface material to the station (Carpenter, 1984). Scattering adds a "tail" of scattered arrivals to the direct wave and after a succession of occurrences, a considerable amount of high-frequency energy is transferred from the direct wave to later phases giving the appearance of a high-frequency cut (Anstey, 1977). Short-path multiples, working in a similar way, have the same effect in that the pulse is broadened, loses its high-frequency components and the energetic part of the waveform is delayed (Anstey, 1977). To have a considerable effect, however, there must be successive reflection coefficients that alternate in sign (i.e. alternating layers of hard and soft rock (Anstey, 1977)). Although this process appears like the high-cut filter effect of absorption, it is not really so. The statistical relationship between the thicknesses of the layers and the

products of the reflection coefficients governs the frequency response of the short-path multiple effect and is not a function of the particular rock as is absorption. On the other hand scattering is related to the degree of inhomogeniety in the geologic section (Anstey, 1977).

The mechanism which has a dominant effect on eliminating high frequencies depends on the geology. Schoenberger et al. (1974) reported a case where absorption and short-path multiples yielded approximately the same amount of attenuation of high frequencies. Highly disturbed zones will be controlled in part by scattering while a thick interval exhibiting little evidence of reflections is most likely to be governed by a true absorption effect, although the effect must persist over a relatively thick interval if it is to yield a measurable frequency loss (Anstey, 1977).

Hypocentral Locations

The HYPO71 Revised (Lee and Lahr, 1975) linear inversion earthquake location program was used in this study. A homogeneous, isotropic half-space velocity model (Vp = 5.85 km/sec, = 0.25) was used. Because of varying thicknesses of near-surface low-velocity material, station time corrections were used. Ward (1980) or Ake (1984) give a detailed discussion of the location procedure for local microearthquakes.

For unlocated events, hypocentral distances were obtained from the expression

$$d = [(1.37)(S-P) - t(sta)]V(p) \qquad (4)$$

where d is the hypocentral distance, V(p) is the P wave velocity, (S-P) is the S-P interval and t(sta) is the station delay accounting for the varying near-surface material thicknesses under each station in the seismic network. Equation (4) assumes a Poisson's ratio of 0.25, which has been found from previous studies to be suitable for the Socorro area (Caravella, 1976; Fender, 1978; Frishman, 1979). Hypocentral information for located events is listed in Appendix 4.

Rise Time Law

The model for this study was based on the relationship

$$\text{tau} = \text{tau s} + C\int_0^T dT/Q \qquad (5)$$

set forth by Gladwin and Stacey (1974) and sometimes referred to as the linear rise time equation (Blair and Spathis, 1982; 1984). Tau is the pulse rise time or equivalently the pulse width of the first half cycle of the waveform when recording ground velocity, tau s is the rise time (pulse width) of the source, C is a constant given the value 0.53 +/- 0.04, Q is the quality factor, and T is the travel time of the wave in the material of quality factor Q. The literature on equation (5) does reveal some uncertainty

in the value of C which will be discussed later. Following the example of Blair and Spathis (1982), equation (5) was transformed from the time to the space domain by substituting R/V(p) for the travel time where R is the raypath distance through the Q material and V(p) the P wave velocity in the material. This transformation was made because of the availability of hypocentral distances and thus raypath distances for the events of this study. Equation (5) took the form

$$\text{tau} = \text{tau s} + C \int_0^R dR/[Qp*Vp] \qquad (6)$$

As discussed previously, only events that were devoid of source propagation effects (i.e. tau s = 0) were used in this study.

Three separate procedures were employed in this study to obtain apparent Q's for the Socorro area. The first procedure assumed a homogeneous half-space and used the form of equation (6)

$$\text{tau} = \frac{C*R(hyp)}{V(av)*Qp(av)} \qquad (7)$$

where R(hyp) is the average hypocentral distance for the respective group, V(av) is the average velocity in the half-space, tau the average pulse width for the group (corrected for instrumental response) and Qp(av) is the average Qp for the half-space of the respective group.

As mentioned previously, there has been some controversy in the literature over the constant C in equation (5). Gladwin and Stacey (1974), working with ultrasonic pulses in an unbroken and massive rock in the Snowy Mountains of S.E. Australia, arrived at a value of C = 0.53 +/- 0.04. They state that their results are independent of source type. They also calculated the value of C for a number theories and concluded that the model of Azimi et al. (1968) was the only case in which the value of C = 0.5 coincided with their own and gave physically reasonable results. Kjartansson (1979) predicted from a constant Q model a value of C = 0.485 for large Q (>20). He then went on to fit the data of McDonal et al. (1958) and Ricker (1953, 1977), both of whom advocated power law relationships for pulse width and time, and found he could fit both data sets with equation (4). However, a value of C = 0.5 was used to obtain a good fit of the data of McDonal et al. (1958), while to fit Ricker's data, a value of C equal to approximately unity was obtained. O'Neill (1984), working with the pulse widths of earthquakes having coda duration magnitudes between 1.2 and 3.9, used C = 0.773. Blair and Spathis (1982) argued against a linear rise time equation and stated that the value of C was source dependent. They did note that the rise time equation was valid under specific conditions, namely the propagation of an impulsive source (tau s = 0). Only events which were believed source independent were used in this study and so

the argument of Blair and Spathis is not relevant here. Blair and Spathis (1984), working in the Mount Isa Mine, Queensland, Australia, concluded that C depends upon not only the seismic source, but also the type of detector used and the local environment of the detector. Thus, there seems to be conflicting views as to what the value of C in equation (5) should be.

Three different values for C were used in the first procedure. C was set equal to 0.5, 0.773 and 1.0 in equation (7) and Qp(av) values were obtained for the various groups. The results, as well as the average Qp values found by Carpenter (1984) for the area are listed in Table 1. Values of Qp obtained when C = 0.773 coincided best with the values calculated by Carpenter (1984).

In the second procedure a layer over a half-space configuration was constructed. The velocity model for the area was a low-velocity layer of varying thickness under the digital stations in the array underlain by a higher velocity half-space. Local explosions (Ward, 1980), refraction studies carried out in Wood's Tunnel in Socorro Mountain (Sanford, personal communication, 1984), refraction studies along the east side of the Rio Grande rift (Olsen et al., 1979) and average velocities of reflected waves through Phanerozoic rocks obtained from COCORP Line 1A (Rinehart, 1979) have given evidence suggesting that 3.4 +/- 0.1 km/sec (1 s.d.) is a good average velocity for P waves in rocks

TABLE 1

AVERAGE APPARENT Qp

Group	C=0.5 Qp(av)	C=0.773 Qp(av)	C=1.0 Qp(av)	Qp - Carpenter (1984)
77-2	55.67	86.07	111.34	71.83 +/- 15.80 (2 s.d.)
77-18	49.55	76.60	99.10	67.85 +/- 16.34
81-4	36.77	56.85	73.54	110.00 +/- 28.19
77-4	47.27	73.09	94.55	82.54 +/- 15.74
77-5	41.23	63.64	82.45	92.69 +/- 18.42
77-15	66.54	102.87	133.09	149.17 +/- 30.59
77-13	44.68	69.06	89.33	68.71 +/- 15.85
77-3	28.35	43.82	56.69	48.20 +/- 5.89
77-17	47.51	73.45	95.02	84.51 +/- 12.19
81-5a	51.37	79.42	102.75	68.69 +/- 13.44
81-5b	31.76	49.10	63.52	45.98 +/- 10.25
77-16	52.73	81.52	105.46	no listing
83-1	65.31	100.97	130.62	135.04 +/- 40.87
83-3	122.25	188.99	244.49	no listing
83-5	203.74	314.97	407.47	103.58 +/- 18.42
83-6	78.86	121.92	157.72	no listing
83-8a	68.65	106.13	137.29	84.29 +/- 21.14
83-8b	69.79	107.89	139.58	no listing
83-8c	71.19	110.05	142.37	248.96 +/- 68.88
83-9	58.30	90.13	116.60	no listing
83-10	63.62	98.35	127.23	no listing
83-11	65.21	100.82	130.42	no listing
83-13a	61.07	94.41	122.13	67.19 +/- 14.47
83-13b	64.11	99.11	128.21	no listing
83-15	31.05	48.00	62.09	no listing

less than 2 km deep in the Socorro area. This was the velocity chosen to represent the low velocity layer in the model for this study. The near-surface low-velocity material in the Socorro area has been shown to cause different time delays for incoming waves at the various stations in the seismic array (Ward, 1981) and these time delays have been attributed to the varying thicknesses and compositions of the low-velocity material underlying the different stations (Carpenter, 1984).

A summary of upper crustal velocities in the Socorro area is given in Rinehart and Sanford (1981) and compiled from numerous studies of the upper 19 km of crust. Figure 31, taken from Carpenter (1984) and originally from Rinehart and Sanford (1981), shows the P wave velocities from which an average value was taken for this study. The P wave velocity of 5.85 +/- 0.02 km/sec (1 s.d.) (Ward et al., 1981) was chosen for the half-space in this study. P wave velocities below 19 km are considerably higher than above this depth, as shown in figure 28, however, first arrivals for local events ("Δ" = 1 - 45 km) do not penetrate this deep and so these higher velocities were not considered in this study.

Near-surface Low-Velocity Layers (LVL)

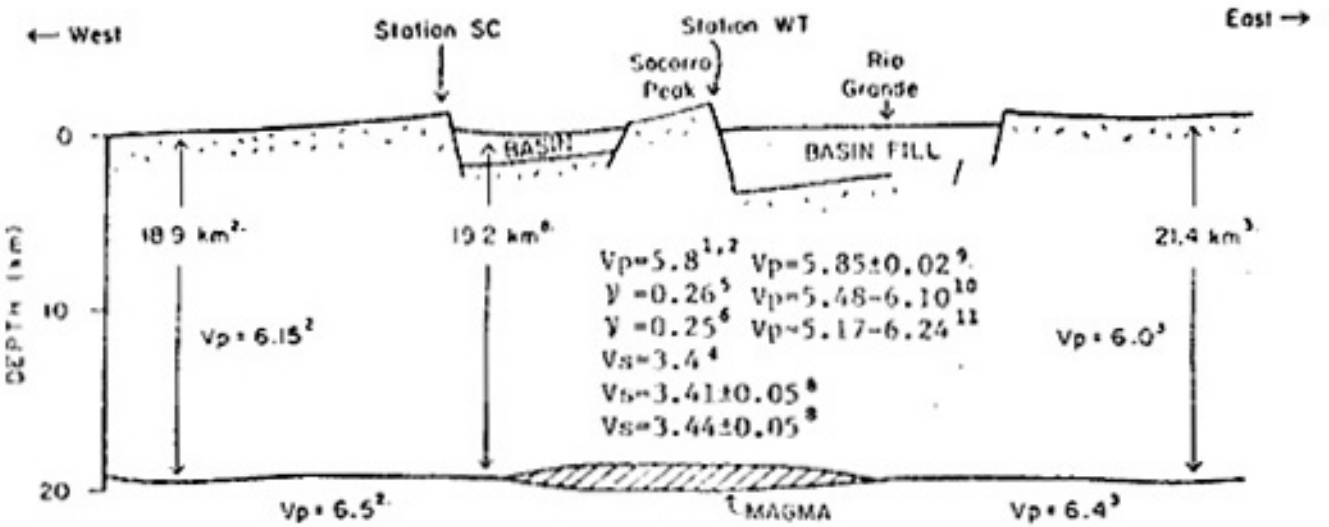

References

1. Sanford et al. (1973)
2. Toppozada and Sanford (1976)
3. Olsen et al. (1979)
4. Keller et al. (1979)
5. Caravella (1976)
6. Fender (1978)
7. Rinehart (1979)
8. Rinehart and Sanford (1981)
9. Ward et al. (1981)-- Average velocity to average depth of hypocenters
10. Ward et al. (1981)-- Velocity in the range 0-4 km
11. Ward et al. (1981)-- Velocity in the range 4 km-average depth of hypocenters

Vp = P-wave velocity in km/s

Vs = S-wave velocity in km/s

γ = Poisson's ratio

Figure 31. A composite geophysical cross section of the central Rio Grande rift at Socorro, New Mexico, adapted from Rinehart and Sanford (1981). Vertical exaggeration is about two.

Station corrections, as mentioned above, reflect the time delays of incoming waves through the low velocity layers. The corrections can be expressed as

$$t(sta) = D/V(1) - D/V(2) \qquad (8)$$

where t(sta) is the observed station correction, D is the distance traveled through the LVL, V(1) is the velocity of the LVL and V(2) is the velocity of the half-space (Carpenter, 1984). By rearranging equation (8) for D and then multiplying D by the cosine of the average angle of incidence for incoming waves at the stations , Carpenter (1984) obtained approximate values for the thicknesses of low-velocity material underlying the different stations in the digital array. Table 2, taken from Carpenter (1984), lists station delays, station corrections adjusted for relative elevation differences between stations and normalized to station CC, LVL thicknesses computed from the normalized corrections and uncertainties of LVL thicknesses for all stations in the digital array.

Q versus Depth

A relatively low Q, low-velocity material will be assumed to overlie a high Q, high-velocity half-space, as represented in figure 32 (from Carpenter, 1984). By combining all the low Q material into one layer, a strong Q gradient near the surface was accounted for (Carpenter, 1984). An increase in apparent Q with distance was observed

TABLE 2

STATION CORRECTIONS AND THICKNESSES OF LOW VELOCITY LAYERS

STATION	t(sta)	t(norm)	thick.	2 s.d.
CC	-0.15 s	0.00 s	0.0 km	0.0 km
CM	0.13	0.28	2.0	0.3
DM	-0.01	0.16	1.1	0.3
IC	0.08	0.21	1.5	0.3
SC	0.15	0.22	1.6	0.3
WT	-0.11	0.05	0.3	0.3

t(sta) taken from Ward (1980)
Table 2 after Carpenter (1984)

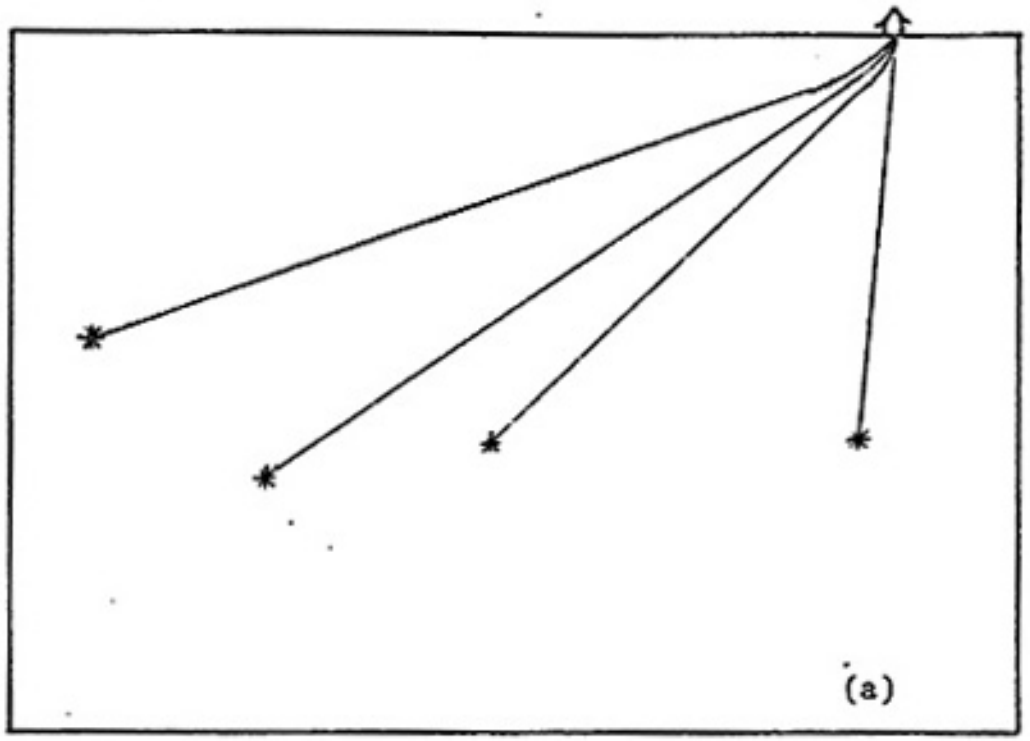

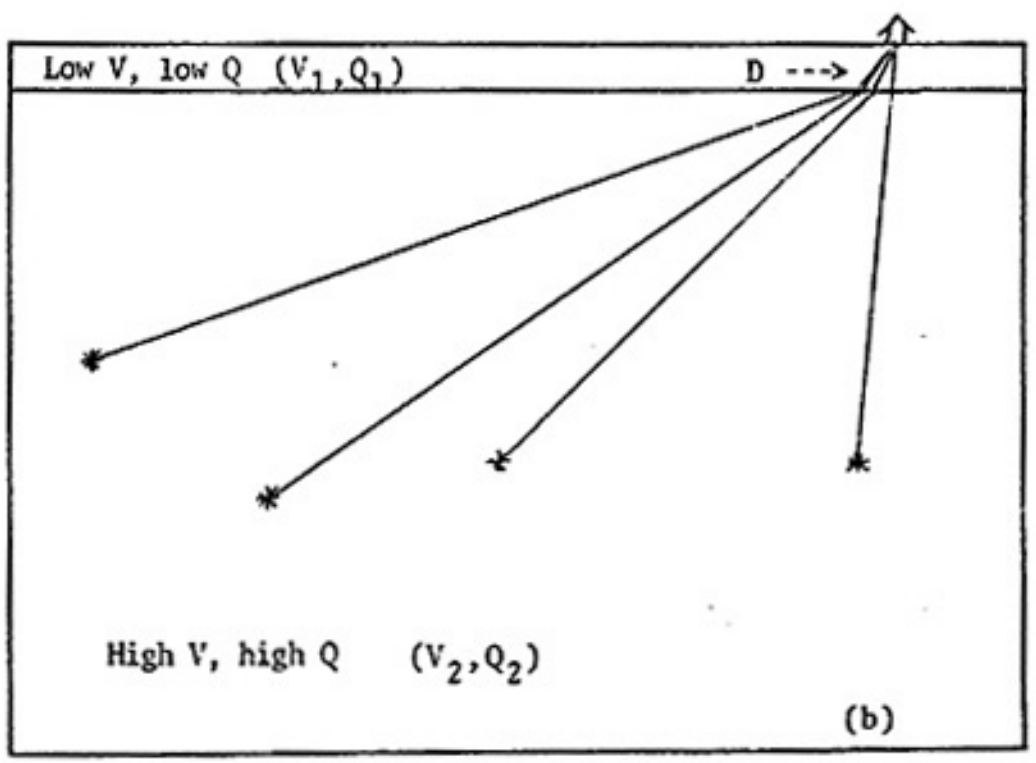

Figure 32. Idealized microearthquake raypaths for events recorded by a station on the surface. (a) The actual raypaths for a rapid increase in velocity with depth near the surface. (b) The layer over a half-space model used to represent (a) in this study (from Carpenter, 1984).

by Carpenter (1984) and suggests Q increases with depth (i.e. earthquakes that are farther away will have a longer travel path through deeper, higher Q material). In the second procedure, a different apparent Qp was assumed for the LVL beneath each station while the apparent Qp of the half-space will be assumed to be a constant both laterally and with depth.

Breaking the integral of equation (6) up into its contributing components for the model of this study (i.e. LVL and half-space) and applying the criterion of source independence, equation (6) can be written as

$$tau = \frac{C*R(LVL)}{V(LVL)Qp(LVL)} + \frac{C*R(HS)}{V(HS)Qp(HS)} \qquad (9)$$

where R,V and Q are the raypath distances, velocities and apparent Q's, respectively, in the LVL and half-space. Apparent Qp values for the low velocity layers under the stations were taken from the results of Carpenter (1984) and apparent Qp's for half-space were computed from equation (9). Again, the three values used in the first procedure for the parameter C were used in these calculations.

A graphical technique was employed to estimate the distances traveled in the LVL and half-space by each event. Epicentral distances and hypocentral depths were obtained for each event from HYP071 solutions. For those events in which no HYP071 solution existed, a hypocentral depth of 8.50 km was assumed, a good average depth for

microearthquakes in the Socorro area (Sanford, personal communication, 1985). Hypocentral distances were calculated from (S-P) intervals obtained from digital print outs of the events and applied to equation (4). From the hypocentral distances and depths, epicentral distances were easily calculated using the Pythagorean theorem.

The hypocenter and receiver locations were drawn to scale and an angle of incidence of the incoming wave impingent at the base of the LVL was assumed. From Snell's Law the refracted angle through the LVL was obtained. Using this calculated refracted angle the raypath in the LVL was drawn. The raypath in the half-space with the associated angle of incidence was drawn next. If the raypath in the half-space intersected the hypocenter the resulting raypaths of the respective layers were measured directly from the graph. If this raypath did not intersect the hypocenter, a new angle of incidence was assumed, new refracted angle calculated and the process repeated until an intersection was obtained. Figure 33 is a representation of this technique. There were obviously inherent errors in measuring and drawing the angles and raypaths but these were felt to be negligible. A listing of the raypath distances in the LVL and half-space used in the following procedures can be found in Appendix 5.

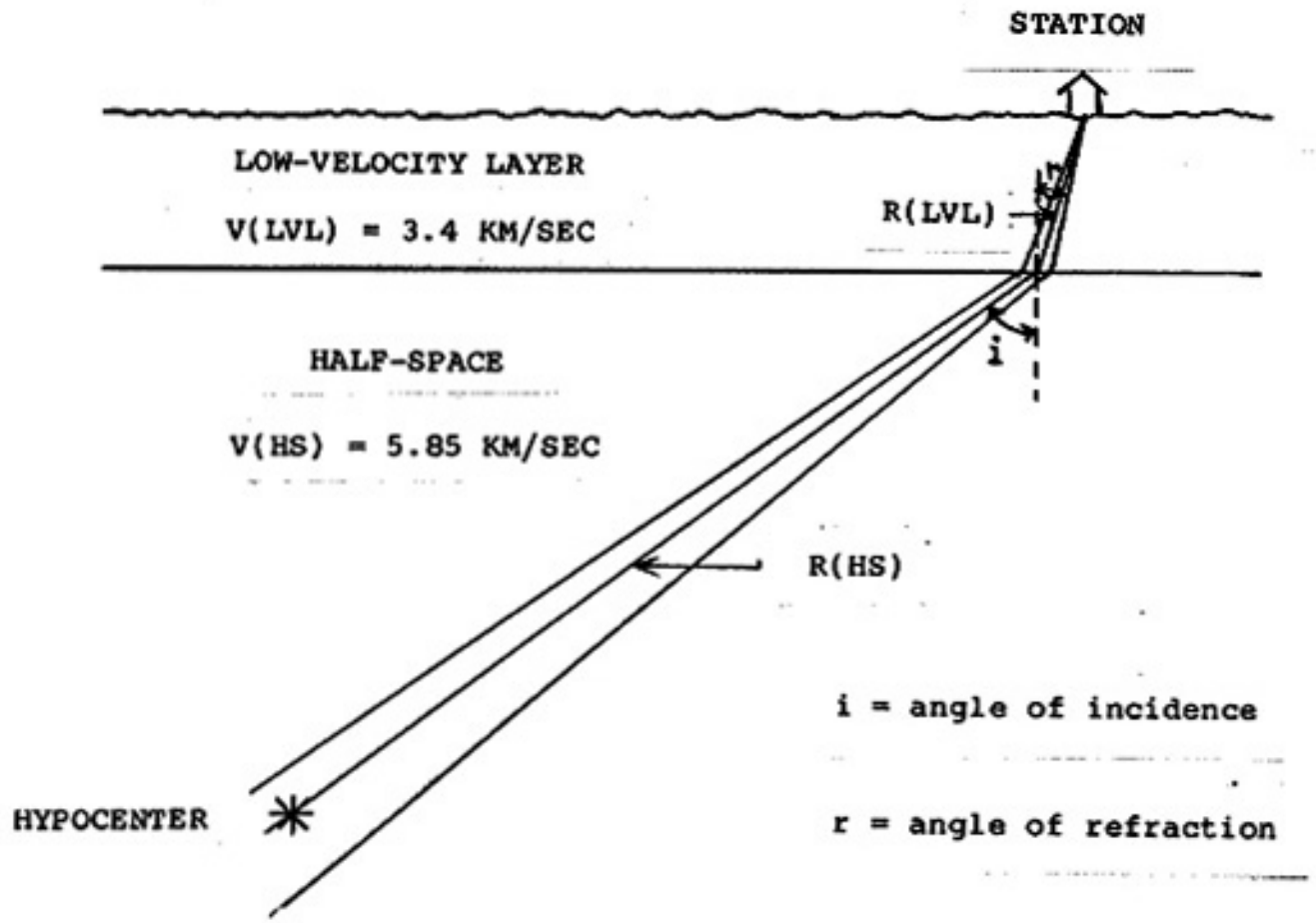

Figure 33. A representation of the graphical technique used to obtain the raypath distances traveled in the low-velocity layer and in the half-space for a duplicate group of events.

TABLE 3

Q(LVL) ESTIMATES FOR EACH STATION

STATION	Qs	Qp
CC	-----	0.00
CM	35.93	25.15
DM	18.83	13.18
IC	34.62	24.23
SC	36.95	25.86
WT	9.83	6.88

TABLE 4

CALCULATED APPARENT Qp FOR HALF-SPACE

GROUP	STATION	C = 0.50	C = 0.773	C = 1.00
77-2	SC	96.95	614.67	-503.74
77-18	SC	73.61	255.46	-9399.02
81-4	SC	42.47	91.85	177.81
77-4	CC	47.28	73.09	94.55
77-5	CC	41.23	63.74	82.46
77-15	CC	66.54	102.88	133.09
77-13	CM	71.99	472.15	-360.11
77-3	DM	38.06	90.50	211.85
77-17	DM	64.63	137.27	257.72
81-5A	IC	80.85	307.15	-1877.22
81-5B	IC	35.47	75.07	140.10
77-16	WT	83.60	204.39	511.86
83-1	WT	188.61	-1916.85	-339.80
83-3	WT	-287.12	-151.11	-126.25
83-5	WT	-548.35	-274.71	-227.51
83-6	WT	-2395.47	-107.34	-135.43
83-8A	WT	217.33	-1068.91	-308.88
83-8B	WT	202.53	-2058.36	-364.89
83-8C	WT	304.98	-478.63	-231.42
83-9	WT	172.44	-1257.79	-282.76
83-10	WT	183.33	-1863.24	-330.30
83-11	WT	201.78	-1120.78	-300.88
83-13	WT	165.13	-5254.35	-358.79
83-13A	WT	191.45	-1376.49	-312.49
83-15	WT	45.44	104.11	224.77

Because the average apparent Qp values obtained by the second method were found in several cases to be significantly lower than the values given by Carpenter (1984), it was thought that the model was too simple. With the low values used for apparent Qp and raypath distances travelled in the LVL, the first term in equation (9) dictates the calculated value of average apparent Qp. By adding additional terms to equation (9) for additional layers in the model, each successively deeper layer having greater thickness and value of apparent Qp values, it was hoped that more realistic values for average apparent Qp's would result. Two, three and four layer models were attempted but a significant change in the resulting average apparent Qp was not observed. The relatively thin, low Q upper layer still dominated.

The third procedure used in this study was a linear inversion of the average pulse widths for the various groups to obtain apparent Qp values for the LVL beneath each station and an average apparent Qp value for the half-space. The inverse problem starts with data (in this case pulse widths) and a general model (equation (6)), and inverts the data to obtain estimates of the model parameters (Qp). The velocities of the respective layers, raypath distances and average pulse widths obtained for the associated groups were the same as those discussed in the previous procedure.

A description of the linear inversion process will not be given here. However, a detailed account of the inversion method used in this study can be found in Jackson (1972). The linear inversion program written for this study can be found in Appendix 6.

It should be mentioned that a linear inversion process was applied to a non-linear model equating pulse width and apparent Qp (see equation 9). An iterative technique was applied to the model in hopes that the iterative process would converge to the (a?) minimum prediction error. The problem is that the linearized method does not "see" the entire error surface but instead sees only that part of the error surface that is linear in the vicinity of the initial guess of the parameter(s) in question (Menke, 1984). If the initial guess is not close enough to the minimum of the error function, the iterative technique may not converge at all or may converge to a local minimum or even a local maximum (Menke, 1984). Only by investigating a variety of initial guesses (which still may not resolve the problem because, theoretically, a sufficient number of guesses can never be obtained) can one be confident that the iterative method really does reach a global minimum on the error surface (Menke, 1984).

The initial model parameters chosen for this study were decided on by combining information based on work by Carpenter (1984), convergence of the apparent Qp values

through an iterative process, and the choice of the "best" solution given various starting parameter groups. The starting values are listed below:

Station	Apparent Qp			
CC	0.0	+/-	0.0	
CM	25.0	+/-	2.0	(1 s.d.)
DM	15.0	+/-	2.0	(1 s.d.)
IC	25.0	+/-	2.0	(1 s.d.)
SC	25.0	+/-	2.0	(1 s.d.)
WT	10.0	+/-	2.0	(1 s.d.)
Half-Space	400.0	+/-	200.0	(1 s.d.).

Station CC was given a LVL apparent Qp of zero since station LVL thicknesses were normalized with respect to station CC and thus this station was assumed to have a zero thickness LVL. These starting values also seemed to give the most physically realistic apparent Qp values as well as exhibit the lowest R parameter values compared with a variety of other starting value combinations. The other combinations of starting values attempted either gave relatively larger R values (R = 1 implies a "reasonable" model) or gave apparent Qp values that did not agree as well (if at all) with values from Carpenter (1984).

As in the previous two procedures the three values for the parameter C were used in separate runs of the inversion program. The apparent Qp values obtained from the runs of the inversion program are listed in Table 5. A general

TABLE 5

APPARENT Qp VALUES FROM LINEAR INVERSION

station	C = 0.50 Apparent Qp	C = 0.773 Apparent Qp	C = 1.00 Apparent Qp
SC	11.49 +/- 0.11	21.77 +/- 0.68	28.64 +/- 0.67
CC	0.00 +/- 0.00	0.00 +/- 0.00	0.00 +/- 0.00
CM	24.26 +/- 6.17	28.13 +/- 2.39	45.85 +/- 7.23
DM	1.97 +/- 2.93	14.23 +/- 0.68	19.72 +/- 1.45
IC	5.31 +/- 0.04	18.84 +/- 1.92	25.95 +/- 1.60
WT	23.17 +/- 0.39	16.15 +/- 0.14	50.56 +/- 0.92
Half-Space	75.09 +/- 1.05	58.95 +/- 5.84	136.37 +/- 4.51

increase in apparent Qp values with the increase in the value of C is expected and observed. There is no obvious "best" group of apparent Qp values that result from the inversion process for the different values of the parameter C. The inversion process using a C = 1.0 did produce a better convergence towards a minimum in prediction errors than the other two inversions using C equal to 0.50 and 0.773.

The most revealing conclusion from the inversion process was based upon the parameter R. In this linear inversion study the parameter R was defined as

$$R = [1/n \sum_{i=1}^{n} (\Delta y_i / \sigma_i)^2]^{1/2} \qquad (10)$$

where:

y = difference between the observed value and the theoretical value of the data.

σ = associated standard deviation of the data.

n = total number of data points.

By weighting all the data correctly by their expected standard deviations we should see that

$$\Delta y_i / \sigma_i = 1 \qquad (11)$$

and so R should likewise be approximately unity. Thus for R = 1, the model is probably reasonable. If R is much less than one, either the estimates for sigma were too large and/or the model is too detailed (more eigenvalues and/or

parameters than are justified by the data). Conversely, for R much greater than unity, the estimates for sigma may have been underestimated and/or the model is too simplistic (too few parameters and/or eigenvalues).

The values of R resulting from the "best" starting values for the parameters for this study were equal to 19.86, 42.70 and 17.37 for the values of C equal to 0.5, 0.773 and 1.0 respectively. These are relatively high values and suggest that either the estimates of the uncertainties of the data were too low and/or the model was too simplistic (too few parameters and/or eigenvalues). Each average pulse width had associated with it an uncertainty of two standard deviations and so it is reasonable to assume that the estimates of uncertainty for the data were reasonable. It therefore seems that the model was too simple to give an accurate account of apparent Qp values for the Socorro area. The inversion suggests then that the geology of the area is structurally quite complex and the model requires a more realistic approximation of the actual physical situation if more accurate values of apparent Qp are to be obtained for the area.

Most other field applications of the rise time law have dealt with relatively small travel distances (on the order of meters) in homogeneous material (Ricker, 1953; Gladwin and Stacey, 1974; Kjartannson, 1978; Wright and Hoy, 1980; and Blair and Spathis, 1982). This study was conducted in a

faulted, and possibly subjected to recent small intrusions of magma to relatively shallow depths. It was not too surprising then that a model consisting of a low Q, low-velocity layer of varying thickness overlying a relatively high Q, high-velocity half-space would give results that imply too simplistic of a model.

Summary and Conclusions

First half-cycles of digitally recorded microearthquakes occurring near Socorro, New Mexico between January, 1977 and November, 1983 were used to obtain a measure of apparent Qp for the Socorro area. A series of criteria were established to select events for this study.

First, cross-correlations of the P-phase were used to separate events into duplicate groups. Second, a noise criterion was set so that events containing appreciable noise would be rejected. Next, a standardized technique was used in measuring the pulse widths. Any abnormally shaped waveforms were either separated from the "normal" group or rejected. Events with clipped waveforms were rejected because duration magnitudes were uncertain, but likely to be greater than imposed magnitude cutoff levels used as a fifth criterion. Events with magnitudes greater than these levels were considered to have some pulse broadening due to the source. Last, any event which displayed an unusual wave character preceding the onset was rejected.

Pulse widths for events in each group which met the above criteria were plotted against duration magnitudes. Groups which displayed an independence of pulse width with magnitude were considered to be free of source effects and thus contain only the response of the path and instrument. An average pulse width and associated standard deviation was calculated for each group.

Pulse broadening due to the instrument impulse response of the digital recording systems were measured in the laboratory and subtracted from the average pulse widths of the groups. Only path information was then contained in the average pulse widths.

The corrected average pulse widths were employed in the rise-time equation along with their respective hypocentral distances and average velocities along the raypaths. Average apparent Qp values were calculated using three different values for the parameter C in the rise time equation with C = 0.773 giving results that agree best with apparent Qp values of Carpenter (1984).

Next,a model consisting of a low Q, low-velocity layer of varying thickness overlying a relatively high Q, high-velocity half-space was constructed and the rise-time equation applied to this model. Apparent Qp values of the LVL under each station were taken from Carpenter (1984) and apparent Qp values for the half-space were calculated using raypath distances in the layer and the half-space which were

obtained from a graphical technique, a velocity of 3.4 km/sec and 5.85 km/sec for the layer and half-space velocities, respectively, and the corrected average pulse widths for the duplicate groups. Three values for the parameter C in the rise time equation that were applied in the first method were also used in this procedure. As the value of C was increased the apparent Qp values in the half-space became negative. This indicated that the values chosen for apparent Qp in the LVL under each station were too small and/or the LVL thicknesses were so large that all the pulse broadening was attributable to travel through the LVL. These negative apparent Qp values could also imply that the model itself is too simple. The half-space apparent Qp values for C = 0.773 ranged from an apparent Qp of -5254 to one of 614. This extreme scatter in the data suggests that the geology in the Socorro area is so varied and complex that the layer over a half-space model is inappropriate.

The third procedure was a linear inversion to obtain apparent Qp values for the LVL under each station and for the half-space. The inversion program was based on the same model as the second method and used the same values for raypath distances and velocities as well as the three values for C. The rise-time equation is non-linear in Q and so an iterative procedure was added to the linear inversion program in hopes of minimizing the prediction errors associated with the apparent Qp values. The inversion

process using C = 1.0 showed a convergent trend while the inversions using C equal to 0.5 and 0.773 did not. However, no obvious "best" group of apparent Qp values resulted from the inversion process for the different values of C. The scalar R parameter, which gives a measure of how reasonable the model is, was equal to 19.86, 42.70 and 17.37 for C equal to 0.50, 0.773 and 1.00, respectively. These relatively high values for R probably imply too simplistic a model.

Future studies employing pulse width measurements to obtain a measure of Q in the Socorro area should entail a more realistic model for the representation of the actual geologic setting. In general, reasonable values of average apparent Qp were obtained for whole path Qp. Attempts to define Qp for specific areas, however, proved inconclusive.

REFERENCES

Ake, J.P., An analysis of the May and July, 1983, Socorro Mountain microearthquake swarms, M.S. Independent Study, New Mexico Inst. of Mining and Technol., 1984.

Ake, J.P., A.R. Sanford and S.P. Jarpe, A magnitude scale for central New Mexico based on signal duration, New Mexico Inst. of Mining and Technol., Geophys. Open-file Report 45, Socorro, 1983.

Al-Sinawi, S., An investigation of body wave velocities, attenuation on elastic parameters of rocks subjected to pressure at room temperature, [Ph.D. thesis], St. Louis University, 1968.

Anstey, N.A., Seismic Interpretation: The Physical Aspect, International Human Resources Development Corporation, Boston, 1977.

Azimi, SH. A., A.V. Kalinin, V.V. Kalinin and B.L. Pivovarov, Impulse and transient characteristics of media with linear and quadratic equation laws, Izv., Earth Physics, No. 2, 42-54,1968.

Birch, F. and D. Bancroft, The effect of pressure on the rigidity of rocks, Jour. of Geol.,46, 59-87 and 113-141, 1938.

Blair, D.P. and A.T. Spathis, Seismic source influence in pulse attenuation studies,Jour. of Geophys. Res.,89, No. B11, 9253-9258, 1984.

Blair, D.P. and A.T. Spathis, Attenuation of explosion-generated in rock forces,Jour. of Geophys. Res.,87, No. B5, 3885-3892, 1982.

Boore, D.M., K.L. Larner and K. Aki, Comparison of two independent methods for the solution of wave-scattering problems:Response of a sedimentary basin to vertically incident SH waves,Jour. of Geophys. Res.,76, 558-569, 1971.

Born, W.T., The attenuation constant of earth materials, Geophysics, 6,132-148, 1941.

Brennan, B.J. and F.D. Stacey, Frequency dependence of elasticity of rock-Test of seismic velocity dispersion, Nature, 268, 220-222,1977.

Brune, J.N., Tectonic stress and the spectra of seismic shear waves from earthquakes, Jour. of Geophys. Res., 75, 4997-5009, 1970.

Caravella, F.J., A study of Poisson's ratio in the upper crust of the Socorro, New Mexico area, M.S. Independent Study, New Mexico Inst. of Mining and Technol., Geophys. Open-file Report 11, 1976.

Carpenter, E.W., Absorption of elastic waves - An operator for a constant Q mechanism: UK Atom. Ener. Auth. AWRE Rep. O-43/66, 1966.

Carpenter, P.J., Apparent Q for upper-crustal rocks in the Rio Grande rift of Central New Mexico from analysis of microearthquakes spectra, [Ph.D. thesis], New Mexico Inst. of Mining and Technol., Socorro, 1984.

Chamberlin, R.M., Cenozoic stratigraphy and structure of the Socorro Peak volcanic center, central New Mexico, New Mexico Bureau of Mines and Mineral Resources Open-file Report 118, 1980.

Chapin, C.E., Evolution of the Rio Grande Rift - a summary, in Reicker, R.E., ed., Rio Grande Rift: Tectonics and Magmatism, A.G.U., Wash. D.C., 1-5, 1979.

Chapin, C.E., R.M. Chamberlin, G.R. Osburn, A.R. Sanford and D.W. White, Exploration framework of the Socorro Geothermal Area, New Mexico, N. Mex. Geol. Soc. Spec. Publ. 7, 114-129, 1978.

Chapin, C.E. and W.R. Seager, Evolution of the Rio Grande rift in the Socorro and Las Cruces area, N. Mex. Geol. Soc. Field Conf. Guideb., 26, 297-321, 1975.

Collins, F. and C.C. Lee, Seismic wave attenuation characteristics from pulse experiments, Geophys., 21, 16-40, 1956.

Cordell, L., Regional geophysical setting of the Rio Grande rift, Geol. Soc. Amer. Bull., 89, 1073-1090, 1978.

Donato, R.J., P.N.S. O'Brien and M.J. Usher, Absorption and dispersion of elastic energy in rocks, Nature, 193, 764-765, 1962.

DeVilbuiss-Monoz, J.W., Wave dispersion and absorption in partially saturated rocks, [Ph.D. thesis], Stanford Univ., 1980.

Eggleston, T.L., D.I. Norman, C.E. Chapin and S. Savin, Geology, alteration, and genesis of the Luis Lopez manganese district, New Mexico, in C. Chapin, ed., N. Mex. Geol. Soc. Guideb. 34, 241-246, 1983.

Fender, J.J., A study of Poisson's ratio in the upper crust in the Socorro, New Mexico area, New Mexico Inst. of Mining and Technol., Geophys. Open-file Rep.

No. 25, 1978.

Frankel, A., The effects of attenuation and site response on the spectra of microearthquakes in the northeastern Caribbean, Bull. Seism. Soc. Am., 72, 1379-1402, 1982.

Frankel, A. and H. Kanamori, Determination of rupture duration and stress drop for earthquakes in southern California, Bull. Seism. Soc. Am., 73, 1527-1551, 1983.

Frishman, M.S., Use of linear inverse techniques to study Poisson's ratio in the upper crust in the Socorro, New Mexico area, New Mexico Inst. of Mining and Technol., Geophys. Open-file Report 27, 1979.

Fuchs, K. and G. Muller, Computation of synthetic seismograms with the reflectivity method and comparison with observations, Geophys. Jour. Roy. Astr. Soc., 23, 417-433, 1971.

Futterman, W.I., Dispersive body waves, Jour. of Geophys. Res., 67, 5277-5291, 1962.

Gardner, G.H.F., M.R.J. Wyllie and D.M. Droschak, Effects of pressure and fluid saturation on the attenuation of elastic waves in sands, Jour. of Petro. Technol., 16, 189-198, 1964.

Gladwin, M.T. and F.D. Stacey, Anelastic degradation of acoustic pulses in rock, Phys. Earth Plan. Int., 8, 332-333, 1974.

Gretenes, P.E.F., An analysis of the observed time discrepancies between continuous and conventional well velocity surveys, Geophys., 26,1-11, 1961.

Gordon, R.B. and D. Radar, Imperfect elasticity of rock: it's enfluence on the velocity of stress waves, Geophys. monographic series, 1971.

Gordon, R.B. and L.A. Davis, Velocity and attenuation of seismic waves in imperfectly elastic rock, Jour. of Geophys. Res., 73, 3917- 3935, 1968.

Hamilton, E.L., Compressional wave attenuation in marine sediments, Geophys., 37, 620-646, 1972.

Hanks, T.C., f max, Bull. Seism. Soc. Am., 72, 1867-1879, 1982.

Jackson, D.D., Interpretation of inaccurate, insufficient and inconsistent data, G.J.R.A.S. 28, 97-109, 1972.

Johnston, D.H. and M.N. Toksoz, Ultrasonic P and S wave attenuation in dry and saturated rocks under pressure, Jour. of Geophys. Res., 85, 925-936, 1980a.

Johnston, D.H. and M.N. Toksoz, Thermal cracking and amplitude dependent attenuation, Jour. of Geophys., 1980b.

Johnston, D.H., M.N. Toksoz and A. Timur, Attenuation of seismic waves in dry and saturated rocks: II. Mechanisms, Geophys., 44, 691-711, 1978.

Johnston, D.H. and M.N. Toksoz, Attenuation of seismic waves in dry and saturated rocks (abstract), Geophys., 42, 1511, 1977.

Kjartansson, E., Constant Q-wave propagation and attenuation, Jour. of Geophys. Res., 84, 4737-4748, 1979.

Klima, K., J. Vaneck and Z. Pros, The attenuation of longitudinal waves in diabase and graywacke under pressures up to 4 kilobars, Studia Geoph. et Geod., 8, 247-254, 1964.

Knopoff, L., Q, Rev. Geophys. Space Phys., 2, 625-660, 1964.

Knopoff, L. and G.J.F. MacDonald, Attenuation of small amplitude stress waves in solids, Rev. Mod. Phys., 30, 1178-1192, 1958.

Kolsky, H., The propagation of stress pulses in viscoelastic solids, Phys. Mag., 1, 693-710, 1956.

Kolsky, H., Stress Waves in Solids, Oxford University Press, Oxford, 1953.

Lee, W.H.K. and J.C. Fahr, HYP071 (revised): A computer program for determining hypocenter, magnitude, and first motion pattern of local earthquakes, U.S. Geological Survey, Open-file Report 75-31, 1975.

Levykin, A.I., Longitudinal and transverse wave absorbtion and velocity in rock specimens at multilateral pressures up to 4000 km/cm, USSR Geophys. Ser. (Engl. transl.), 1, Physics of the Solid Earth, 94-98, 1965.

Liu, H.P., D.L. Anderson and H. Kanamori, Velocity dispersion due to anelasticity: Implications for seismology and mantle composition, Geophys. Jour. Roy. Astr. Soc., 47, 41-58, 1976.

Lockner, D., J.B. Walsh and J. Byerlee, Changes in seismic velocity and attenuation during deformation of granite,

Jour. of Geophys. Res., 82, 5374-5378, 1977.

Lominitz, C., Linear dissipation in solids, Jour. Appl. Phys., 28, 201-205, 1957.

McDonal, F.J., F.A. Angona, R.L. Sengbush, R.G. van Nostrand and J.E. White, Attenuation of shear and compressional waves in Pierre shale, Geophys., 23, 421-439, 1958.

McKavanagh, B. and F.D. Stacey, Mechanical hysteresis in rocks at low strain amplitudes and seismic frequencies, Phys. Earth Plan. Int., 8, 246-250, 1974.

Menke, W., Geophysical Data Analysis: Discrete Inverse Theory, Academic Press, Inc., Orlando, 1984.

Munasinghe, M. and G.W. Farnell, Finite difference analysis of Rayleigh wave scattering at vertical discontinuities, Jour. of Geophys. Res., 78, 2454-2466, 1973.

Newton, C.A., D.J. Cash, K.H. Olsen and others, LASL seismic programs in the vicinity of Los Alamos, New Mexico, Los Alamos Scientic Laboratory Informal Report LA-6406-MS, 42, 1976.

Nur, A. and K. Winkler, The role of friction and fluid flow in wave attenuation in rocks (abst.), Geophys., 45, 591-592, 1980.

Nur, A. and G. Simmons, The effect of viscosity of a fluid phase on velocity in low porosity rocks, Earth Planet. Sci. Lett., 7, 99-108, 1969.

O'Brien, P.N.S., A discussion on the nature and magnitude of elastic absorbtion in seismic prospecting, Geophys. Prop., 261-273, 1960.

O'Connell, R.J. and B. Budiansky, Viscoelastic properties of fluid saturated cracked solids, Jour. of Geophys. Res., 82, 5719-5736, 1977.

Olsen, K.H., G.R. Keller and J.N. Stewart, Crustal structure along the Rio Grande rift from seismic refraction profiles, in R.E. Riecker, ed., Rio Grande Rift: Tectonics and Magmatism, Am. Geophys. Un., Wash., D.C., 127-143, 1979.

O'Neill, M.E., Source dimensions and stress drops of small earthquakes near Parkfield, California, Bull. Seism. Soc. Am.,74, 27-40, 1984.

Pandit, B.I. and J.C. Savage, An experimental test of Lomnitz's theory of internal friction in rocks, Jour.

of Geophys. Res., 78, 6097-6099, 1973.

Peselnick,L., H.P. Liu and K.R. Harper, Observations of details of hysteresis loops in Westerly granite, Geophys. Res. Lett., 6, 693-696, 1979.

Peselnick, L. and W.F. Outerbridge, Internal friction and rigidity modulus of Solenhofen limestone over a wide frequency range, USGS Prof., No. 400B, 1961.

Reilinger, R. and J. Oliver, Modern uplift associated with a proposed magma body in the vicinity of Socorro, New Mexico, Geology, 4, 573-586, 1976.

Reiter, M. and C.T. Smith, Subsurface temperature data in the Socorro Peak KGRA, New Mexico, Geothermal Magazine, 5, 37-41, 1977.

Rejas, A., Geology of the Cerros de Amado area, M.S. thesis, New Mexico Inst. of Mining and Technol., 1965.

Ricker, N., Transient Waves in Visco-Elastic Media, 278 pp., Elsevier, Amsterdam, 1977.

Ricker, N., The form and laws of propagation of seismic wavelets, Geophys., 18, 10-40, 1953.

Rinehart, E.J., The determination of an upper crustal model for the Rio Grande rift near Socorro, New Mexico, employing S-wave reflections produced by local microearthquakes, [Ph.D. thesis], New Mexico Inst. of Mining and Technol., Geophys. Open-file Report 29, 1979.

Rinehart, E.J. and A.R. Sanford, Upper crustal structure of the Rio Gran de rift near Socorro, New Mexico, from inversion of microearthquakeS-wave reflections, Bull. Seism. Soc. Am., 71, 437-450, 1981.

Sanford, A.R., J.P. Ake, S.P. Jarpe, P.J. Carpenter and L. Jaksha, Source independent spectra up to M = 1.2 implied from duplication of P- phase waveforms in a Rio Grande rift microearthquake swarm, New Mexico Inst. of Mining and Technol.,Geophys. Open-file Report 48, Socorro, 1983b.

Sanford, A.R., P.J. Carpenter and E.J. Rinehart, Characteristics of a microearthquake swarm in the Rio Grande rift near Socorro, New Mexico, New Mexico Inst. of Mining and Technol., Geophys. Open- file Report 43, Socorro, 1983c.

Sanford, A.R., K.H. Olsen and L.H. Jaksha, Seismicity of the Rio Grande rift, in R.L. Rieckey, ed., Rio Grande

Rift: Tectonics and Magmatism, Am. Geophys. Un., Washington, D.C., 145-168, 1979.

Sanford, A.R., R.P. Mott, Jr., P.J. Shuleski, E.J. Rinehart, F.J. Caravella, R.M. Ward and T.C. Wallace, Geophysical evidence for a magma body in the crust in the vicinity of Socorro, N.M., in Heacock, J.G. ed.,The Earth's Crust, Amer. Geophys. Union Monograph 20, Wash. D.C., 385-403, 1977.

Sanford, A.R., Gravity surveys in central Socorro County, New Mexico, N. Mex. Bureau of Mines and Mineral Resource, Circ. 91, Socorro, 1968.

Schreiber, E., O.L. Anderson and N. Soga, Elastic Constants and Their Measurements, McGraw-Hill Book Co., Inc., New York, 1973.

Sheriff, R.E., Encyclopedic Dictionary of Exploration of Geophysics, Society of Exploration Geophysicists, Tulsa, 1984.

Spencer, J.W, Jr., Stress relaxations at low frequencies in fluid saturated rocks: attenuation and modulus dispersion, Jour. of Geophys. Res., 1803-1812, 1981.

Spetzler, H. and D.L. Anderson, The effect of temperature and partial melting on velocity and attenuation in a simple binary system, Jour. of Geophys. Res., 73, 6051-6060, 1968.

Strick, E., An explanation of observed time discrepancies between continuous and conventional well velocity surveys, Geophysics, 36, 285-295, 1971.

Strick, E., A predicted pedestal effect for pulse propagation in constant Q solids, Geophysics, 35, 387-403, 1970.

Strick, E., The determination of Q, dynamic viscosity and creep curves from wave propagation measurements, Geophys. Jour. Roy. Astron. Soc., 13, 197-218, 1967.

Tittman, B.R., J. Nadler, V.A. Clark, L.A. Ahlberg and T.W. Spencer, Frequency dependence of seismic dissipation in saturated rocks, Geophys. Res. Lett., 8, 36-38, 1981.

Tittman, B.R., Internal friction measurements and their implications in seismic Q structure models of the crust, in J.G.Heacock, ed., The Earth's Crust, Am. Geophys. Un. Mon. 20, 197-213, 1977.

Toksoz, M.N. and D.H. Johnston, Seismic Wave Attenuation, Society of Exploration Geophysicists, Tulsa, 1981.

Toksoz, M.N., D.H. Johnston and A. Timur, Attenuation of seismic waves in dry and saturated rocks. I. Laboratory measurements, Geophysics, 44, 681-690, 1979.

Usher, M.J., Elastic behavior of rocks at low frequencies, Geophys. Prosp., 10, 119-127, 1962.

Volarvich, M.P. and G.I. Gurevich, Investigation of dynamic moduli of elasticity for rocks in relation to temperature, Bull. Aca. Sci. USSR, Geophysics, 4, 1-9, 1957.

Walsh, J.B., W.F. Brace and W.R. Wawersik, Attenuation of stress waves in Cedar City quartz diorite, Air Force Weapons Lab. Tech. Rep. AFWL-TR-70-8, 1970.

Walsh, J.B., Seismic wave attenuation in rocks due to friction, Jour. of Geophys. Res., 71, 2591-2599, 1966.

Ward, R.M., Determination of three-dimensional velocity anomalies within the upper crust in the vicinity of Socorro, New Mexico, using first P-arrival times from local earthquakes, [Ph.D.thesis], New Mexico Inst. of Mining and Technol., Geophys. Open-file Report 34b, 1980.

Ward, R.M., J.W. Schlue and A.R. Sanford, Three dimensional velocity anomalies in the upper crust near Socoro, New Mexico, Geophys. Res. Lett., 8, 553-556, 1981.

White, J.E., Static friction as a source of seismic attenuation, Geophysics, 31, 333-339, 1966.

Winkler, K. and A. Nur, Poor fluids and seismic attenuations in rocks, Geophys. Res. Lett., 6, 1-4, 1979.

Wright, C. and D. Hoy, A note on pulse broadening and anelastic attenuation in near-surface rocks, Phys. Earth Planet. Inter., 25, 1-8, 1981.

Wyllie, M.R.J., G.H.F. Gardner and A.R. Gregory, Studies of elastic wave attenuation in porous media, Geophysics, 27, 569-589, 1962.

Zemanek, J. and I. Rudnick, Attenuation and dispersion of elastic waves in a cylindrical bar, Jour. Acoust. Soc. Am., 33, 1283-1288, 1961.

Zener, C., Elasticity and anelasticity of metals, University of Chicago, Chicago, 1948.

Appendix 1

This appendix contains a listing of the measured and corrected average pulse widths and associated recording instruments and filter settings used. The pulse broadening due to the impulse responses of the two recording systems for a one millisecond input pulse for the various filter settings is also tabulated. The one millisecond input pulse has not been subtracted from the pulse broadening values.

Appendix 1a. Listing of the measured and corrected average pulse widths and associated recording instruments and filter settings.

GROUP	DATES	TAU (MEASURED)	INSTRUMENT DR100	INSTRUMENT DR100A	FILTER SETTING LOW	FILTER SETTING HIGH	TAU (CORRECTED)
77-2	30/05/77-02/06/77	0.0221	X		05	00	0.0164
77-3	14/07/77	0.0429	X		00	00	0.0350
77-4	17/07/77	0.0352	X		00	00	0.0273
77-5	17/08/77-18/08/77	0.0357	X		00	00	0.0278
77-13	14/06/77-15/06/77	0.0327	X		05	30	0.0208
77-15	16/08/77-17/08/77	0.0382	X		00	00	0.0303
77-16	28/08/77	0.0318	X		00	00	0.0239
77-17	29/08/77	0.0515	X		00	00	0.0436
77-18	05/10/77-11/10/77	0.0268	X		00	00	0.0189
81-4	17/06/81	0.0442	X		00	30	0.0288
81-5A	18/06/81-19/06/81	0.0441	X		00	30	0.0287
81-5B	20/06/81-05/07/81	0.0432	X		00	30	0.0188
83-1	14/05/83-30/05/83	0.0374		X	00	30	0.0126
83-3	29/05/83-30/05/83	0.0307		X	00	30	0.0066
83-5	11/06/83-12/06/83	0.0319		X	00	30	0.0071
83-6	11/06/83	0.0331		X	00	30	0.0083
83-8A	14/07/83-15/07/83	0.0369		X	00	30	0.0121
83-8B	14/07/83-15/07/83	0.0374		X	00	30	0.0126
83-8C	14/07/83	0.0357		X	00	30	0.0100
83-9	16/07/83	0.0372		X	00	30	0.0124
83-10	16/07/83-20/07/83	0.0374		X	00	30	0.0126
83-11	16/07/83	0.0370		X	00	30	0.0122
83-13A	16/07/83-20/07/83	0.0378		X	00	30	0.0130
83-13B	16/07/83-17/07/83	0.0375		X	00	30	0.0127
83-15	19/07/83	0.0477		X	00	30	0.0229

Appendix 1b. Listing of the pulse broadening due to the input responses of the two recording systems. The 1 millisecond input pulses have not been subtracted from these values.

Filter setting		DR100	DR100A
low	high	(sec.)	(sec.)
00	00	0.0089	0.0204
05	00	0.0067	0.0176
00	30	0.0164	0.0291
05	30	0.0129	0.0223

Appendix 2

This appendix contains a listing of the P-phase and full-wave cross-correlation coefficients for events in this study. A cross-correlation coefficient of 1.000 signifies an event was used as the master in the cross-correlation. Also listed is the noise criterion for events and the reason an event was rejected from the study, the possible reasons being:

1) P-phase cross-correlation coefficient less than 0.700.

2) Twice the standard deviation of the average amplitude of 35 data points preceding the onset of an event which is greater than 10% of the maximum amplitude of the first half-cycle of the event.

3) Abnormal shape of the first half-cycle of an event.

4) Clipped waveform.

5) Magnitude of an event exceeded the magnitude cutoff level for source independence for a specific station.

6) Unusual wave character preceding the onset of an event.

Appendix 2. Listing of P-phase and full-wave cross-correlation coefficients for events of this study. Noise criterion and reason for rejection of event also listed.

GROUP	EVENT DATE & TIME	STATION	P-PHASE COEFF.	FULL-WAVE COEFF.	NOISE CRITERION	REJECTED EVENTS 1	2	3	4	5	6
77-2											
	02-JUN-77 065041	SC	1.000	1.000	0.0014				X		
	02-JUN-77 065349	SC	0.777	0.831	0.0649						
	02-JUN-77 065523	SC	0.820	0.690	0.0061						
	02-JUN-77 114205	SC	0.923	0.788	0.0225						
	30-MAY-77 065553	SC	0.815	-----	0.0146						
	30-MAY-77 070053	SC	0.568	-----	0.0515	X					
	30-MAY-77 070757	SC	0.722	-----	0.0188						
	30-MAY-77 071235	SC	0.831	-----	0.0087				X		
	30-MAY-77 071339	SC	0.920	-----	0.0302						
	30-MAY-77 071613	SC	0.905	-----	0.0102				X		
	30-MAY-77 072519	SC	0.722	-----	0.0103				X		
	30-MAY-77 071645	SC	0.863	-----	0.0100				X		
	30-MAY-77 091627	SC	0.807	-----	0.0230						
	30-MAY-77 100331	SC	-0.878	-----	0.0038				X		
	30-MAY-77 070327	SC	-0.684	-----	0.0389	X					
	30-MAY-77 071533	SC	-0.917	-----	0.0320						
77-3											
	14-JUL-77 023407	DM	1.000	1.000	0.0203						
	14-JUL-77 100035	DM	0.765	0.250	0.0169						
	14-JUL-77 113159	DM	0.986	0.955	0.0145						
77-4											
	17-AUG-77 153725	CC	1.000	1.000	0.0102						
	17-AUG-77 155303	CC	0.925	0.556	0.0444						
77-5											
	17-AUG-77 060323	CC	1.000	1.000	0.0041						
	18-AUG-77 093019	CC	0.950	0.843	0.0156						
77-6											
	18-AUG-77 103819	CC	1.000	1.000	0.0269			X			
	18-AUG-77 103915	CC	0.810	0.383	0.0683						
77-7											
	18-AUG-77 103915	WT	1.000	1.000	0.0493						X
	18-AUG-77 103819	WT	0.791	0.830	0.0063						X
	18-AUG-77 103853	WT	0.508	0.628	0.7976	X					
	19-AUG-77 035103	WT	0.608	0.745	0.0307	X					
	26-AUG-77 103301	WT	0.306	0.667	0.2444	X					
77-8											
	22-SEP-77 052035	WT	1.000	1.000	0.0624						
	22-SEP-77 191933	WT	0.389	0.689	------	X					
77-9											
	30-MAY-77 065553	CC	1.000	1.000	0.1313		X				
	30-MAY-77 070055	CC	0.850	0.308	0.3754		X				
	30-MAY-77 070119	CC	0.888	0.637	0.0092						
77-13											
	14-JUN-77 234649	CM	1.000	1.000	0.0088						

GROUP	EVENT DATE & TIME	STATION	P-PHASE COEFF.	FULL-WAVE COEFF.	NOISE CRITERION	REJECTED EVENTS 1 2 3 4 5 6
	15-JUN-77 030921	CM	0.965	0.949	0.0034	
	15-JUN-77 054715	CM	0.776	0.886	0.1249	X
77-14						
	13-AUG-77 190657	WT	1.000	1.000	0.0660	
	13-AUG-77 191109	WT	0.474	0.689	0.2340	X
	14-AUG-77 024527	WT	0.586	0.662	0.1178	X
	14-AUG-77 054551	WT	0.214	0.584	0.0903	X
	14-AUG-77 063419	WT	0.275	0.593	1.2834	X
	14-AUG-77 064813	WT	0.321	0.628	0.0219	X
	14-AUG-77 221649	WT	0.595	0.740	0.1459	X
	17-AUG-77 043655	WT	0.734	0.661	0.1256	X
	27-AUG-77 021311	WT	0.292	0.526	0.1469	X
77-15						
	16-AUG-77 154927	CC	1.000	1.000	0.0201	
	16-AUG-77 120833	CC	0.919	0.747	0.0268	
77-16						
	28-AUG-77 013207	WT	1.000	1.000	0.0124	
	28-AUG-77 015633	WT	0.831	0.800	0.0394	
77-17						
	29-AUG-77 014231	DM	1.000	-----	0.0128	
	29-AUG-77 035643	DM	0.739	-----	0.0394	
77-18						
	05-OCT-77 051727	SC	1.000	1.000	0.0126	
	08-OCT-77 050309	SC	0.725	0.763	0.0155	
	11-OCT-77 043823	SC	0.756	0.860	0.0000	
77-19						
	12-OCT-77 210017	FM	1.000	-----	0.0069	X
	12-OCT-77 212033	FM	0.969	-----	0.0171	X
77-20						
	25-OCT-77 125225	FM	1.000	1.000	0.0046	X
	25-OCT-77 150331	FM	0.515	0.855	0.0210	X
77-21						
	09-NOV-77 070101	FM	1.000	1.000	0.1114	X
	09-NOV-77 071207	FM	0.931	0.448	0.0591	
77-22						
	09-NOV-77 071205	CM	1.000	1.000	0.0023	
	09-NOV-77 102909	CM	0.853	0.470	0.0188	
81-1						
	29-MAR-81 065935	SNM	1.000	-----	0.0174	X
	30-MAR-77 065934	SNM	0.853	-----	0.0166	X
81-2						
	16-JUN-81 064955	SNM	1.000	-----	0.0175	X
	16-JUN-81 075529	SNM	0.830	-----	0.0567	X
	16-JUN-81 120437	SNM	0.356	-----	0.1508	X
81-3						
	17-JUN-81 203031	IC	1.000	-----	0.0309	
	17-JUN-81 213651	IC	0.900	-----	0.0063	
	17-JUN-81 213707	IC	0.873	-----	0.0781	
	17-JUN-81 230727	IC	0.908	-----	0.0018	X
	18-JUN-81 014235	IC	0.804	-----	0.0327	
81-4						
	17-JUN-81 203033	SC	1.000	-----	0.0359	
	17-JUN-81 213639	SC	0.972	-----	0.0091	
	17-JUN-81 230721	SC	0.987	-----	0.0022	X
81-5						

GROUP	EVENT DATE & TIME	STATION	P-PHASE COEFF.	FULL-WAVE COEFF.	NOISE CRITERION	REJECTED EVENTS 1 2 3 4 5 6
	18-JUN-81 101925	IC	1.000	-----	0.0014	
	19-JUN-81 182847	IC	0.893	-----	0.0270	
	*20-JUN-81 162247	IC	0.899	-----	0.0053	
	22-JUN-81 024057	IC	0.877	-----	0.0086	X
	22-JUN-81 024115	IC	0.879	-----	0.0049	X
	*22-JUN-81 024345	IC	0.901	-----	0.0037	
	*05-JUL-81 112259	IC	0.783	-----	0.0037	
81-6						
	20-JUN-81 162247	SNM	-----	-----	0.3835	X
	20-JUN-81 024345	SNM	-----	-----	0.1273	X
83-1						
	14-MAY-83 010216	WT	1.000	1.000	0.0385	
	14-MAY-83 010830	WT	0.860	0.879	0.0012	X
	14-MAY-83 023914	WT	0.963	0.920	0.1195	X
	14-MAY-83 024142	WT	0.949	0.936	0.0422	
	14-MAY-83 040244	WT	0.939	0.882	0.0232	
	14-MAY-83 050202	WT	0.819	0.919	0.0326	
	14-MAY-83 052416	WT	0.784	0.915	0.0697	X
	14-MAY-83 081126	WT	0.764	0.865	0.0576	
	14-MAY-83 144318	WT	0.856	0.880	0.0236	
	14-MAY-83 025452	WT	0.916	0.868	0.0604	X
	14-MAY-83 083704	WT	0.802	0.883	0.0786	
	14-MAY-83 084938	WT	0.776	0.835	0.0340	
	14-MAY-83 030000	WT	-----	0.851	0.1285	X
	14-MAY-83 040320	WT	-----	0.929	0.1038	X
	30-MAY-83 050722	WT	0.918 .	0.925	0.0254	
83-2						
	29-MAY-83 041636	WT	1.000	1.000	0.0018	X
	29-MAY-83 050652	WT	0.523	0.725	0.0017	X
83-3						
	29-MAY-83 053153	WT	1.000	1.000	0.0081	
	29-MAY-83 055412	WT	0.965	0.850	0.0022	X
	29-MAY-83 060520	WT	0.837	0.682	0.0375	
	29-MAY-83 064812	WT	0.982	0.941	0.0181	
	30-MAY-83 074507	WT	0.927	0.898	0.0005	X
83-4						
	08-JUN-83 075808	WT	-----	1.000	0.1814	X
	08-JUN-83 093600	WT	-----	0.976	0.1091	X
	09-JUN-83 062951	WT	1.000	0.939	0.0339	X
	09-JUN-83 090558	WT	0.742	0.911	0.0888	X
	09-JUN-83 083936	WT	0.824	0.932	0.0465	X
	09-JUN-83 062134	WT	0.856	0.854	0.0182	X
83-5						
	11-JUN-83 100319	WT	1.000	1.000	0.0236	
	11-JUN-83 114310	WT	0.932	0.948	0.0185	
	11-JUN-83 120423	WT	0.959	0.902	0.0132	
	11-JUN-83 125737	WT	0.971	0.953	0.0216	
	12-JUN-83 223221	WT	0.979	0.840	0.0853	
83-6						
	11-JUN-83 104743	WT	1.000	1.000	0.0614	
	11-JUN-83 105603	WT	0.867	0.919	0.0329	
83-7						
	11-JUN-83 130945	WT	-----	1.000	0.0575	
	11-JUN-83 132051	WT	-----	0.851	0.1113	X
83-8						

GROUP	EVENT DATE & TIME	STATION	P-PHASE COEFF.	FULL-WAVE COEFF.	NOISE CRITERION	REJECTED EVENTS 1 2 3 4 5 6
	A14-JUL-83 055229	WT	1.000	1.000	0.0369	
	14-JUL-83 110945	WT	0.680	0.578	0.0106	X
	14-JUL-83 113948	WT	0.853	0.793	0.0274	X
	A14-JUL-83 161755	WT	0.927	0.776	0.0363	
	B15-JUL-83 085104	WT	0.898	0.442	0.0042	
	B15-JUL-83 063609	WT	0.914	0.843	0.0383	
	A14-JUL-83 064957	WT	0.828	0.781	0.0146	
	B14-JUL-83 081017	WT	0.957	0.883	0.0117	
	A14-JUL-83 081407	WT	0.827	0.746	0.0209	
	B14-JUL-83 084647	WT	0.916	0.850	0.0713	
	B14-JUL-83 112333	WT	0.932	0.852	0.0073	
	C14-JUL-83 124242	WT	0.951	0.853	0.0207	
	14-JUL-83 135114	WT	0.938	0.777	0.0945	X
	A14-JUL-83 135126	WT	0.897	0.814	0.0202	
	C14-JUL-83 161323	WT	0.980	0.838	0.0398	
	B14-JUL-83 194904	WT	0.891	0.810	0.0860	
	A14-JUL-83 210553	WT	0.852	0.892	0.0482	
	A14-JUL-83 043238	WT	0.831	0.807	0.0112	
	A15-JUL-83 051410	WT	0.816	0.765	0.0101	
83-9						
	16-JUL-83 013113	WT	1.000	1.000	0.0274	
	16-JUL-83 064412	WT	0.955	0.642	0.0093	
83-10						
	20-JUL-83 014607	WT	1.000	1.000	0.0345	
	20-JUL-83 015202	WT	0.795	0.363	0.0215	
	20-JUL-83 041107	WT	0.792	0.344	0.0259	
	20-JUL-83 152552	WT	0.783	0.233	0.0994	
	20-JUL-83 152552*	WT	0.814	-----	0.1296	X
	20-JUL-83 154322	WT	0.792	0.258	0.0496	
	16-JUL-83 061207	WT	0.776	0.382	0.0054	X
	16-JUL-83 085950	WT	0.727	0.394	0.0007	X
	20-JUL-83 013031	WT	0.831	0.255	0.0106	
	20-JUL-83 004155	WT	0.827	0.259	0.0028	X
	15-JUL-83 200213	WT	0.746	0.242	0.0487	
	16-JUL-83 032147	WT	0.720	0.329	0.0856	X
	20-JUL-83 010026	WT	0.828	0.264	0.0306	
83-11						
	16-JUL-83 032849	WT	1.000	1.000	0.0041	
	16-JUL-83 043554	WT	0.915	0.922	0.0117	
83-12						
	16-JUL-83 043637	WT	1.000	1.000	0.0930	X
	16-JUL-83 061024	WT	0.791	0.541	0.0268	X
	16-JUL-83 061024*	WT	0.836	0.673	0.0418	X
83-13						
	A16-JUL-83 033026	WT	1.000	1.000	0.0019	
	B16-JUL-83 063234	WT	0.919	0.863	0.0040	
	B16-JUL-83 064412	WT	0.886	0.813	0.0093	
	A16-JUL-83 074504	WT	0.965	0.893	0.0074	
	B16-JUL-83 074504*	WT	0.881	0.808	0.0813	
	B16-JUL-83 080659	WT	0.883	0.637	0.0349	
	A16-JUL-83 125535	WT	0.866	0.546	0.0257	
	B16-JUL-83 150554	WT	0.913	0.572	0.0322	
	16-JUL-83 173952	WT	0.937	0.493	0.0046	X
	B16-JUL-83 215020	WT	0.863	0.638	0.0088	
	B16-JUL-83 222040	WT	0.846	0.661	0.0249	

GROUP	EVENT DATE & TIME	STATION	P-PHASE COEFF.	FULL-WAVE COEFF.	NOISE CRITERION	REJECTED EVENTS 1 2 3 4 5 6
	A16-JUL-83 222816	WT	0.925	0.446	0.0090	
	16-JUL-83 224850	WT	0.832	0.643	0.0005	X
	B16-JUL-83 225218	WT	0.863	0.282	0.0133	
	B16-JUL-83 230054	WT	0.845	0.814	0.0177	
	B17-JUL-83 010301	WT	0.770	0.334	0.0058	
	A17-JUL-83 024240	WT	0.931	0.683	0.0017	
	B17-JUL-83 024404	WT	0.858	0.806	0.0083	
	B17-JUL-83 041904	WT	0.917	0.410	0.0434	
	A17-JUL-83 054522	WT	0.930	0.327	0.0084	
	A17-JUL-83 061512	WT	0.906	0.409	0.0056	
	B17-JUL-83 121303	WT	0.811	0.680	0.0286	
	A17-JUL-83 140653	WT	0.949	0.408	0.0097	
	B17-JUL-83 141324	WT	0.912	0.287	0.0169	
	A17-JUL-83 142709	WT	0.954	0.304	0.0108	
	B17-JUL-83 155058	WT	0.885	0.326	0.0231	
	A17-JUL-83 212547	WT	0.835	0.291	0.0309	
	A17-JUL-83 224531	WT	0.908	0.373	0.0013	
	A17-JUL-83 232656	WT	0.822	0.331	0.0252	
	A20-JUL-83 165028	WT	0.845	0.486	0.0144	
	A18-JUL-83 013858	WT	0.878	0.497	0.0095	
	A18-JUL-83 110937	WT	0.894	0.601	0.0110	
	A19-JUL-83 212922	WT	0.883	0.484	0.0401	
	20-JUL-83 165716	WT	0.878	0.420	0.0142	X
	A20-JUL-83 172246	WT	0.887	0.389	0.0132	
	B16-JUL-83 220910	WT	0.863	0.675	0.0276	
	16-JUL-83 031037	WT	0.902	0.637	0.0190	X
	17-JUL-83 113258	WT	0.890	0.378	0.0003	X
	A17-JUL-83 113545	WT	0.932	0.435	0.0102	
	20-JUL-83 004155	WT	0.952	0.688	0.0028	X
	A20-JUL-83 041107	WT	0.947	0.662	0.0259	
	16-JUL-83 085950	WT	0.900	0.698	0.0007	X
	A16-JUL-83 043554	WT	0.946	0.287	0.0117	
	B16-JUL-83 043647	WT	0.729	0.776	0.0936	
	17-JUL-83 145309	WT	-----	0.319	0.1390	X
	16-JUL-83 220613	WT	-----	0.399	0.1241	X
83-14						
	18-JUL-83 175922	WT	-----	1.000	0.2828	X
	18-JUL-83 200029	WT	-----	0.711	0.3513	X
	18-JUL-83 200034	WT	-----	0.620	0.4877	X
	18-JUL-83 201217	WT	-----	0.641	0.1735	X
83-15						
	18-JUL-83 215100	WT	-----	1.000	0.3166	X
	19-JUL-83 005647	WT	-----	0.880	0.1194	X
	19-JUL-83 024715	WT	1.000	0.836	0.0778	
	19-JUL-83 024957	WT	-----	0.863	0.1050	X
	19-JUL-83 025313	WT	0.905	0.875	0.0853	
	19-JUL-83 025707	WT	0.973	0.749	0.0301	
	19-JUL-83 030009	WT	-----	0.765	0.6015	X
	19-JUL-83 032953	WT	-----	0.903	0.1250	X
	19-JUL-83 032847	WT	-----	0.857	0.2967	X
	19-JUL-83 033945	WT	0.774	0.320	0.0318	
	19-JUL-83 034125	WT	-----	0.718	0.1884	X
	19-JUL-83 034325	WT	0.759	0.415	0.0605	
	19-JUL-83 034733	WT	0.922	0.707	0.0750	
	19-JUL-83 035447	WT	-----	0.823	0.2395	X

GROUP	EVENT DATE & TIME	STATION	P-PHASE COEFF.	FULL-WAVE COEFF.	NOISE CRITERION	REJECTED EVENTS 1 2 3 4 5 6
	19-JUL-83 035509	WT	0.936	0.812	0.0798	
	19-JUL-83 040045	WT	0.762	0.181	0.0946	
	19-JUL-83 040327	WT	0.825	0.375	0.0671	
	19-JUL-83 040533	WT	0.701	0.580	0.0576	
	19-JUL-83 040609	WT	-----	0.454	0.2667	X
	19-JUL-83 042535	WT	0.876	0.722	0.0143	
	19-JUL-83 044633	WT	0.976	0.754	0.0268	
83-16						
	20-JUL-83 185217	WT	1.000	1.000	0.0570	X
	20-JUL-83 185342	WT	0.749	0.908	0.0345	
	20-JUL-83 030237	WT	0.577	0.870	0.0442	X
83-17						
	26-JUL-83 124902	WT	1.000	1.000	0.0026	
	26-JUL-83 175503	WT	0.976	0.961	0.0019	

Appendix 3

This appendix contains a listing of the measured pulse widths, their associated estimated errors, magnitudes, digital amplitudes and gain settings for events which displayed an independence of pulse width with magnitude.

Appendix 3. Listing of measured pulse widths, their estimated errors (sigma +/-), magnitudes, digital amplitudes and gain settings for events which displayed an independence of pulse width with magnitude.

GROUP	EVENT DATE/TIME/STATION	TAU (MEASURED)	SIGMA (+/-)	MAGNITUDE	DIGITAL AMPLITUDE	GAIN
77-2						
	02-JUN-77 065349 SC	0.0248	0.0023	-1.32	177	84
	02-JUN-77 065523 SC	0.0213	0.0008	-0.91	368	84
	02-JUN-77 114205 SC	0.0205	0.0015	-1.32	179	84
	30-MAY-77 065553 SC	0.0217	0.0010	-0.06	1704	84
	30-MAY-77 070757 SC	0.0217	0.0021	0.00	1926	84
	30-MAY-77 071339 SC	0.0214	0.0004	-0.63	613	84
	30-MAY-77 091627 SC	0.0237	0.0014	-0.85	417	84
	30-MAY-77 071533 SC	0.0219	0.0006	-0.63	613	84
77-3						
	14-JUL-77 023407 DM	0.0435	0.0010	-0.20	80	72
	14-JUL-77 100035 DM	0.0418	0.0016	-0.09	151	72
	14-JUL-77 113159 DM	0.0435	0.0012	-0.20	118	72
77-4						
	17-AUG-77 153725 CC	0.0348	0.0019	0.21	408	84
	17-AUG-77 155303 CC	0.0356	0.0012	-0.21	190	84
77-5						
	17-AUG-77 060323 CC	0.0355	0.0020	0.32	817	84
	18-AUG-77 093019 CC	0.0359	0.0026	-0.59	147	84
77-13						
	14-JUN-77 234649 CM	0.0343	0.0018	-0.19	341	72
	15-JUN-77 030921 CM	0.0311	0.0015	0.28	791	72
77-15						
	16-AUG-77 154927 CC	0.0386	0.0027	0.64	819	84
	16-AUG-77 120833 CC	0.0377	0.0021	0.47	384	84
77-16						
	28-AUG-77 013207 WT	0.0316	0.0019	-0.14	329	84
	28-AUG-77 015633 WT	0.0320	0.0010	-0.52	176	84
77-17						
	29-AUG-77 014231 DM	0.0520	0.0012	-0.32	358	84
	29-AUG-77 035643 DM	0.0509	0.0009	-0.71	150	84
77-18						
	05-OCT-77 051727 SC	0.0269	0.0010	-0.05	350	66
	08-OCT-77 050309 SC	0.0251	0.0020	-0.39	158	66
	11-OCT-77 043823 SC	0.0285	0.0033	-0.31	181	66
77-22						
	09-NOV-77 071205 CM	0.0447	0.0019	0.41	988	60
	09-NOV-77 102909 CM	0.0521	0.0008	-0.95	87	60
81-3						
	17-JUN-81 203031 IC	0.0367	0.0019	-0.05	541	72
	17-JUN-81 213651 IC	0.0403	0.0009	0.30	900	72
	17-JUN-81 213707 IC	0.0394	0.0013	-0.39	331	72
	18-JUN-81 014235 IC	0.0427	0.0021	-1.22	102	72
81-4						
	17-JUN-81 203033 SC	0.0440	0.0019	-0.76	197	72

	17-JUN-81 213639	SC	0.0443	0.0014	-0.29	382	72
81-5							
	B18-JUN-81 101925	IC	0.0354	0.0019	0.58	1313	72
	B19-JUN-81 182847	IC	0.0329	0.0020	-1.15	112	72
	A20-JUN-81 162247	IC	0.0431	0.0021	-0.07	527	72
	A22-JUN-81 024345	IC	0.0450	0.0013	0.60	1340	72
	A05-JUL-81 112259	IC	0.0442	0.0010	-0.78	128	72
83-1							
	14-MAY-83 010216	WT	0.0354	0.0023	-1.36	533	84
	14-MAY-83 024142	WT	0.0367	0.0009	-0.20	992	84
	14-MAY-83 040244	WT	0.0369	0.0023	-1.56	425	84
	14-MAY-83 050202	WT	0.0389	0.0022	-1.68	496	84
	14-MAY-83 081126	WT	0.0381	0.0008	-1.68	234	84
	14-MAY-83 144318	WT	0.0363	0.0019	-0.09	1696	84
	14-MAY-83 083704	WT	0.0386	0.0013	-1.81	274	84
	14-MAY-83 084938	WT	0.0383	0.0006	-1.88	233	84
	30-MAY-83 050722	WT	0.0371	0.0023	-1.62	341	84
83-3							
	29-MAY-83 053153	WT	0.0314	0.0018	-0.67	1197	84
	29-MAY-83 060520	WT	0.0293	0.0018	-1.46	199	84
	29-MAY-83 064812	WT	0.0314	0.0021	-1.56	292	84
83-5							
	11-JUN-83 100319	WT	0.0320	0.0016	-0.97	413	84
	11-JUN-83 114310	WT	0.0330	0.0010	-0.41	204	84
	11-JUN-83 120423	WT	0.0298	0.0021	-0.78	736	84
	11-JUN-83 125737	WT	0.0319	0.0019	-0.84	597	84
	12-JUN-83 223221	WT	0.0328	0.0025	-1.11	288	84
83-6							
	11-JUN-83 104743	WT	0.0331	0.0018	-2.11	167	84
	11-JUN-83 105603	WT	0.0330	0.0013	-2.30	325	84
83-8A							
	14-JUL-83 055229	WT	0.0363	0.0021	-1.74	208	78
	14-JUL-83 161755	WT	0.0370	0.0020	-1.46	269	78
	14-JUL-83 064957	WT	0.0386	0.0009	-1.04	256	78
	14-JUL-83 081407	WT	0.0357	0.0011	-2.30	118	78
	14-JUL-83 135126	WT	0.0365	0.0009	-0.84	278	78
	14-JUL-83 210553	WT	0.0384	0.0021	-1.64	173	78
	14-JUL-83 043238	WT	0.0382	0.0013	-1.46	301	78
	15-JUL-83 051410	WT	0.0346	0.0031	-1.36	263	78
83-8B							
	15-JUL-83 085104	WT	0.0364	0.0026	-1.04	512	78
	15-JUL-83 063609	WT	0.0376	0.0032	-2.11	104	78
	14-JUL-83 081017	WT	0.0374	0.0026	-0.78	304	78
	14-JUL-83 084647	WT	0.0376	0.0029	-2.11	61	78
	14-JUL-83 112333	WT	0.0376	0.0027	-0.52	392	78
	14-JUL-83 194904	WT	0.0376	0.0026	-0.92	338	78
83-8C							
	14-JUL-83 124242	WT	0.0359	0.0016	-0.88	344	78
	14-JUL-83 161323	WT	0.0355	0.0014	-1.68	208	78
83-9							
	16-JUL-83 013113	WT	0.0376	0.0026	-1.95	255	78
	16-JUL-83 064412	WT	0.0368	0.0018	-1.95	255	78
83-10							
	20-JUL-83 014607	WT	0.0338	0.0011	-1.81	236	78
	20-JUL-83 015202	WT	0.0362	0.0016	-1.46	290	78

	20-JUL-83 041107	WT	0.0385	0.0012	-2.11	320	78
	20-JUL-83 152552	WT	0.0331	0.0014	-1.38	348	78
	20-JUL-83 154322	WT	0.0366	0.0010	-1.98	210	78
	20-JUL-83 013031	WT	0.0314	0.0010	-1.68	250	78
	15-JUL-83 200213	WT	0.0257	0.0011	-1.95	128	78
	20-JUL-83 010026	WT	0.0336	-0.0009	-1.95	252	78
83-11							
	16-JUL-83 032849	WT	0.0370	0.0012	-1.46	303	78
	16-JUL-83 043554	WT	0.0370	0.0008	-1.04	402	78
83-13A							
	16-JUL-83 033026	WT	0.0382	0.0015	-0.13	972	78
	16-JUL-83 074504	WT	0.0387	0.0013	-2.20	180	78
	16-JUL-83 125535	WT	0.0370	0.0028	-2.30	127	78
	16-JUL-83 222816	WT	0.0383	0.0002	-2.30	137	78
	17-JUL-83 024240	WT	0.0418	0.0030	-0.52	609	78
	17-JUL-83 054522	WT	0.0376	0.0020	-1.27	219	78
	17-JUL-83 061512	WT	0.0371	0.0012	-1.81	215	78
	17-JUL-83 140653	WT	0.0384	0.0005	-1.68	201	78
	17-JUL-83 142709	WT	0.0397	0.0010	-0.43	638	78
	17-JUL-83 212547	WT	0.0321	0.0019	-2.30	152	78
	17-JUL-83 224531	WT	0.0379	0.0021	0.00	1856	78
	17-JUL-83 232656	WT	0.0357	0.0021	-2.11	192	78
	20-JUL-83 165028	WT	0.0342	0.0017	-0.30	808	78
	18-JUL-83 013858	WT	0.0374	0.0025	-2.40	177	78
	18-JUL-83 110937	WT	0.0362	0.0012	-1.68	326	78
	19-JUL-83 212922	WT	0.0310	0.0015	-2.11	348	78
	20-JUL-83 172246	WT	0.0383	0.0029	-0.59	636	78
	17-JUL-83 113545	WT	0.0389	0.0027	-1.46	312	78
	20-JUL-83 041107	WT	0.0385	0.0012	-2.11	320	78
	16-JUL-83 043554	WT	0.0368	0.0018	-1.19	420	78
83-13B							
	16-JUL-83 063234	WT	0.0368	0.0012	-0.72	511	78
	16-JUL-83 064412	WT	0.0369	0.0016	-1.68	255	78
	16-JUL-83 074504*	WT	0.0368	0.0023	-2.23	166	78
	16-JUL-83 080659	WT	0.0363	0.0023	-2.30	139	78
	16-JUL-83 150554	WT	0.0377	0.0019	-0.90	230	78
	16-JUL-83 215020	WT	0.0370	0.0022	-0.78	701	78
	16-JUL-83 222040	WT	0.0381	0.0027	-2.11	153	78
	16-JUL-83 225218	WT	0.0385	0.0033	-0.84	447	78
	16-JUL-83 230054	WT	0.0380	0.0028	-1.81	429	78
	17-JUL-83 010301	WT	0.0372	0.0022	-1.56	309	78
	17-JUL-83 024404	WT	0.0362	0.0022	-1.36	383	78
	17-JUL-83 041904	WT	0.0396	0.0008	-1.74	372	78
	17-JUL-83 121303	WT	0.0388	0.0036	-2.30	139	78
	17-JUL-83 141324	WT	0.0359	0.0017	-1.81	177	78
	17-JUL-83 155058	WT	0.0376	0.0018	-1.81	185	78
	16-JUL-83 220910	WT	0.0369	0.0023	-0.90	599	78
	16-JUL-83 043647	WT	0.0387	0.0035	-2.11	192	78
83-15							
	19-JUL-83 024715	WT	0.0447	0.0016	-2.52	449	78
	19-JUL-83 025313	WT	0.0461	0.0015	-2.95	204	78
	19-JUL-83 025707	WT	0.0504	0.0021	-1.68	1985	78
	19-JUL-83 033945	WT	0.0476	0.0021	-2.11	725	78
	19-JUL-83 034325	WT	0.0441	0.0003	-1.81	848	78
	19-JUL-83 034733	WT	0.0521	0.0042	-2.20	547	78

	19-JUL-83 035509	WT	0.0502	0.0014	-2.79	563	78
	19-JUL-83 040045	WT	0.0480	0.0015	-2.40	351	78
	19-JUL-83 040327	WT	0.0480	0.0005	-2.30	535	78
	19-JUL-83 040533	WT	0.0496	0.0021	-2.11	792	78
	19-JUL-83 042535	WT	0.0464	0.0017	-1.88	1609	78
	19-JUL-83 044633	WT	0.0453	0.0020	-1.95	1042	78
83-17							
	26-JUL-83 124902	WT	0.0406	0.0006	-0.13	898	72
	26-JUL-83 175503	WT	0.0420	0.0008	-0.23	567	72

Appendix 4

This appendix contains a listing of the hypocentral information for locatable events and their average values for the associated groups.

Appendix 4. Listing of hypocentral information for locatable events and their average values.

GROUP	EVENT DATE/TIME/STATION		HYP. DIST.	HYP. DEPTH	EPI. DIST.	LAT.	LONG.
77-2							
	02-JUN-77 065523	SC	8.70	8.22	2.85	34.0117	107.0587
	02-JUN-77 114205	SC	8.19	7.73	2.71	34.0117	107.0603
	30-MAY-77 071339	SC	10.43	8.50	6.40	--------	--------
	30-MAY-77 091627	SC	9.71	8.50	4.69	--------	--------
	30-MAY-77 071533	SC	10.19	8.50	5.62	--------	--------
	average		9.44	8.29	4.52		
77-3							
	14-JUL-77 023407	DM	11.07	7.20	8.41	34.1587	106.8750
	14-JUL-77 113159	DM	11.12	7.38	8.32	34.1548	106.8778
	average		11.10	7.29	8.37		
77-4							
	17-AUG-77 153725	CC	15.72	6.34	-----	34.2628	106.9190
	17-AUG-77 155303	CC	14.48	5.08	-----	34.2568	106.9248
	average		15.10	5.71	13.98		
77-5							
	17-AUG-77 060323	CC	13.41	7.40	11.18	34.1630	106.8630
77-13							
	14-JUN-77 234649	CM	9.42	8.50	-----	--------	--------
	15-JUN-77 030921	CM	9.34	8.50	-----	--------	--------
	average		9.38	8.50	3.97	--------	--------
77-15							
	16-AUG-77 154927	CC	24.35	8.50	-----	--------	--------
	16-AUG-77 120833	CC	22.83	8.50	-----	--------	--------
	average		23.59	8.50	22.01	--------	--------
77-16							
	28-AUG-77 013207	WT	14.51	8.50	-----	--------	--------
	28-AUG-77 015633	WT	14.23	8.50	-----	--------	--------
	average		14.37	8.50	11.59	--------	--------
77-17							
	29-AUG-77 014231	DM	25.71	8.50	-----	--------	--------
	29-AUG-77 035643	DM	17.61	8.50	-----	--------	--------
	average		21.66	8.50	19.92	--------	--------
77-18							
	05-OCT-77 051727	SC	9.79	8.50	-----	--------	--------
	08-OCT-77 050309	SC	9.63	8.50	-----	--------	--------
	average		9.71	8.50	4.69	--------	--------
81-4							
	17-JUN-81 203033	SC	11.31	8.50	-----	--------	--------
	17-JUN-81 230721	SC	10.83	8.50	-----	--------	--------
	average		11.07	8.50	7.09	--------	--------
81-5							
	B18-JUN-81 101925	IC	10.34	8.00	-----	34.0700	106.9800
	B19-JUN-81 182847	IC	9.78	8.50	-----	--------	--------
	20-JUN-81 162247	IC	9.38	8.50	-----	--------	--------
	A22-JUN-81 024057	IC	9.14	7.00	-----	--------	--------
	22-JUN-81 024115	IC	10.34	7.00	-----	34.0700	107.0300
	A22-JUN-81 024345	IC	10.26	8.50	-----	--------	--------

	A05-JUL-81	112259	IC	8.82	8.50	-----	-------	--------
		A average		10.06	8.25	5.76	-------	--------
		B average		9.49	8.50	4.22	-------	--------
83-1								
	14-MAY-83	010216	WT	8.43	7.76	3.30	34.0595	106.9777
	14-MAY-83	010830	WT	9.38	9.14	-----	34.0618	106.9650
	14-MAY-83	024142	WT	10.71	10.18	-----	34.0605	106.9790
	14-MAY-83	144318	WT	8.85	8.51	-----	34.0592	106.9672
		average		9.34	8.90	2.83	-------	--------
83-3								
	30-MAY-83	074507	WT	9.14	6.52	6.40	34.0285	106.9918
83-5								
	11-JUN-83	114310	WT	16.40	11.31	-----	34.0262	107.0020
	11-JUN-83	120423	WT	15.24	10.45	-----	34.0245	107.0515
	11-JUN-83	125737	WT	18.05	12.22	-----	34.0343	107.0823
		average		16.56	11.33	12.08	-------	--------
83-6								
	11-JUN-83	104743	WT	7.37	7.37	00.00	-------	--------
	11-JUN-83	105603	WT	7.37	7.37	00.00	-------	--------
		average		7.37	7.37	00.00	-------	--------
83-8a								
	14-JUL-83	055229	WT	-----	9.09	-----	34.0637	106.9618
	14-JUL-83	161755	WT	-----	9.68	-----	34.0672	106.9763
	14-JUL-83	135126	WT	-----	9.96	-----	34.0718	106.9723
	15-JUL-83	051410	WT	-----	8.99	-----	34.0645	106.9607
		average		9.43	9.43	00.00	-------	--------
83-8b								
	15-JUL-83	085104	WT	-----	9.84	-----	34.0718	106.9638
	14-JUL-83	112333	WT	-----	10.16	-----	34.0718	106.9638
		average		10.00	10.00	00.00	-------	--------
83-8c								
	14-JUL-83	124242	WT	-----	8.67	-----	34.0738	106.9548
	14-JUL-83	161323	WT	-----	8.90	-----	34.0525	106.9653
		average		8.79	8.79	00.00	-------	--------
83-9								
	16-JUL-83	064412	WT	8.17	8.17	00.00	-------	--------
83-1								
	20-JUL-83	014607	WT	-----	9.29	-----	34.0528	106.9635
	20-JUL-83	041107	WT	-----	9.26	-----	34.0708	106.9560
	16-JUL-83	061207	WT	-----	8.14	-----	34.0597	106.9653
	16-JUL-83	085950	WT	-----	8.62	-----	34.0512	106.9617
	20-JUL-83	004155	WT	9.09	8.90	1.84	34.0590	106.9583
		average		9.09	8.90	1.84	-------	--------
83-11								
	16-JUL-83	043554	WT	9.02	8.76	2.15	34.0550	106.9600
83-13a								
	16-JUL-83	043554	WT	9.02	8.76	2.15	34.0550	106.9600
	18-JUL-83	110937	WT	-----	8.58	00.00	34.0680	106.9578
	20-JUL-83	041107	WT	-----	9.26	00.00	34.0708	106.9560
		average		8.87	8.87	00.00	-------	--------
83-13								
	16-JUL-83	215020	WT	-----	9.20	00.00	34.0503	106.9635
	16-JUL-83	230054	WT	-----	8.36	00.00	34.0477	106.9600
		average		9.20	8.78	2.75	-------	--------

83-15

19-JUL-83 034325	WT*	8.03	8.03	00.00	34.0643	106.9627

Appendix 5

This appendix contains a listing of the raypath distances of the groups for the low-velocity layers and half-space, the hypocentral distances and the average velocity through the layer and half-space.

Appendix 5. Listing of raypath distances for the low-velocity layers and half-space, the hypocentral distances, and the average velocities through the layer and half-space.

GROUP	STATION	R(LVL)	R(HS)	R(HYP)	VEL(AV)
77-2	SC	1.675 km	7.80 km	9.44 km	5.17 km/sec
77-18	SC	1.675	8.08	9.71	5.18
81-4	SC	1.738	9.40	11.07	5.23
77-4	CC	0.000	15.10	15.10	5.85
77-5	CC	0.000	13.41	13.41	5.85
77-15	CC	0.000	23.59	23.59	5.85
77-13	CM	2.075	7.30	9.38	5.05
77-3	DM	1.225	9.50	11.10	5.59
77-17	DM	1.300	22.00	21.66	5.23
81-5A	IC	1.613	8.53	10.06	5.21
81-5B	IC	1.563	7.98	9.49	5.21
77-16	WT	0.450	13.97	14.37	5.70
83-1	WT	0.400	8.94	9.34	5.67
83-3	WT	0.430	8.70	9.14	5.66
83-5	WT	0.450	16.15	16.56	5.72
83-6	WT	0.400	6.97	7.37	5.63
83-8	WT	0.400	9.03	9.43	5.68
83-8A	WT	0.400	9.60	10.00	5.69
83-8B	WT	0.400	8.39	8.79	5.66
83-9	WT	0.400	7.77	8.17	5.65
83-10	WT	0.400	8.69	9.09	5.67
83-11	WT	0.400	8.62	9.02	5.67
83-13	WT	0.400	8.60	9.00	5.67
83-13A	WT	0.410	8.82	9.20	5.66
83-15	WT	0.400	7.63	8.03	5.65

Appendix 6

This appendix contains a listing of the linear inversion program used in this study.

Appendix 6. Listing of linear inversion program.

```
C THIS IS A LINEAR INVERSE MODEL TO COMPUTE THE ABSORBTION COEF-
C  FICIENTS (Q) FOR A LAYER OVER A HALF-SPACE LOCATED WITHIN THE
C  NMIMT SEISMIC ARRAY.  IT INVOLVES AN OVER CONSTRAINED CASE
C  (MORE KNOWNS (N) THAN UNKNOWNS (M)) THAT USES EIGENVALUES AND
C  EIGENVECTORS TO OBTAIN A SOLUTION.  INCLUDED IN THE PROGRAM ARE
C  COMPUTATIONS OF THE TRADE OFF PARAMETER (r), THE SCALAR R (SIM-
C  ILAR TO THE CHI SQUARED TEST), AND USES WIEGHTED VALUES FOR THE
C  KNOWNS & UNKNOWNS.

  PARAMETER MDIM=30

  REAL LAMINV(MDIM,MDIM), NEWQ(MDIM)
  DIMENSION A(MDIM,MDIM), AT(MDIM,MDIM), ATA(MDIM,MDIM), DELQ(MD
     *    IM), DELT(MDIM), DIRAC(MDIM,MDIM), EVAL(MDIM), HHT(MDIM,MDIM),
     *    HMAT(MDIM,MDIM), HT(MDIM,MDIM), Q(MDIM), R(MDIM,MDIM),
     *    ROC(MDIM),RMAT(MDIM,MDIM), SIGT(MDIM), SMAT(MDIM,MDIM),
     *    SMR(MDIM), TAU(MDIM), TAUTH(MDIM), TAWQ(MDIM), UNC(MDIM),
     *    UMAT(MDIM,MDIM), VAL(MDIM), VEC(MDIM,MDIM), VECLAM(MDIM,MDIM),
     *    VELOC(MDIM), VECT(MDIM,MDIM), VL(MDIM,MDIM), WK(MDIM),VAR(MDIM)
     *    ,DELTT(MDIM)

C THE FOLLOWING IS A LISTING OF THE ABOVE DIMENSIONED PARAMETERS

C A=A MATRIX
C AT=A TRANSPOSE MATRIX
C ATA=A TRANSPOSE A MATRIX
C DELQ=CALCULATED VALUE OF THE RESPECTIVE ABSORBTION COEFFICIENT
C DELT=DIFFERENCE BETWEEN THEORETICAL AND OBSERVED TAU DIVIDED BY
C      ITS STANDARD DEVIATION
C DIRAC=DIRAC FUNCTION IN MATRIX FORM
C EVAL=EIGENVALUE (ORDERED IN DECREASING VALUE LARGEST TO SMALLEST)
C HHT=H H TRANSPOSE MATRIX
C HMAT=H MATRIX
C HT=H TRANSPOSE MATRIX
C Q=ABSORBTION COEFFICIENT OF RESPECTIVE LAYER AND STATION
C R=RAY PATH OF RESPECTIVE TAU
C RMAT=R MATRIX
C ROC=DUMMY VARIABLE TO AID IN COMPUTATION OF SMR
C SIGT=STANDARD DEVIATION OF RESPECTIVE TAU
C SMAT=S MATRIX
C SMR=TRADE OFF PARAMTER (SMALL R - r)
C TAU=PULSE RISE TIME OF EVENT AT A SPECIFIC STATION (TAU 1/2)
C TAUTH=THEORETICAL VALUE OF TAU AS A FUNCTION OF Q
C TAWQ=UNCERTAINTY IN RESPECTIVE Q
C UNC=COMPUTED UNCERTAINTY IN RESPECTIVE Q
C UMAT=U MATRIX
C VAL=COMPUTED EIGENVALUE
C VEC=COMPUTED EIGENVECTOR
C VECLAM=PRODUCT OF MATRIX MULTIPLICATION OF ORDERED EIGENVECTORS
C        AND LAMBDAINVERSE MATRIX USED TO COMPUTE HMAT
C VELOC=VELOCITY OF RESPECTIVE LAYER
```

```
C VECT=COMPUTED EIGENVECTORS ARRANGED LARGEST TO SMALLEST
C VL=EQUIVILENT OF VECLAM EXCEPT USED TO COMPUTE UMAT
C WK=WORK AREA APPROPRIATED FOR COMPUTATION SPACE OF SUBROUTINE EIGRS

C SET DISPLAY MODE

  WRITE(5,1)
  ACCEPT*, NUNIT

  OPEN (UNIT=3,DEVICE='LPT',ACCESS='SEQOUT')
  OPEN (UNIT=1,DEVICE='DSK',FILE='QINV.DAT',ACCESS='SEQIN')

C READ IN # OF PARAMETERS & # OF DATA

  READ(1,2)M,N

  WRITE(NUNIT,200)N
  WRITE(NUNIT,210)M

C INPUT OBSERVED TAU'S AND ASSOCIATED TRAVEL PATH DISTANCES.
C          DATA IS ARRANGED SUCH THAT RAY PATH DISTANCES IN THE LOW
C          VELOCITY LAYER FOR STATIONS SC,CC,CM,DM,IC, & WT ARE IN
C          THE SECOND THROUGH SIXTH ROWS.  RAY PATH DISTANCES IN THE
C   HALF SPACE FOR EVENTS ARE IN THE SEVENTH ROW.

  DO 10 I=1,N
10            READ(1,3) (TAU(I),(R(I,J),J=1,M))

  WRITE(NUNIT,220)
  DO 20 I=1,N
20            WRITE(NUNIT,230) (I,TAU(I),(R(I,J),J=1,M))

C INPUT UNCERTAINTIES IN TAU

  DO 30 I=1,N
30            READ(1,4) SIGT(I)

  WRITE(NUNIT,240)
        DO 35 I=1,N
35            WRITE(NUNIT,255) I,SIGT(I)

C INPUT VELOCITIES OF LAYERS, FIRST GUESSES AT RESPECTIVE Q'S, &
C   ASSOCIATED UNCERTAINTIES IN Q'S

  DO 40 I=1,M
40            READ(1,5) VELOC(I),Q(I),TAWQ(I)

  WRITE(NUNIT,260)
  DO 45 I=1,M
45            WRITE(NUNIT,270) VELOC(I),Q(I),TAWQ(I)

C COMPUTE DIRAC DELTA MATRIX FOR LATER USE

  DO 50 I=1,M
  DO 50 J=1,M
```

```
      DIRAC(I,J)=0.
50            IF(I.EQ.J) DIRAC(I,J)=1.0

C INITIALIZE TEST VALUE FOR NEGATIVE Q VALUES (IFLG) & INITIALIZE
C     COUNTER TO STOP ITERATION OF INVERSION AT 7 RUNS

   L=0
55       IFLG=0
   L=L+1

   WRITE(NUNIT,275)L
   DO 56 I=1,M
56            WRITE(NUNIT,270) VELOC(I),Q(I),TAWQ(I)

C COMPUTE THEORETICAL MODEL (& INITIALIZE AZIMI'S CONSTANT)

   AZ=0.50

   WRITE(NUNIT,271)AZ
271         FORMAT(//,'********** AZ=',F5.3,' **********')
   DO 70 I=1,N
      TAUTH(I)=0.0
   DO 60 J=1,M
60            TAUTH(I)=(AZ*R(I,J))/(Q(J)*VELOC(J))+TAUTH(I)
70            DELT(I)=(TAU(I)-TAUTH(I))/SIGT(I)

   WRITE(NUNIT,280)
   WRITE(NUNIT,285) (I,DELT(I),I=1,N)

C COMPUTE SCALAR R PARAMETER

   SCALR=0.0
   DO 75 I=1,N
75            SCALR=(DELT(I)**2)+SCALR
   SCALR=SQRT(SCALR/N)

   WRITE(NUNIT,520)
   WRITE(NUNIT,530) SCALR

C COMPUTE A MATRIX

   DO 80 I=1,N
   DO 80 J=1,M
80            A(I,J)=TAWQ(J)*((-AZ*R(I,J))/((VELOC(J)*Q(J)**2)*SIGT(I)))

   WRITE(NUNIT,300)
   WRITE(NUNIT,310) ((I,J,A(I,J),J=1,M),I=1,N)

C COMPUTE A TRANSPOSE MATRIX

   DO 90 J=1,M
   DO 90 I=1,N
90            AT(J,I)=A(I,J)

   WRITE(NUNIT,320)
```

```
      WRITE(NUNIT,330) ((AT(I,J),J=1,N),I=1,M)

C COMPUTE A TRANSPOSE A MATRIX

      CALL VMULFF (AT,A,M,N,M,MDIM,MDIM,ATA,MDIM,IER)

      WRITE(NUNIT,340)
      WRITE(NUNIT,350) ((I,J,ATA(I,J),J=1,M),I=1,M)

C COMPUTE EIGENVALUES(SQUARED) & EIGENVECTORS OF A TRANSPOSE A MATRIX

      CALL VCVTFS (ATA,M,MDIM,ATA)
      JOBN=1
      CALL EIGRS (ATA,M,JOBN,VAL,VEC,MDIM,WK,IER)

      WRITE(NUNIT,355)WK
      WRITE(NUNIT,365)IER
      WRITE(NUNIT,360)
      WRITE(NUNIT,350) ((I,J,VEC(I,J),J=1,M),I=1,M)
      WRITE(NUNIT,370)
      WRITE(NUNIT,380) (I,VAL(I),I=1,M)

C REORDER SQUARED EIGENVALUES (& MATCHING EIGENVECTORS) LARGEST TO
C   SMALLEST (EIGRS COMPUTES SMALLEST TO LARGEST)

      DO 100 J=1,M
         EVAL(J)=VAL(M-J+1)
      DO 100 I=1,M
100           VECT(I,J)=VEC(I,M-J+1)
      M1=M

      WRITE(NUNIT,385) M1
333        WRITE(NUNIT,390)
      WRITE(NUNIT,350) ((I,J,VECT(I,J),J=1,M),I=1,M)
      WRITE(NUNIT,400)
      WRITE(NUNIT,380) (I,EVAL(I),I=1,M)

C COMPUTE VARIANCES & UNCERTAINITIES USING EIGENVALUES & EIGENVECTORS

      DO 110 I=1,M
110           VAR(I)=0.0
      DO 120 I=1,M
      DO 120 J=1,M1
120           VAR(I)=(VECT(I,J)/SQRT(EVAL(J)))**2 + VAR(I)
      DO 130 I=1,M
130           VAR(I)=TAWO(I)*SQRT(VAR(I))

            WRITE(NUNIT,405)
            WRITE(NUNIT,380) (I,VAR(I),I=1,M)

C COMPUTE LAMBDAINVERSE MATRIX

      DO 140 J=1,M
      DO 140 I=1,M
         LAMINV(I,J)=0.0
```

```
140          IF(I.EQ.J)LAMINV(I,J)=1.0/SQRT(ABS(EVAL(J)))

  WRITE(NUNIT,410)
  WRITE(NUNIT,350) ((I,J,LAMINV(I,J),J=1,M),I=1,M)

C COMPUTE U MATRIX (U=A*VECT*LAMBDAINVERSE)

  CALL VMULFF (VECT,LAMINV,M,M,M,MDIM,MDIM,VL,MDIM,IER)
  CALL VMULFF (A,VL,N,M,M,MDIM,MDIM,UMAT,MDIM,IER)

  WRITE(NUNIT,420)
  WRITE(NUNIT,310) ((I,J,UMAT(I,J),J=1,M),I=1,N)

C COMPUTE TRADE OFF PARAMETER (SMALL R )

  DO 160 K=1,M
     SMR(K)=0.0
  DO 160 I=1,M
     ROC(I)=0.0
  DO 150 J=1,M1
150          ROC(I)=(VECT(K,J)*VECT(I,J))+ROC(I)
160          SMR(K)=(ROC(I)-DIRAC(K,I))**2+SMR(K)

  WRITE(NUNIT,430)
  WRITE(NUNIT,380) (I,SMR(I),I=1,M)

C COMPUTE H MATRIX ("THE NATURAL INVERSE OF A")
C     (H=VECT*LAMBDAINVERSE*U TRANSPOSE)

  CALL VMULFF (VECT,LAMINV,M,M1,M1,MDIM,MDIM,VECLAM,MDIM,IER)
  CALL VMULFP (VECLAM,UMAT,M,M1,N,MDIM,MDIM,HMAT,MDIM,IER)

  WRITE(NUNIT,440)
  WRITE(NUNIT,330) ((HMAT(I,J),J=1,N),I=1,M)

C COMPUTE EIGEN SOL'N FOR MODEL PARAMETERS

  CALL VMULFP (HMAT,DELT,M,N,1,MDIM,MDIM,DELQ,MDIM,IER)
  DO 170 I=1,M
170          NEWQ(I)=TAWQ(I)*DELQ(I)+Q(I)

  WRITE(NUNIT,450)
  WRITE(NUNIT,455) (I,NEWQ(I),I=1,M)

C       TEST FOR ZERO OR NEGATIVE Q VALUES & IF FOUND REITERATE ENTIRE
C   INVERSION PROCESS

  DO 175 I=1,M
175          IF(NEWQ(I).LT.0.0)IFLG=1
  IF(IFLG.EQ.1)GO TO 194
C COMPUTE H TRANSPOSE MATRIX

  DO 180 J=1,N
  DO 180 I=1,M
180          HT(J,I)=HMAT(I,J)
```

```
      WRITE(NUNIT,460)
      WRITE(NUNIT,310) ((I,J,HT(I,J),J=1,M),I=1,N)

C CALCULATE UNCERTAINTIES OF PARAMETERS

      CALL VMULFF (HMAT,HT,M,N,M,MDIM,MDIM,HHT,MDIM,IER)

      WRITE(NUNIT,470)
      WRITE(NUNIT,350) ((I,J,HHT(I,J),J=1,M),I=1,M)

      DO 185 I=1,M
185           UNC(I)=TAWQ(I)*SQRT(HHT(I,I))

      WRITE(NUNIT,480)
      WRITE(NUNIT,380) (I,UNC(I),I=1,M)
      WRITE(NUNIT,300)
      WRITE(NUNIT,310) ((I,J,A(I,J),J=1,M),I=1,N)
      WRITE(NUNIT,440)
      WRITE(NUNIT,330) ((HMAT(I,J),J=1,N),I=1,M)

C COMPUTE R MATRIX

      CALL VMULFF (HMAT,A,M,N,M,MDIM,MDIM,RMAT,MDIM,IER)

      WRITE(NUNIT,485)IER
      WRITE(NUNIT,490)
      WRITE(NUNIT,350) ((I,J,RMAT(I,J),J=1,M),I=1,M)

C COMPUTE S MATRIX

      CALL VMULFF (A,HMAT,N,M,N,MDIM,MDIM,SMAT,MDIM,IER)

      WRITE(NUNIT,500)
      WRITE(NUNIT,510) ((SMAT(I,J),J=1,N),I=1,N)

C RECOMPUTE DELTA TAU VALUES FOR NEXT ITERATION

      DO 192 I=1,N
         TAUTH(I)=0.0
      DO 191 J=1,M
191           TAUTH(I)=(AZ*R(I,J))/(NEWQ(J)*VELOC(J))+TAUTH(I)
192           DELTT(I)=(TAU(I)-TAUTH(I))/SIGT(I)

      WRITE(NUNIT,280)
      WRITE(NUNIT,290) (I,DELTT(I),I=1,N)

C COMPUTE SCALAR R PARAMETER WITH APPROPRIATE # OF EIGENVALUES

            SCALR=0.0
            DO 193 I=1,N
193            SCALR=(DELTT(I)**2)+SCALR
            SCALR=SQRT(SCALR/N)

            WRITE(NUNIT,535) M1,SCALR
```

```
C REITERATE PROCESS W/ONE LESS EIGENVALUE & CORRESPONDI<NG
C   EIGENVECTOR

  M1=M1-1
  IF(M1.LT.0) GO TO 999

        WRITE(NUNIT,540)
  WRITE(NUNIT,545) M1
  GO TO 333

C REINITIALIZE NEGATIVE Q VALUES OF STATIONS TO 3/4 OF THEIR
C    PREVIOUS VALUE BUT KEEP POSITIVE Q"S THE SAME & LOOP BACK
C    TO REITERATE INVERSION PROCESS. NEGATIVE Q VALUES OBTAINED
C          FOR THE HALF SPACE ARE REINITIALIZED TO 1/2 OF THEIR
C          PREVIOUS VALUE.  LIMITS ARE ALSO SET TO VALUES FOR Q IN
C    THE LAYER AND IN THE HALF SPACE.

194       WRITE(NUNIT,550)

  DO 199 I=1,M
    IF(NEWQ(I))195,195,197
195         IF(I.GT.6)GO TO 196
            Q(I)=Q(I)*0.75
            GO TO 198
196           Q(I)=Q(I)*0.50
    GO TO 199
197           Q(I)=NEWQ(I)
198     IF((I.LT.7).AND.(Q(I).LT.3.0))Q(I)=3.0
  IF((I.EQ.2).AND.(Q(I).EQ.3.0))Q(I)=0.0
  IF((I.LT.7).AND.(Q(I).GT.200.0))Q(I)=25.0
  IF((I.EQ.6).AND.(Q(I).GT.30.0))Q(I)=10.0
199       IF((I.EQ.7).AND.(Q(I).LT.50.0))Q(I)=50.0
  IF(L .GT. 7)GO TO 998
  GO TO 55

C!!!!!!!!!!!!!BE SURE THAT YOU'VE USED THE CORRECT M & N VARIABLES
C                 IN THE FORMAT STATEMENTS!!!!!!!!!!!!!!!!!!!!!!!!!!


1 FORMAT('    TYPE 3 FOR LPT OUTPUT OR 5 FOR TTY OUTPUT    ')
2 FORMAT(I3,2X,I3)
3 FORMAT(2X,F7.5,5X,7(F7.4,2X))
4 FORMAT(2X,F7.5,2X)
5 FORMAT(F5.3,5X,F6.2,5X,F6.2)
200       FORMAT(/,5X,'NUMBER OF DATA =',I3)
210       FORMAT(/,5X,'NUMBER OF PARAMETERS =',I3)
220       FORMAT(/,9X,'TAU',11X,'R(1)',9X,'R(2)',9X,'R(3)',9X,'R(4)')
230       FORMAT(1x,I3,2X,F8.5,3X,7(F10.3,3X))
240       FORMAT(/,20X,'UNCERTAINTY IN RESPECTIVE TAU')
250       FORMAT(24(/,2X,'I=',I2,4X,'SIGT=',F8.5))
255     FORMAT(/,2X,'I=',I2,4X,'SIGT=',F8.5)
260       FORMAT(/,5X,'VELOCITY',10X,'ABSORBTION COEFFICIENT (Q)',5X,
     *    'UNCERTAINTY IN Q')
270       FORMAT(6X,F5.3,20X,F5.1,22X,F5.1)
```

```
275       FORMAT(///,1X,94('*'),/,40('*'),' ITERATION # =',I3,1X,38('*')
     *   ,/,1X,94('*'),///)
280       FORMAT(/,10X,'DIFFERENCE IN OBSERVED TAU FROM THEORETICAL TAU')
285     FORMAT(24(/,2X,'I=',I2,4X,'DELT=',F12.6))
290       FORMAT(24(/,2X,'I=',I2,4X,'DELTT=',F12.6))
300       FORMAT(/,35X,'A MATRIX')
310       FORMAT(24(/,7(2X,'I=',I2,2X,'J=',I2,E19.10)))
320       FORMAT(/,25X,'A TRANSPOSE MATRIX')
330       FORMAT(7(/,1X,24(F7.4,1X)))
340       FORMAT(/,25X,'A TRANSPOSE A MATRIX')
350       FORMAT(7(/,7(2X,'I=',I2,2X,'J=',I2,E19.10)))
355       FORMAT(/,5X,'WORK AREA FOR EIGRS',F15.8)
360       FORMAT(/,25X,'COMPUTED EIGENVECTORS')
365       FORMAT(/,5X,'ERROR INFORMATION FOR EIGRS',I20)
370       FORMAT(/,25X,'COMPUTED EIGENVALUES SQUARED')
380       FORMAT(7(/,2X,'I=',I2,4X,F12.6))
385       FORMAT(/,30('*'),' # OF EIGENVALUES USED FOR THIS ITERATION ='
     *  I2,1X,30('*'))
390       FORMAT(/,25X,'ORDERED EIGENVECTORS')
400       FORMAT(/,25X,'ORDERED EIGENVALUES SQUARED')
405     FORMAT(/,25X,'UNCERTAINTIES OF Q"S USING EIGENVECTORS/VALUES')
410       FORMAT(/,25X,'LAMBDAINVERS MATRIX')
420       FORMAT(/,25X,'U MATRIX')
430       FORMAT(/,25X,'TRADE OFF PARAMETER (SMALL r)')
440       FORMAT(/,35X,'H MATRIX')
450       FORMAT(/,10X,'NEW Q VALUES COMPUTED FROM EIGENVALUES/VECTORS')
455       FORMAT(7(/,2X,'J=',I2,4X,'NEWQ=',F12.6))
460       FORMAT(/,25X,'H TRANSPOSE MATRIX')
470       FORMAT(/,25X,'H H TRANSPOSE MATRIX')
480       FORMAT(/,25X,'UNCERTAINTY IN Q CALCULATED USING DIAGONAL OF
     *HHT')
485       FORMAT(/,5X,'ERROR INFORMATION FOR R MATRIX',I20)
490       FORMAT(/,35X,'R MATRIX')
500       FORMAT(/,35X,'S MATRIX')
510       FORMAT(24(/,1X,24(F6.4,1X)))
520       FORMAT(/,25X,'SCALAR R PARAMETER')
530       FORMAT(10X,'SCALAR R=',F10.5)
535     FORMAT(/,25X,'SCALAR R COMPUTED WITH',I2,' EIGENVALUE(S)',/,
     *    20X,' R= ',F10.5)
540     FORMAT(/,60('*'))
545       FORMAT(/,5X,'# OF EIGENVALUES USED M1=',I3)
550       FORMAT(/,'******NEGATIVE Q VALUE FOUND!!  RESET VALUE TO HALF
     * ITS PREVIOUS VALUE & LOOP BACK TO REITERATE INVERSION PROCESS
     ************')
560       FORMAT(///,95('$'),/,25('-'),'ITERATION LIMIT EXCEEDED!!! KIC
     *K OUT OF PROGRAM',25('-'),/,95('$'))


998       WRITE(NUNIT,560)
999       STOP
  END
```